SYNTHESIS AND CHARACTERIZATION OF CONJUGATED POLYMERS VIA TRADITIONAL AND NON-TRADITIONAL POLYCONDENSATION TECHNIQUES.

by

NARAYAN MUKHERJEE

A dissertation submitted to the Graduate Faculty in Chemistry in partial fulfillment of the requirements for the degree of Doctor of Philosophy, The City University of New York

2008

This manuscript has been read and accepted for the
Graduate Faculty in Chemistry in satisfaction of the
dissertation requirement for the degree of Doctor of Philosophy.

01.25.2008	Dr. Ralf M Peetz
Date	Chair of Examining Committee
01.31.2008	Dr. Gerald Koeppl
Date	Executive Officer

Prof. Nan-Loh Yang

Dr. Bonnie Gersten

Supervision Committee

THE CITY UNIVERSITY OF NEW YORK

Abstract

SYNTHESIS AND CHARACTERIZATIONS OF CONJUGATED POLYMERS VIA TRADITIONAL AND NON-TRADITIONAL POLYCONDENSATION TECHNIQUES.

by

Narayan Mukherjee

Adviser: Professor Ralf M. Peetz

This doctoral thesis is focused on the novel and facile synthesis and characterization of conjugated cyclic and linear oligomers and polymers containing heteroatoms, via acyclic diene metathesis (ADMET) or traditional polycondensation techniques. All products are soluble, and have a highly defined all-*trans* microstructure without defects. All monomers utilized were designed, synthesized, and characterized accordingly.

Poly(*p*-phenylene vinylene) (PPV) type oligomers were synthesized via ADMET with a ruthenium-based Grubbs-type catalyst. The ADMET could be optimized to produce individual oligomers in high yields and exclusively *trans*-configured at the vinylene bonds. These oligomers constitute valuable oligomeric building blocks in a variety of applications.

A series of homologous conjugated oligomers and polymers with siloxane, silylene, germylene, and stannylene linkages integrated into the conjugated backbone and different lateral solublizing side-chains could be synthesized in a unified synthetic strategy, using ruthenium-based ADMET under the same conditions for all cases. Products were isolated in 89-95%-yields with exclusively all-*trans*-configured vinylene bonds. Analysis by means of ^{1}H-, ^{13}C-, ^{29}Si-, and ^{119}Sn-NMR, ATR-FTIR, GPC, etc. indicated that the siloxane condensates consisted exclusively of macrocycles (cyclic oligomers) whereas

silane, germane, stannane-based monomers mainly yielded higher molecular weight linear polycondensates. The optical absorption and emission properties proved that all heteroatomic linkages participate in the electronic conjugation. Thus a facile synthetic access to homologous heteroatom containing conjugated polymers and macrocycles with no defect structures and all-*trans* configured vinylene bonds is available.

A new class of homologous soluble and processable polyazines is presented, synthesized via polycondensation of alpha-omega-diformyl functional aromats with flexible side chains, i.e., side-chain substituted oligo(*p*-phenylene vinylene) (OPV) blocks, with hydrazine. The reaction conditions were investigated and the products analyzed by means of ^{1}H-, ^{13}C-, ^{15}N-NMR, ATR/FTIR, GPC, etc. indicating exclusively all-*trans* configured C=N–N=C linkages. The optical properties showed a red shift in absorption and emission maxima of ~31–60 nm relative to the monomers, due to active conjugation through the azine linkage, with an orange-red emission. Thin films of OPV-polyazines readily undergo n-doping, resulting in a rare example of OPV-type materials with n-type behavior.

Acknowledgements

It is my pleasure to thank all those people who made this thesis possible.

I express my sincere gratitude to my Ph.D. supervisor, Prof. Ralf M. Peetz. His encouragement, support, and his unique way to explain things in a simple manner, helped me a lot to understand the chemistry. He also gave me enough freedom to work in his lab.

I am grateful to Prof. Nan-Loh Yang and Dr. Bonnie Gersten for serving as thesis committee members and their constructive criticism of my work.

I am indebted to Dr. Hsin Wang for his help and advice with all NMR experiments.

I wish to thank Mr. Tai Park for his help with Chromatography (GPC) and thermal characterization experiments.

I would like to thank all my colleagues for providing a fun environment. Special thanks goes to Mr. Rajesh Sardar, and Dr. Neeraja Vinduyala for their sincere help. Especially Mr. Chivin Sun helped me a lot with monomer/trimer synthesis in polyazine project (Chapter 5).

I also enjoyed working with many undergraduates especially Bilal Marie, Steven Schultz, Olga Naglyuk and Fiza Quadri. I would like to thank all of them for their numerous contributions.

The financial supports from different sources particularly from the City University of New York and NSF-MRI are gratefully acknowledged.

Lastly and most importantly, I owe thank to my family particularly, my parents for their continuous support and encouragement. Without their support, it would have not been possible for me to complete this thesis. I dedicate this thesis to them.

I wish to express my warm and sincere thanks to all other people whose names are not mentioned above for their help.

Table of Contents

List of Schemes

List of Figures

List of Tables

1 Introduction

1.1 Conjugated polymers

Polymers are typically known as insulators. In 1977, Shirakawa et al. found that polyacetylene, which is the simplest conjugated polymer, can be made conductive (band gap 1.5 eV) after suitable doping. [1] Conjugated polymers exhibit semi-conducting properties due to the delocalization of conjugated p electrons along the polymer main chain. These materials, often considered as 4th generation of polymeric materials, show a characteristics band gap between the p (bonding) and p* (antibonding) molecular orbital, usually 1- 4 eV, (before or after doping).

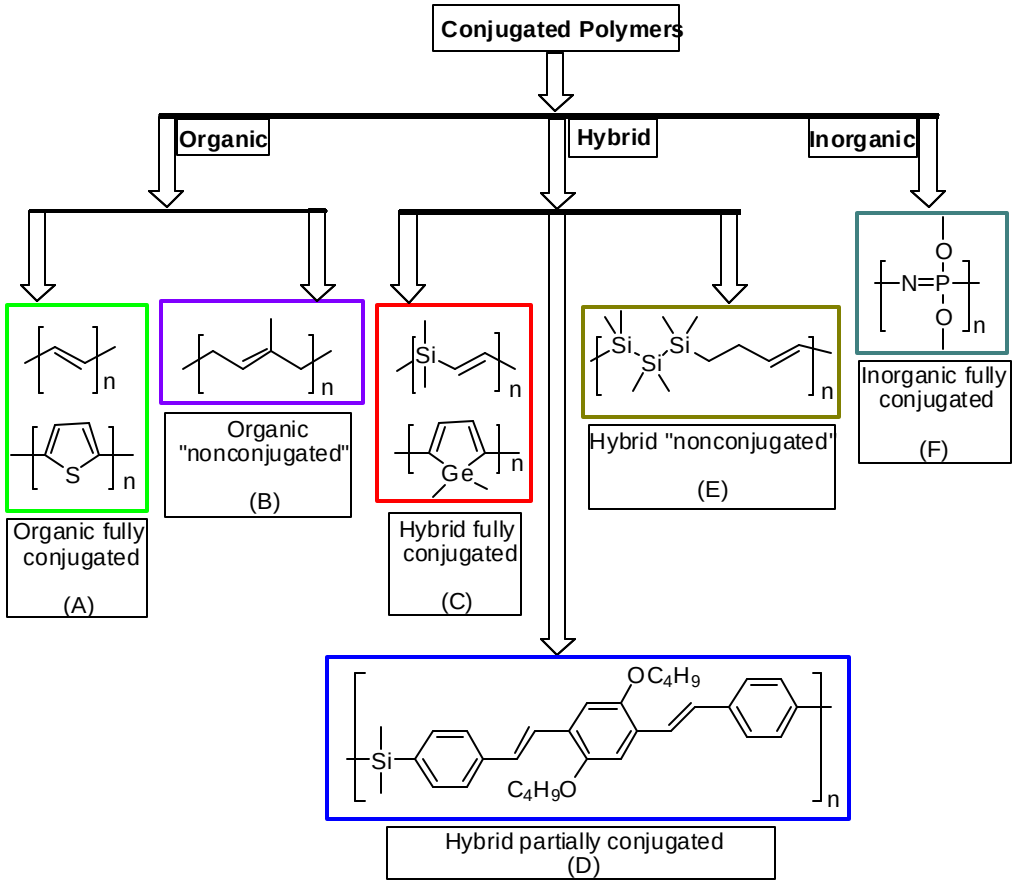

Scheme.1.1 Classification of conjugated polymers based on bonding

1.2 Opto-electronic properties of conjugated polymers

Electronic transitions (excitation and emission) and charge transport are observed in many inorganic as well as organic materials, when they are exposed to certain electromagnetic radiation. Obeying the Frank-Condon principle (in an electronic transition the nuclei do not change their position), electrons may move between a higher occupied molecular orbital (HOMO) and a lower unoccupied molecular orbital (LUMO). For conjugated organic systems a "free electron model" [the p electron is a domain of uniform energy, confined by boundary walls, i.e., a square well potential] is generally applicable where the lowest electronic transition involved is an electronic transition between the "filled band" (formed by overlapping of HOMOs) to an "empty band" (formed by overlapping of LUMOs).

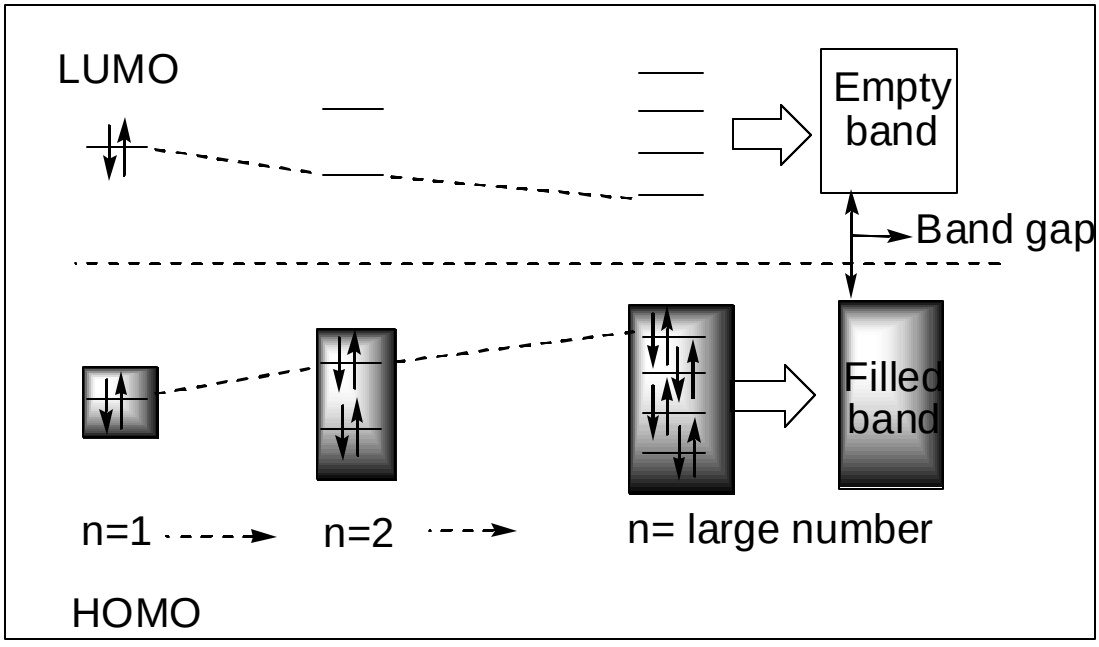

Scheme: 1.2 Formation of bands in organic conjugated molecules. (n= number of double bonds) [Adopted and modified from ref. 2(a)]

When the electron from the excited state (singlet*) relaxes back to its ground state (singlet) this may involve a singlet* to singlet transition [the energy difference is lost either via a radiative (fluorescence) or non-radiative (heat emission) mechanism]. Another possibilty for the relaxation is a singlet* to triplet* to singlet transition [involving inter-system crossing and/or phosphorescence].

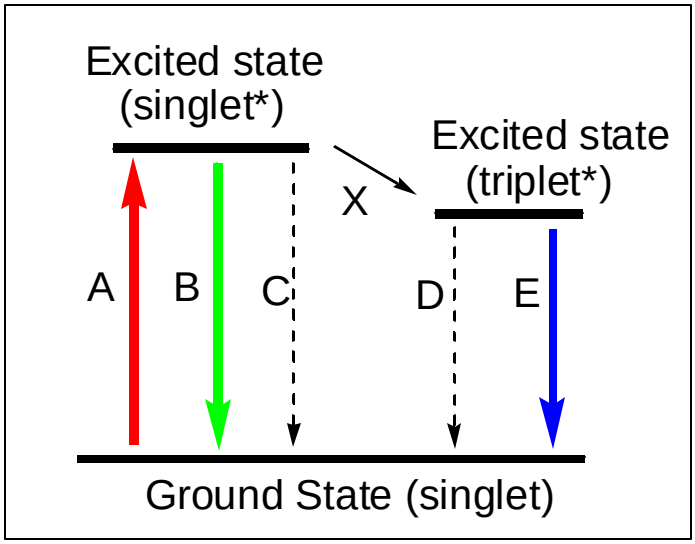

Scheme: 1.3 Electron transitions: A) Excitation (singlet to singlet*) B) radiative relaxation (fluorescence: singlet* to singlet) C) non-radiative relaxation (singlet* to singlet) D) non-radiative relaxation (triplet* to singlet) E) radiative relaxation (phosphorescence: triplet* to singlet) X) inter system crossing (singlet* to triplet*)

In conjugated oligomers/polymers two major factors affect the conjugation and hence the optoelectronic properties. As the number of repeat units increases in conjugated polymers, the delocalization of p-electrons becomes more extensive (After a certain number of repeat units the properties approach a limit after which the extension of the conjugated system by one repeat unit does not resultin additional changes). Typically, the HOMO-LUMO bandgap in such systems decreases when the conjugated system is extended, making electron excitations less energetically costly. However, as the

conjugated polymers usually have a rigid backbone, they easily aggregate and form crystalline domains in solid state via p-p stacking. This aggregation significantly reduces the fluorescence efficiency by means of quenching. By introducing long and branched side chains the aggregation can be reduced and fluorescence effiences are thus increased.

Electroluminescence materials properties have been known from inorganic compounds for many years. [2] In the mid 1980's Tang and Van Slyke developed a two-layer sublimated molecular electro-luminescence device. It consisted of a hole transport layer (aromatic diamine), an electron transport and emissive layer (8-hydroxyquinoline aluminum) .[3]

The phenomenon of electroluminescence from polymeric materials was reported for the first time in 1990: Friend et al. observed that poly(phenylene vinylene) (PPV) and its derivatives emit light when positioned between two electrodes under an electric current.[4] This triggered extensive research activity to investigate conjugated polymers both theoretically and experimentally. Thus conjugated polymers expand the scope for organic compounds not only as possible conducting materials but also as materials for electroluminescence applications, due to their synthetic flexibility, and potential processing advantages. [2,5] Nowadays it is possible to design conjugated polymeric systems (by tuning specific properties in order to obtain desired functions), in which a multitude of the mentioned photonic phenomena can be observed (until recently this was only valid for inorganic compounds). Thus, these polymers have been investigated and used for variety of applications - for example in light emitting diodes (LED), photodiodes, light emitting electrochemical cells, field effect transistors, photovoltaic cells, piezo- and pyro-electric materials, photo detector devices, laser dyes, as well as

optical data storage materials, molecular switches, for signal processing applications and as nonlinear optical materials. [6-13]

1.3 Importance of well-defined p-conjugated oligomers

Oligomers can serve as model systems for any analogous polymer and often allow to predict specific properties of the polymers based on extrapolation of the observed oligomer properties.[14] Detailed microstructure analysis and/or other characterizations are often difficult due to a limited solubility of the polymeric materials. Furthermore structural defects are often encountered due to the aggregration, monomer residues and other impurities (e.g. metal catalysts) from the synthetic process. By design and use of oligomers with well-defined microstructures and conjugation lengths it is possible to address these problems. Conjugated oligomers are usually soluble in many common organic solvents and easily purified. Through investigation of homologous series of oligomers with defined length and conformation, structure/property relationships can be deduced, which help to understand and predict the properties of analogous polymeric systems. It has been shown both theoretically and experimentally that the effective conjugation reaches its maximum after ~ 8 repeating units. In fact, even 3-4 repeating units will achieve around ~ 80% of the effective conjugation, depending on the particular system.[15] Furthermore, for several years conjugated oligomers themselves, have become attractive for many opto-electronic applications because of their specific and highly defined structure. Organic light emitters or molecular wires are examples of potential areas for these materials.[9,16]

1.4 Poly(p-phenylene vinylene).

Among the conjugated polymers, poly(p-phenylene vinylene) (PPV), has its own place as it is one of the cheaper and intensely studied systems due to its' electroluminescence properties.[4] Unsubstituted PPV, is a bright yellow, fluorescent polymer with emission maxima at 551 nm and 520 nm.[17] PPV is insoluble, infusible, and cannot be processed. Although conjugated, the backbone of this polymer is not strictly planar, but slightly twisted (10 °) due to steric interactions between H-atoms of the phenyl ring and vinylene bonds.[18] The HOMO-LUMO bad gap of these types of polymers (and their copolymers) can be controlled by using adequate substitution on either the phenyl ring or the internal vinylene bonds, or both.

The first soluble and fusible PPV derivative was reported by Hörhold et al. [19] In 1987 Murase et al. reported a modified sulfonium precursor route (originally developed by Wessling and Zimmerman) in order to synthesize soluble substituted PPV derivatives, which was then used by Burroughes et al. in 1990 in order to develop electroluminescence devices, based on PPV.[20]

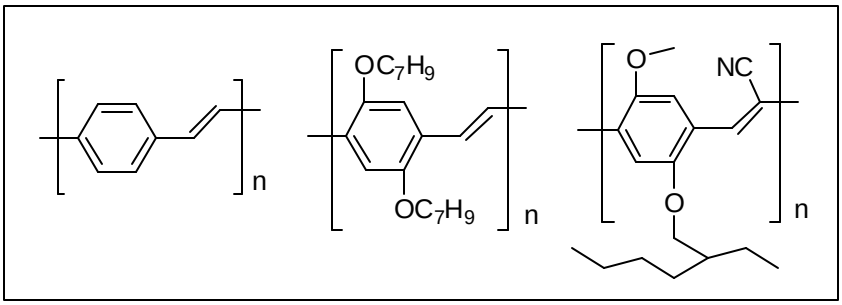

Scheme: 1.4 Examples of different PPV systems

In 1988, Wudl et al. reported the synthesis of dialkoxy substituted PPV, a soluble conjugated polymer.[21] Later this type of system (with different side chain substitution)

was used by Heeger et al. to make a mechanically flexible light emitting diode. [21] Many other methods have been reported to prepare PPV derivatives and copolymers suitable for electroluminescence applications with higher efficiencies and improved lifetimes of the respective devices. One of the alternative routes to synthesize PPV is based on the elimination of sulfinyl or sulfonyl groups instead of sulfino group, reported by Vanderzande et al.[22] Recently Jin et al. reported the synthesis of alkylsilylphenyl-substituted PPV, which has some unique properties like good solubility, thermal stability, uniform film morphology, and the color of the emission can be slightly tuned by changing the position of the substituent in the side group along the back bone.[23]

1.5 Effect of spacer group in conjugated polymers

Although it is generally accepted that for conducting properties a polymer needs a conjugated backbone, in 1988 M. Thakur reported that a conjugated backbone *"is not a pre-requisite for a polymer to be conductive"*.[24] Polymers having "non-conjugated backbones" after doping, may exhibit conductivity almost as good as a p-conjugated polymers. As an example, when polyisoprene (natural rubber) is doped with iodine, the conductivity of the material increases by about 100 billion times. From that time, many theoretical and experimental studies on organic conjugated polymers with spacer groups between conjugated structural elements in the backbone have been reported.[25,26]

One of the simple ways to synthesize such materials is to place a proper spacer moiety between specificly designed conjugated blocks. As a result, one can precisely control solubility, aggregation, absorption and emission, conductivity, charge carrier mobility, redox potentials, and stability toward external factors of the materials by selecting the proper combination of conjugating block and spacer. The conjugated block will exhibit

the opto-electronic properties like a conjugated oligomer, although the overall material will behave as a less rigid polymer, thus overcoming the problems associated with conventional long chain fully conjugated polymers.

Using group-IV elements as a spacer group (other than carbon, e.g. Si, Ge, Sn) has recently received a lot of attention in this area, as delocalization of electrons in a controlled manner through out the polymer chain is possible via so-called s-p and p-$3d_{Si}$ interaction (lowering the LUMO level of the conjugated block, thus reducing the barrier for charge injection and transportation). These types of materials are organic –inorganic hybrids in nature, featuring elements from both sides and spanning the gap between classical conjugated organic polymers and inorganic materials. Although a large number of materials have been developed and synthesized including some polysilane-based materials, systematic control over structures, and understanding of corresponding structure/property relationship is limited due to synthetic limitations of making both monomers and polymers.[27-30]

1.6. Metathesis polymerizations

1.6.1 Metathesis

The word "metathesis" originates from the Greek metatithenai (to transpose) [Meta (change) and Tithenai (to place)]. The term is used as a common phrase for any kind of change. In chemistry, it represents an exchange of atoms and atom groups between two different molecules in a certain fashion.

The concept of Olefin Metathesis describes the thermodynamically controlled redistribution of unsaturated carbon–carbon bonds occur in the presence of metal carbene

complexes.[31] It could be Homo-metathesis (when single species is used) or Cross-metathesis (when two different species react).

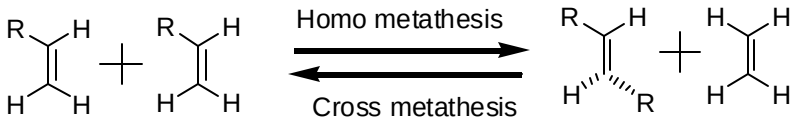

Scheme 1.5 Olefin metathesis

Metathesis reactions have been known for almost fifty years. In 1957 H. S. Eleuterio reported on the polymerization of cyclic olefins using transitional metal oxide catalysts to produce an amorphous unsaturated linear polymer.[32] In 1960 the same type of catalyst was reported by E. F. Peters et al. in a U.S. Patent for metathesis reactions of hydrocarbons.[33] During the same time, Truett et al. reported the use of $TiCl_4/LiAlR_4$ in the ring opening polymerization of norbornene type monomers.[34] In the early 60's G. Natta *et al.* showed that a Ziegler-Natta-type catalyst ($AlEt_3$ and $TiCl_4$ or $ZrCl_4$ or VCl_4) can also be used to for metathesis polymerization.[35] Later, the same group showed that the $WCl_6/AlCl_2Et/EtOH$ and $MoCl_5/AlEt_3$ type systems may even produce exclusively stereo-specific polymers from cyclic olefins via a ring opening mode.[36] During the late 60's N. Calderon *et al.* reported for the first time the polymerization of unsaturated hydrocarbons via skeletal transformation in the presence of $WCl_6/AlCl_2Et/EtOH$.[37,38] This group also proposed a three-step metathesis reaction pathway involving biolefin-metal complex formation, transalkylidenation, and olefin exchange, using deuterium exchange reaction of 2-butene. This report also proved that the olefin metathesis reaction works both for ring opening and acyclic mode under suitable conditions.

1.6.2 Mechanism

Different reaction mechanisms were proposed after the initial break-through report on the skeletal transformations of unsaturated hydrocarbons. After the initial complexation of the transition metal and carbon-carbon double bond, an intermediate formed, followed by olefin exchange. Formation of a "cyclobutanation complex" of ligand-bound olefin, metallacycle, metallhydrid or a metalltetracarben-complex were proposed by different groups as a intermediate species formed during the reaction. [39-42]

The commonly accepted olefin metathesis mechanism was proposed by Chauvin and Hérisson in 1971, involving a [2+2] cyclo-addition type reaction between a transition metal alkylidene (Metal=C) complex and the proper olefin, to form a metallacyclobutane type intermediate. This intermediate then breaks apart in a reverse fashion to afford either the new alkylidene-complex (which further reacts with another olefin) and olefin (productive) or may produce the starting compounds (regenerative). The reaction is thermodynamically controlled, highly reversible, and always equilibrium mixtures of olefins are obtained (exceptions are thermodynamically highly stable cyclic ring type species). [43-45] The key step of the mechanism is shown in Scheme 1.6.

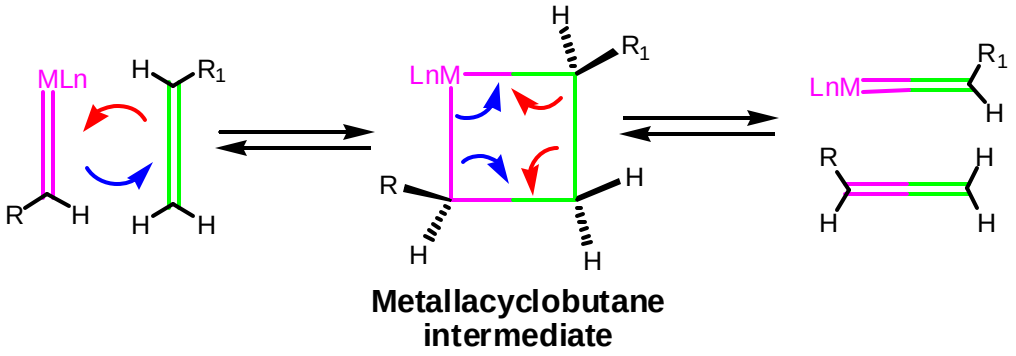

Scheme: 1.6 Simple schematic diagram of metathesis mechanism

1.6.3 Catalysts

The catalysts used in metathesis reactions can be broadly classified into two categories.

1.6.3.1 Classical multicomponent catalysts

The “classical” catalysts are multi-components systems and one can distinguish between “homogeneous” and “heterogeneous” systems.

The “homogeneous” systems consist of mainly three components: [31, 37, 46-49]

1. A transitional metal (oxy) halides: e.g. WCl_6, $WOCl_4$, $MoCl_5$, $TiCl_4$, $ZrCl_4$, VCl_4.

2. An organometallic species having metal-alkyl linkage: eg $AlEtCl_2$, $AlEt_3$, $Sn(Alkyl)_4$.

3. An "activator": e.g. EtOH, Et_2O

The “heterogeneous” systems consist of transition metal oxides embedded in an inorganic matrix/ support. e.g WO_3/Al_2O_3 (SiO_2), Re_2O_7/Al_2O_3 (SiO_2) + $Sn(Alkyl)_4$

1.6.3.2 Stable transitional metal alkylidenes

Generally, W, Mo or Ru based metal-alkylidene complexes are employed in metathesis. These stable “single site” metal-alkylidene complexes are soluble in organic solvents, easily removable after reaction and the amount of active species used is precisely defined, whereas in “traditional” systems, the active species form only in situ in a small quantities. Two types of metal-alkylidene-complexes are commercially available and used for all practical purposes.

Schrock-type (W or Mo based) complexes are the most reactive. Scheme 1.7 illustrates the general structure of Schrock-alkylidene-complexes. The main system features two t-butyloxy- ligands (R_2), which are usually partially fluorinated along with a metal=C (alkylidene) and metal=N linkage (imido linkage).[50,51] By varying the ligand and the

central atom (Mo or W) the specificity and the reactivity of catalyst can be strongly varied.[52] The "molybdenum-version" of the catalyst in generally reacts much faster towards terminal olefins than the "tungsten-version".[53] The nature and steric interaction of Imido- ligands also play an important role in the activity of the catalyst systems, particularly if the olefin substrate features significant steric bulk.

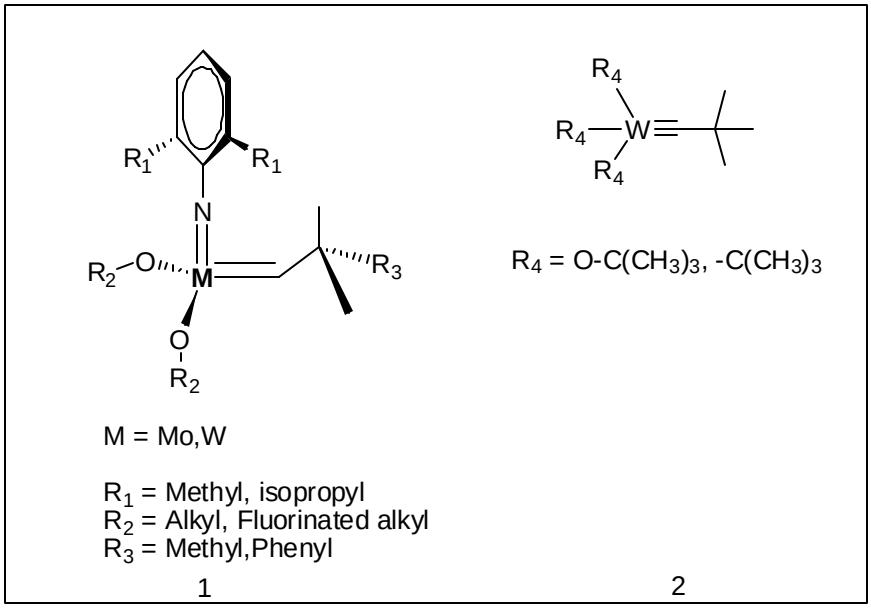

Scheme: 1.7 Mo and W based metathesis catalyst: 1) General representation of Mo and W-based Schrock catalyst (Examples of substitutions are included but not limited) 2) W based Schrock alkyne metathesis catalyst.

The second group of catalysts is Ru – based alkylidene-systems developed in the early 90's and known as Grubbs type catalysts, shown in Scheme 1.8. The 1st generation system features two triphenyl phosphine type ligands along with two metal-halogen and a metal=C (benzylidene) linkages.[54] The major challenge to this system was its relatively low reactivity. The 2nd generation catalyst was developed from the combination of the 1st Generation Catalyst and alkoxy-protected 1,3-dimesityl-4,5-dihydroimidazol-2-ylidene.[55] One of the triphenyl phosphine ligand is replaced by a N-heterocyclic carbene (more

basic and hence better sigma donation-ability towards metal center) in order to improve the reactivity. More recently, a 3rd generation Ru-based catalyst, (also known as Grubbs-Hoveyda 1st generation catalyst) has been reported, where one triphenyl phosphine ligand is replaced by *o*-isopropoxyphenylmethylene ligand. [56]

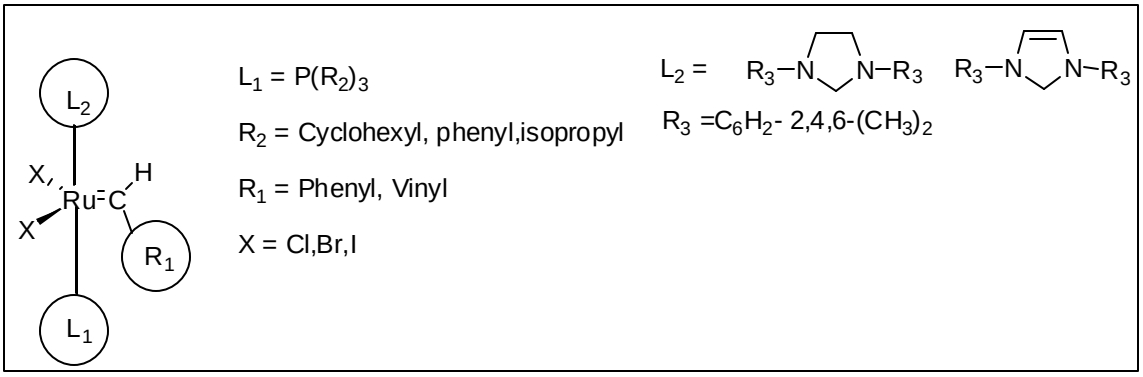

A

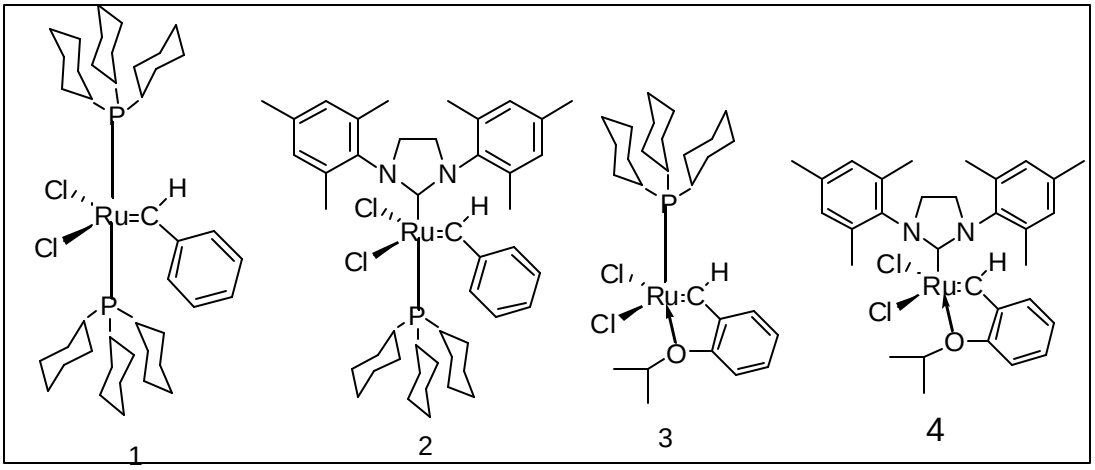

B

Scheme: 1.8 Ru based metathesis catalyst: A) General representation of Ru-based catalyst (Examples of substitutions are included but not limited) B) Representative Ru-based catalyst (commercially available): 1) Grubbs 1st generation 2) Grubbs 2nd generation 3) Grubbs-Hoveyda 1st generation 4) Grubbs-Hoveyda 2nd generation catalyst.

In a Grubbs-Hoveyda 2nd generation catalyst, the triphenyl phosphine ligand of the Grubbs-Hoveyda 1st generation catalyst is replaced by the N-heterocyclic carbene.[57] All of these new catalysts are still less reactive compared to Schrock catalysts but active enough for a variety of metathesis reactions, not too costly and easily available. They can tolerate a wide range of polar functional/ pendent groups and solvents (a water soluble Grubbs catalyst is also reported) and it can easily be removed after the reaction simply by passing through a silica gel column.[58,59]

1.6.4 Acyclic Diene Metathesis (ADMET)

Different modes of the metathesis reaction such as ring opening metathesis, ring closing metathesis, cross metathesis have been well known for many years.[60-62] Acyclic Diene Metathesis (ADMET) is more recent and can be considered a "non-traditional" condensation reaction to make oligomeric/polymeric materials, in which terminal divinyl functional monomers can be polymerized using either Schrock or Grubbs type complexes.[63] Although the term ADMET was first coined by Wagner et al. in the late 80's, in 1973, Dall'Asta et al. reported the metathetic polycondensation of alpha-omega-dienes (1,4-pentadiene, 1,5-hexadiene and 1,7-octadiene) in the presence of Lewis base-modified 4-component catalysts yielding stereo-specific regular oligomers with minimal by-product formation.[64] In 1982, Dolgoplosk et al. also reported this type of reaction and proved both polycondensation and cyclodegradation are possible using suitable starting compounds.[65]

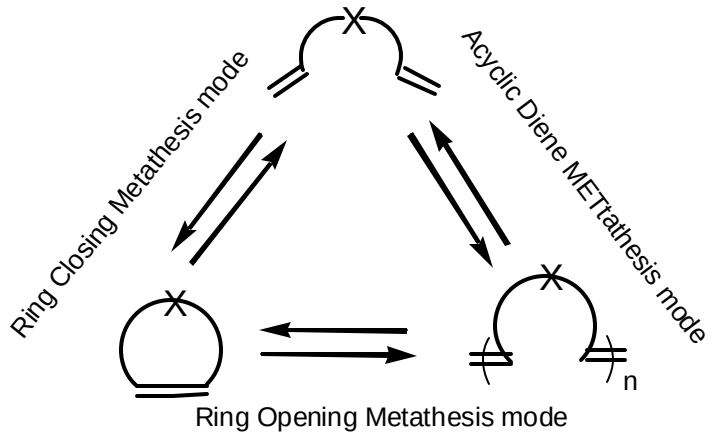

Scheme: 1.9 Major modes of olefin metathesis 1) Acyclic Diene Metathesis (ADMET), 2) Ring Opening Metathesis (ROM) 3) Ring Closing Metathesis (RCM) [for cross metathesis see Scheme 1.5] [31(f)]

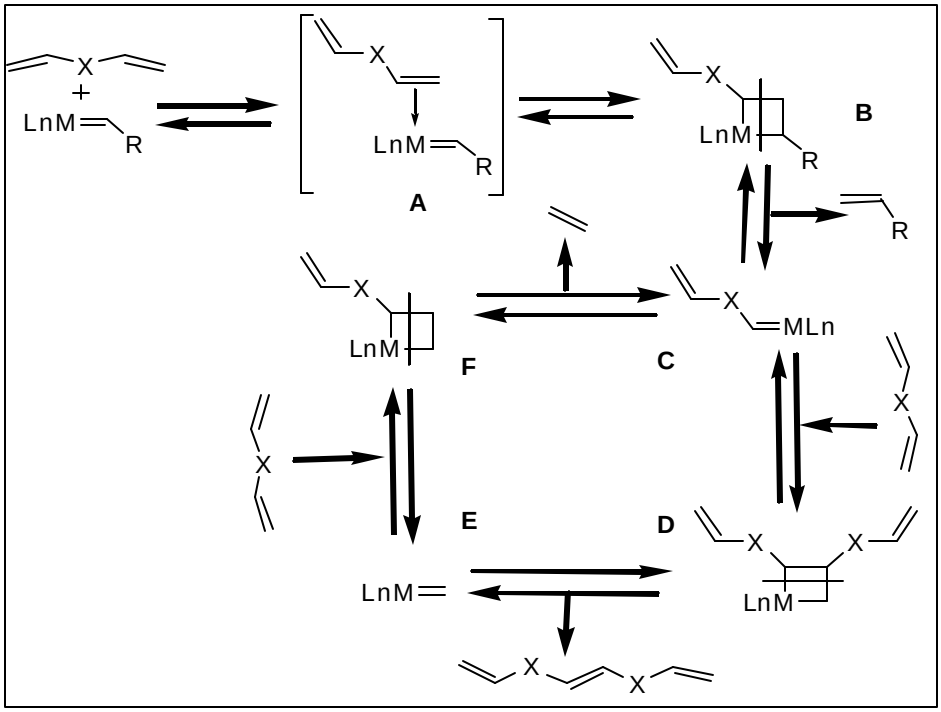

Scheme: 1.10 ADMET catalytic cycle. [63(h)]

The ADMET is characterized by the formation of a metallacyclobutane ring (as mentioned above), a reaction intermediate that is also formed during Ring Opening Metathesis Polymerization (ROMP) [another olefin metathesis technique to synthesize

polymers].[66] Several aspects of the ADMET process are different from ROMP. Each step in the reaction is reversible and in equilibrium, and by removing the side product (usually ethane) one can drive the reaction equilibrium to the product side, i.e. the polymer. This is generally done by intermittently applying vacuum, or slowly streaming inert gas, in order to remove the by-product as it forms (release of ring strain is the main driving force of ROMP). The ADMET proceeds via two metallacyclobutane intermediates (Scheme 1.10, **D** and **F**), (ROMP: one intermediate). The "true catalyst" in the ADMET system is the methylidene complex **E (**Scheme 1.10**)**. Depending on the structures of monomer and the catalyst complex, ADMET can be employed for polymerization of an array of monomers with the tolerance of wide varieties of functional groups, producing well-defined linear, cyclic, olefin-containing, oligomers and polymers.[63]

1.6.4.1 ADMET - synthesis of conjugated polymers

A convenient way to synthesize vinylene containing conjugated polymers is the ADMET polycondensation method. Mo or W based Schrock catalysts have been reported for the synthesis of PPV –type oligomers and polymers, but challenges include the handling of catalyst under rigorous condition, intolerance against polar functional/ pendent group in the substrate, choice of solvent and removal of catalyst residue after reaction. [67-70]

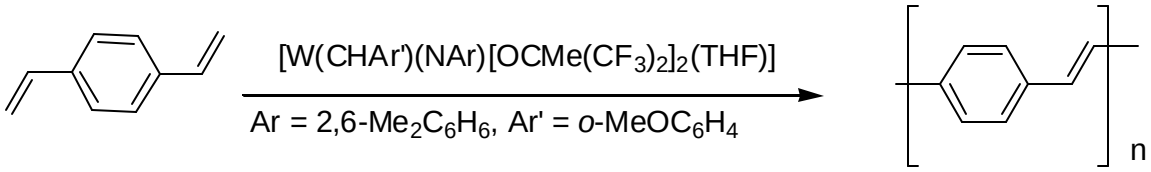

Scheme: 1.11 Synthesis of PPV via ADMET using Schrock catalyst (W based)

Although ruthenium based catalysts have been successfully used for ADMET in general, less reports are found on synthesizing PPV-type and other relevant conjugated polymers. Very recently, the use of a Grubbs catalyst to synthesize PPV type oligo/polymers using medium to long alkoxy or alkyl side chains has been reported by Thorn-Csanyi et al. and by Nomura et al.[71,72]

1.6.4.2 ADMET - synthesis of heteroatom containing conjugated polymers

During the last 10 years Wagener et al. have reported on the synthesis of heteroatom (silicon/germanium/tin) containing polymers using ADMET.[73,74] Cyclolinear carbosilane polymers made via ADMET have been reported by Interrante et al.. [75]

However, hardly any attention has been focused on the the synthesis of silicon/germanium/tin containing conjugated polymers via ADMET, as the vinyl derivatives of silicon compounds are very unreactive towards homometathesis due to steric and electronic effects originating from the silyl group, stimulating non-productive cleavage of the metallacyclobutane intermediate containing two silyl groups attached to adjacent carbonatoms.[76] A few silicon-containing monomers undergo "silylative coupling", as reported by Marciniec et al., and the ADMET of thiophene containing silane polymers as reported by Bazan et al. are "exceptions" with no follow-up reports, probably due to problematic side-reactions.[77-79] In silicon/germanium/tin containing conjugated oligomers and polymers, the organo-silicon/germanium/tin moiety acts as a "spacer group" between the p-conjugation of the conjugated oligomer block, generating a well defined conjugation unit, usually with a band gap corresponding to a blue emission.(difficult to make from inorganic counterparts).[80-82]

1.7 Schiff-base polycondensation

Schiff base or imines are a well-known class of compounds, which are synthesized by the condensation reaction of an aldehyde or ketone with an amine.[83]

These materials have been extensively studied due to their high coordination ability, which is further increased in presence of other polar functional groups, with a wide range of transitional and lanthanide metals to form chelate metal complexes and due to their applications mainly as catalysts both in synthetic organic chemistry and biologically active systems.[84, 85]

Adams et al. reported on the first synthesis of polymeric Schiff's bases in 1923 by polycondensation reaction between an aromatic dialdehyde e.g. terephthaldehyde and an aromatic diamine e.g benzidine or o-anisidine.[86] Most of the synthesized polyimines reported until the late 1960's were mainly insoluble, infusible and low-molecular weight compounds.[84(a)] However, D'Alelio et al. showed that different aromatic polyimines exhibit high thermally stability and can be potentially used as engineering materials.[87]

After the discovery of electroluminescence in polymers (PPV, see above), interest in this area of research was revived as some of the soluble conjugated polyimines are isoelectronic with PPV/polythiophene type polymers and hence could potentially be used in optoelectronic applications.[88] Similarly, polyazine synthesized from glyoxal and hydrazine is the "nitrogen-analog" of polyacetylene, with better oxidation and thermal stability.[89] Another classical example is the polycondensate of p-benzoquinone with p-phenylenediamine, which is structurally similar to the oxidized form of polyaniline.[90]

Along with the afore-mentioned properties, aromatic polyimines also exhibit liquid-crystallinity, form mesophases (either via main chain or a suitable side chain) under appropriate conditions.[91]

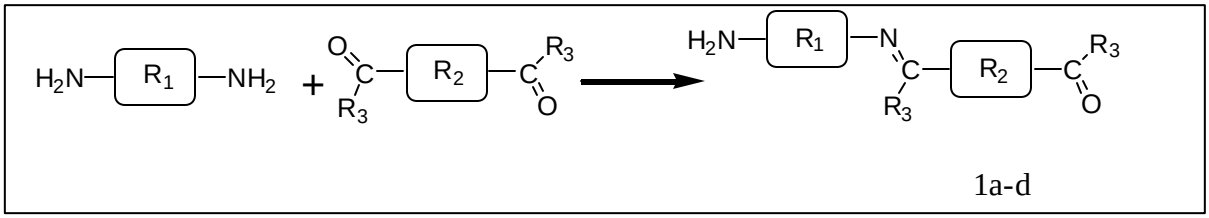

1a-d

R_1	R_2	R_3	Polymer
Aryl or alkyl	Aryl or alkyl	H	**1a**
n=1	Aryl or alkyl	H	**1b**
Aryl or alkyl	Aryl or alkyl	Aryl or alkyl	**1c**
n=1	Aryl or alkyl	Aryl or alkyl	**1d**

1a = polyazomethines [PAM], **1b** = polyazines [when diamines or hydrazine are used in the polycondensation reactions with any dialdehyde compound.]
1c = polyketamines [PAM], **1d** = polyketazines [when diamines or hydrazine are used in the polycondensation reactions with any diketone compound.]

Scheme: 1.12 General Schiff base synthesis.[93]

1.7.1. Polyazines – synthesis and conducting properties

Polyazines (PAZs) are a sub-class of poly Schiff-base polymers, and feature HC=N-N=CH linkages that are isoelectronic with butadienyl units, and thus also seem suitable for conjugated organic materials.[92, 93] Typical characteristics of PAZs include thermal stability, strength, high modulus.[94] Recently, some Schiff-base polymers have been

receiving attention due to their semi-conducting and non-linear optical properties.[95] Introducing flexible side chains to rigid polymers helps overcome the usually limited processability owing to high melting points and low solubility, thus enabling systematic structure/property investigations.[96]

PAZs with alternating aromatic and azine units have been reported with substituted thiophene as the aromatic part. [97] The solubility of these materials highly depends on the presence of flexible side chains. Mainly three synthetic approaches have been utilized, e.g. melt polymerization, polymerization under azeotropic conditions, and polymerization in the presence of a water-absorbing agent. However in all cases syn-anti isomerism (10-30% syn) with respect to the azine linkage was observed, which strongly affects the thermal and structural properties of the polymer, thus limiting the optoelectronic applications.[97]

1.8. Applications of conjugated polymers (LED)

Light emitting diodes, are among the important commercial applications for conjugated polymers where the emitter color can be tuned by adjusting the chemical structures of the emitter materials.[2, 4, 11, 98] A typical LED consists of an emitter layer "sandwiched" between two electrodes as shown in Scheme 1.13. When a bias is applied, the cathode (generally low work-function metals, e.g., Ca, Al) injects electrons into the polymeric material and creates negative charges (polarons/bipolarons carrying single/double negative formal charges). The anode is generally a transparent material, i.e.,indium titanium oxide (ITO) and injects electron holes into the polymeric material, creating positive charges (polarons/bipolarons with single/double positive formal charges).

Polarons and bipolarons are radical species with positive or negative charge and usually formed in the presence of doping agent. They carry charges intra-molecularly along the polymer chains. When both positive and negative polarons/bipolarons meet each other, a neutral excited species (exciton) is formed in a charge recombination process. This exciton is singlet in nature and may emit light via electronic relaxation (singlet* to singlet transition) or may undergo non-radiative thermal decay (see above for more details). As the probability of the singlet* to triplet is 3 times that of a singlet* to singlet transition, the electroluminescence efficiency of a conjugated polymer can theoretically not exceed 25%. [98] In practical examples, efficiencies of light-emitting diodes (usually 2-5%) are limited by charge injection and charge transport (mainly due to the relatively "high energy barrier" at the electrode/polymer interface). Use of polymer blends and copolymers in multi-layer systems (up to 7 layers) have been reported in efforts to improve the efficiencies to as high as 10% as well as to create white light emitting diodes. [98-100]

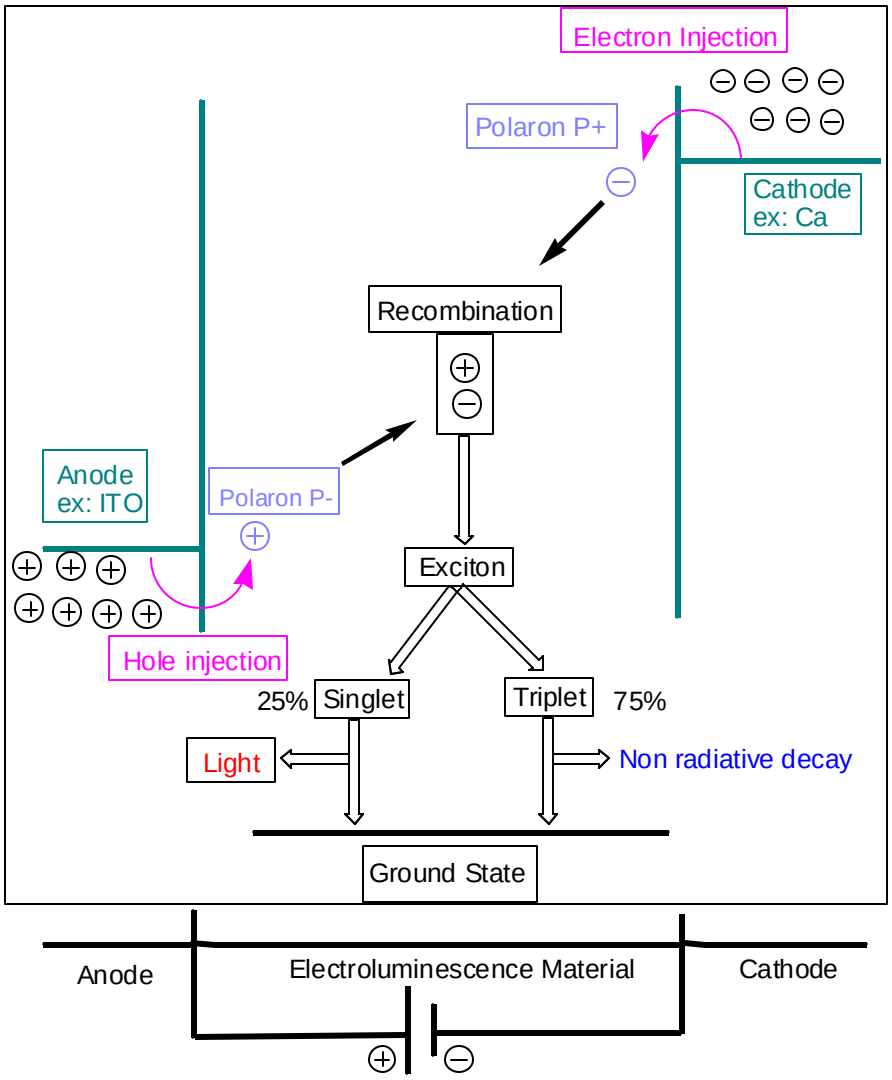

(A)

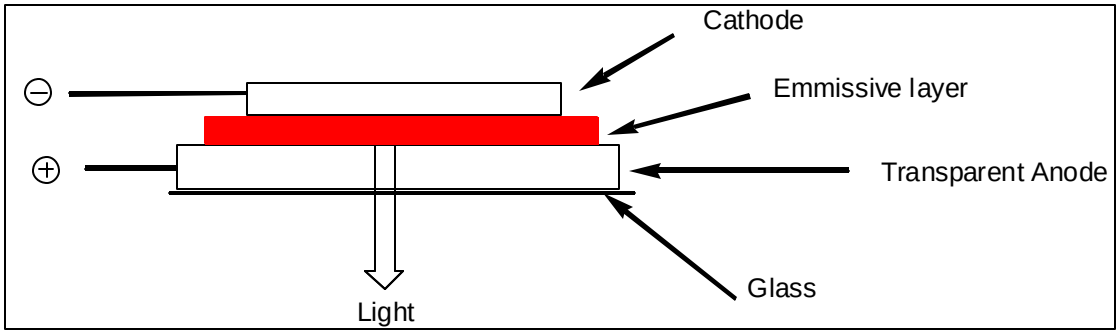

(B)

Scheme: 1.13 (A) "Mechanism" of light emitting in a typical polymer light emitting diode (PLED) (B) Typical Construction and components of a PLED system.

2 Synthesis of dimethoxy PPV using Grubbs-type catalysts

2.1 Objective

The objective of this work was to synthesize PPV type oligo/polymers using a 4th generation Ru-based Grubbs catalyst, which is also known as Grubbs-Hoveyda 2nd generation catalyst. This catalyst is less reactive compared to Schrock systems (less moisture and air sensitive) but active enough for the planned ADMET polycondensation. At the same time it can tolerate a wide range of polar functional and/or pendent groups and it can easily be removed after the reaction simply by passing the reaction mixture through a short silica gel column. In order to prove the effective functional group tolerance of these catalysts especially Grubbs-Hoveyda 2nd generation catalyst, a simple dimethoxy-substituted monomer was selected, where the oxygen atom is highly exposed to the transition metal center of the catalyst. This approach demonstrates by proof of principlethe effectiveness of the system. It is important to note that while higher alkoxy substituted side chain yield more soluble products; it becomes more difficult to separate single oligomers e.g. dimeric, trimeric, tetrameric units as the molcules quickly become too similar to separate. Chosing the methoxy group emphasizes the solubility differences of the individual oligomers; enable more selective synthesis and isolation. In 2004 however, Thorn-Csanyi *et. al.* reported the use of Grubbs 2nd generation catalyst to synthesize PPV oligomers using medium to long alkoxy side chains under very similar conditions.[71]

2.2 Results and discussions

2.2.1 Monomer synthesis

2,5-Dimethoxy phenylene vinylene oligomers, particularly dimer and trimer were synthesized using the ADMET-polycondensation reaction. In order to yield these

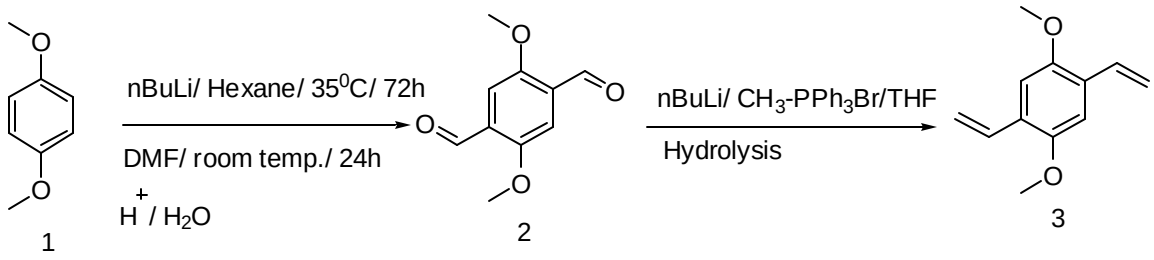

Scheme: 2.1 Synthesis of 1,4-dimethoxy-2,5-divinylbenzene

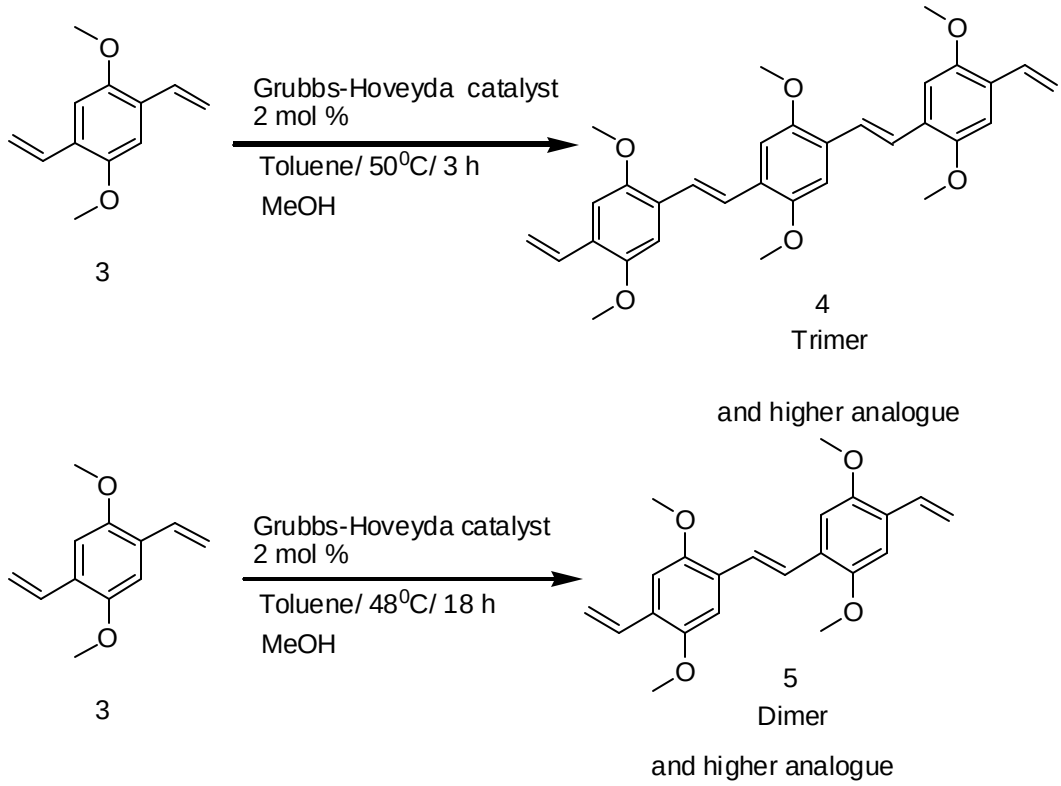

Scheme: 2.2 Synthesis of Dimeric and trimeric unit from 1,4-dimethoxy-2,5-divinylbenzene

oligomers, we first synthesized the monomer (Scheme 2.1). 1,4-dimethoxy-2,5-dialdehyde-benzene (precursor of the monomer) was made from 1,4-dimethoxy benzene. In a first step 1,4-dimethoxy benzene was lithiated using n-butyl lithium, followed by addition of DMF. Finally the reaction mixture was hydrolyzed (via acid catalysis) to yield 1,4-dimethoxy-2,5-dialdehydebenzene. In a second step, the aldehyde group was converted to a vinyl group via a standard Wittig reaction using excess phosphorus ylide, which could be removed by passing the crude product mixture through a silica gel column. (Scheme.2.1)

2.2.2 ADMET polycondensation

2,5-Dimethoxy phenylene vinylene oligomers, particularly dimer and trimer were synthesized in high yield using the ADMET-polycondensation reaction using Grubbs-Hoveyda catalyst (Scheme.2.2). In this metathesis reaction the solvent/ temperature/ ratio of catalyst: monomer / and type of catalyst were varied. The by-product ethylene was removed intermittently by applying vacuum, which also helped to drive the reaction equilibrium towards the product side.

In order to synthesize the oligomeric PPV, the reaction was carried out at temperatures from 25 ^{0}C to 70 ^{0}C. No product formation was observed at room temperature (table 2.1, entry 1) whereas at 70 ^{0}C a 6%-yield in trimer was isolated (table 2.1, entry 7). The optimum reaction temperature proved to be around 50 ^{0}C when up to 38 % trimer and 5% dimer (table 2.1, entry 12) were isolated. The relative amount of catalyst was varied from 1mol% (table 2.1, entry 1) to 4 mol% (table 2.1, entry 3) [mol catalyst/ mol monomer]

and was observed that the reaction yielded highest percentage in trimer at 2 mol% catalyst (table 2.1, entries 5, 11, 12).

Table 2.1 Representaive table for ADMET reaction1,4-dimethoxy-2,5-divinylbenzene*

	Catalyst (mol%)	**Solvent**	**Time (h)**	**Temperature (^{0}C)**	**Product**	
					Isolated total mass % (mg)	**Isolated dimer or trimer %**
1	1	DCM	18	25	98	Traces of trimer
2	2	DCM	18	55	95	5 % trimer
3	4	DCM	18	55	90	8 % trimer
4	2	Toluene	18	48	81	25 % trimer **10** % dimer
5	2	Toluene	18	42	80	31 % trimer **8** % dimer
6	2	Toluene	16	55	80	28 % trimer 5 % dimer
7	2	Toluene	48	70	75	6 % trimer
8	2	Toluene	12	70	77	12 % trimer
9	2	Toluene	6	70	75	8 % trimer
10	2	Toluene	6	32	92	7 % trimer 3 % dimer
11	2	Toluene	12	50	80	32 % trimer 5 % dimer
12	2	Toluene	3	50	79 (395)	**38** % trimer 5 % dimer
13	2 $^+$	Toluene	18	50	98 (490)	Traces of trimer

* Catalyst: Grubbs-Hoveyda catalyst, amount of monomer used: 500 mg)
$^+$ Catalyst: Grubbs 1st generation catalyst**.**

While varying the solvent it was found that the aromatic solvent (e.g. toluene) worked (table 2.1, entry 6) better compared to the halogenated solvent (i.e., dichloromethane) (table 2.1, entry 3) under comparable conditions.

Generally most of the reactions were carried out ca. 12 h but longer reaction time such as 48h (table 2.1, entry 7) resulted in mostly insoluble product (crosslinked or higher homologs) whereas even 3 h reaction time (table 2.1, entry 12) was enough to produce 38% trimer under controlled condition.

It is to be noted that the Grubbs 1st generation catalyst did not produce any ADMET product at all (data not shown), probably due to the lower reactivity of catalyst.

The dimer was obtained under very similar conditions to trimer but a longer reaction time was required coupled with a slightly lower temperature (table 2.1, entries 4,5) in order to get a higher relative yield. As the dimer unit is soluble in methanol during the follow up process (along with catalyst residue and unreacted monomer) the reaction solutions were concentrated and passed through a silica gel column

2.3.3 Characterizations of materials

2.3.3.1 NMR

The structures of dimer and trimer were confirmed by ^{1}H NMR spectroscopy, as shown in figures 2.1 and 2.2 below. The proton resonances of methoxy and terminal vinyl group are useful for the structure determinations as they change in a characteristic in the homologous series. The structures showed exclusive all-trans configurations at the vinylene bonds, a result of the specificity of the substitution pattern in the metalla-cyclobutane intermediate transition state (see schematic of catalytic cycle above).

In the homologous series, the methoxy signals changed from 3.82 ppm (monomer) to 3.87 ppm (dimer) and 3.88/3.92 ppm (trimer) due to an increase in conjugation. Furthermore the trimeric unit showed two different singlets for inner-ring (3.92) and outer-ring (3.88) methyloxy with signal intensities ~1:2 respectively. The relative resonance intensities from the terminal vinyl groups at 5.71 and 5.25 ppm gradually decreased from monomer to dimer to trimer as expected and at the same time an internal trans vinylene signal appeared at 7.41ppm (dimer) and 7.44 ppm (trimer). The aromatic protons also showed different intensities from monomer (6.97) to dimer (7.04, 7.13) or trimer (7.01,7.14,7.16) due to their different positions with respect to methoxy and internal vinylene groups.

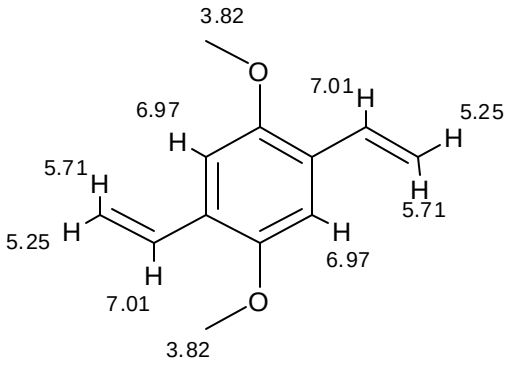

a

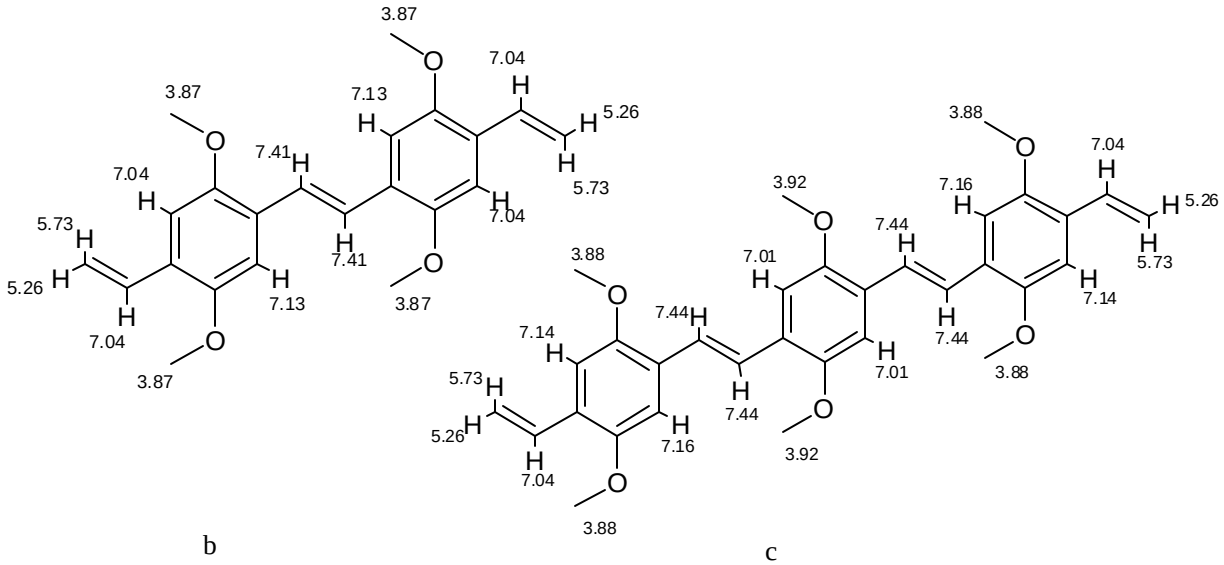

b c

Fig. 2.1 [1]HNMR assignment of 1,4-dimethoxy-2,5-divinylbenzene a)monomer b) dimer c) trimer

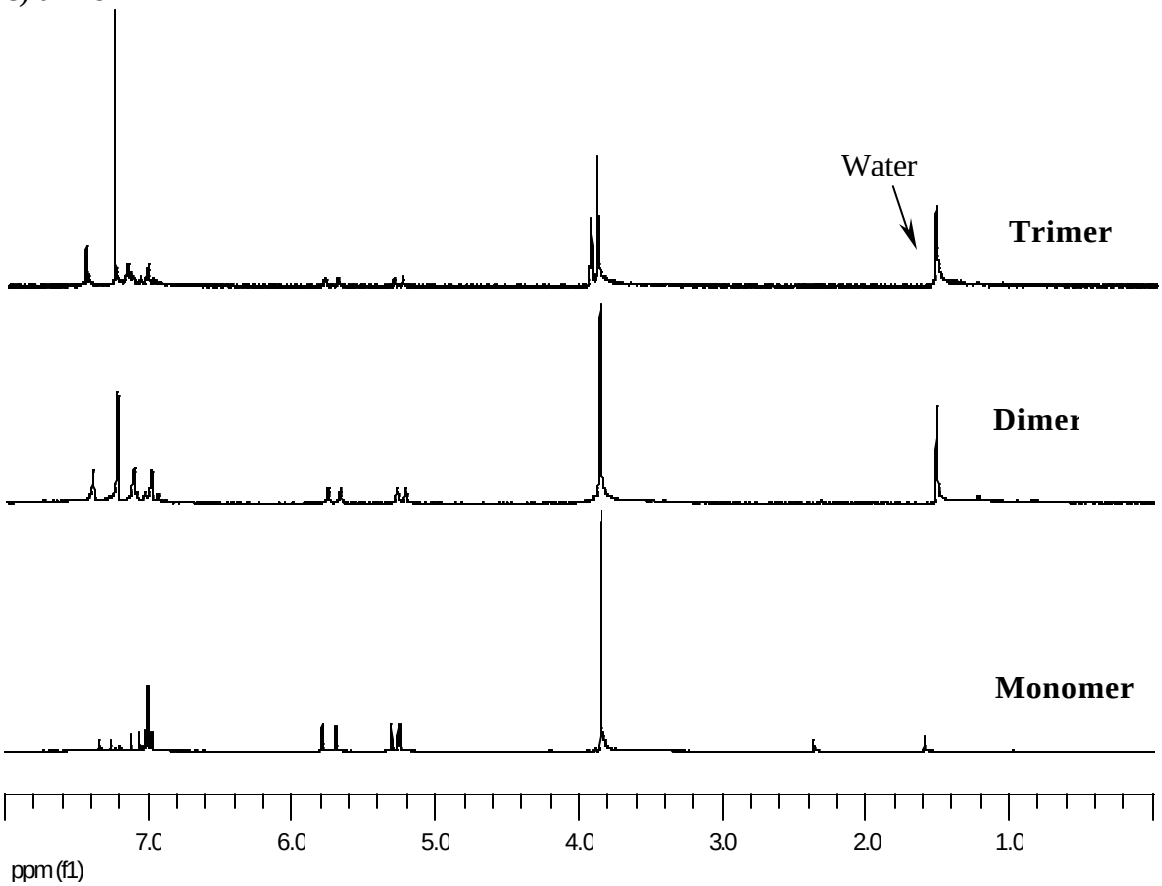

Fig. 2.2 NMR data of monomer/ dimer and trimer unit of 1,4-dimethoxy-2,5-divinylbenzene

2.3.3.2 FT-IR

FT-IR studies (Fig. 2.3 and 2.4) confirmed conclusions from the ^{1}H NMR spectroscopic analysis. Important IR frequency values for monomer, dimer and trimer are listed below. C=C stretching intensities (with conjugation) increased from monomer (1672,1622) to dimer (1620,1605) to trimer (1619,1601) and aromatic C=C stretching vibration intensities (1490,1461 cm^{-1} for monomer, 1497,1462 cm^{-1} for dimer and 1505, 1465 cm^{-1} for trimer) also increased but with a shift towards higher frequencies. Signals at ~ 994 and 906 cm^{-1} indicate the presence of terminal vinyl bonds in the monomer, whereas in higher oligomers a new peak appeared at ~ 963 cm^{-1}, indicating formation of the *trans* double bond (out of plane bending mode) during polymerization. ADMET results in *trans* configured double bonds for this type of system with a very defined microstructure.

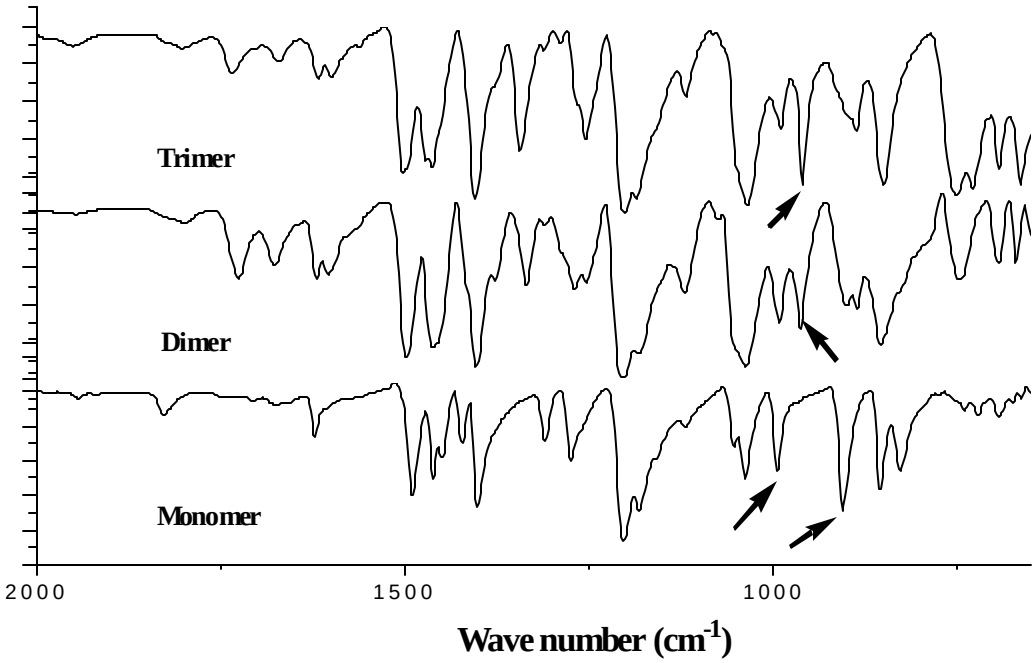

Fig. 2.3 FTIR spectra of monomeric, dimeric and trimeric unit of 1,4-dimethoxy-2,5-divinylbenzene (Zoomed version)

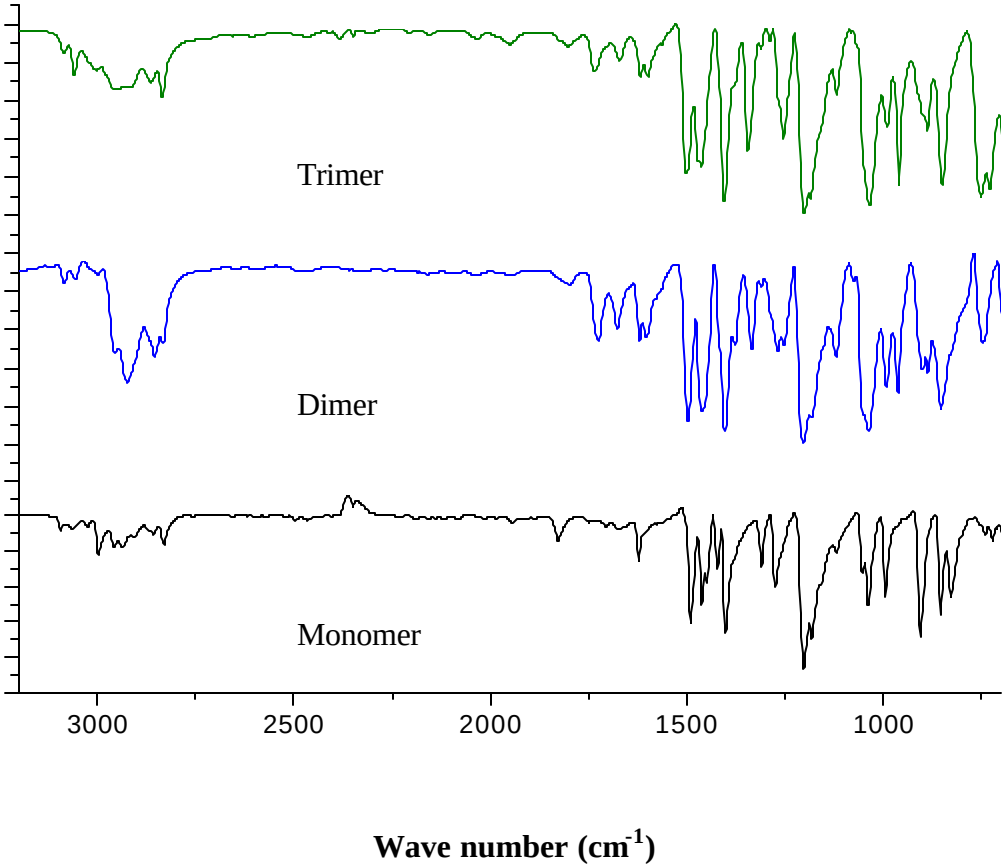

Fig. 2.4 FTIR spectra of monomer and polymeric unit of 1,4-dimethoxy-2,5-divinylbenzene

Table 2.2. FTIR- data of monomer, dimer and trimer of 1,4-dimethoxy-2,5-divinylbenzene

Monomer	Dimer	Trimer	
3093	3083	3086	C-H stretching (CH=)CH_2
3064	3054	3059	C-H stretching (CH=)CH_2
3024, 2996	2997	3009,3001	Aromatic C-H stretching
2956	2954	2960,2947	Aliphatic C-H stretching
2933	2922	2933	Aromatic overtone
2905		2916	
2857	2853	2866	-O-CH_3 symmetrical stretching
2830	2832	2836	
1827	1798	1805	Aromatic overtone
	1725	1737	
	1677	1672	
1672,1622	1620,1605	1619,1601	C=C stretching with conjugation
		1563	
1490	1497	1505	Aromatic C=C stretching vibration
1461	1462	1473,1465	Aliphatic C-H asymmetric deformation Aromatic C=C stretching vibration
1449			
1422			
1402	1403	1407	-CH_3 deformation
	1377		
	1377,1335	1346	Aliphatic C-H twisting of -CH_2-
1309	1310	1313	
		1291	
1275	1269,1253	1256	
1203	1204	1204	Asymmetric C-O-C stretching
1182		1188	
1119	1120	1121	Phenylene. C-H in plane bending
	1074		
1053			
1038	1037	1034	Symmetric. C-O-C stretching
994	991	989	CH(=CH_2) oop deformation
	963	960	Trans vinylene oop –CH-deformation
906	900	900	CH(=CH_2) oop deformation
	886	887	
855	854	850	Phenylene –CH- oop deformation
827			
740	747	752	Phenylene. C-H OOP bending
721		729	Aliphatic. C-C vibration
694	694	694	-CH_2 rocking
675	670	665	
664	649		

OOP = out of plane

2.3.3.3 Optical properties

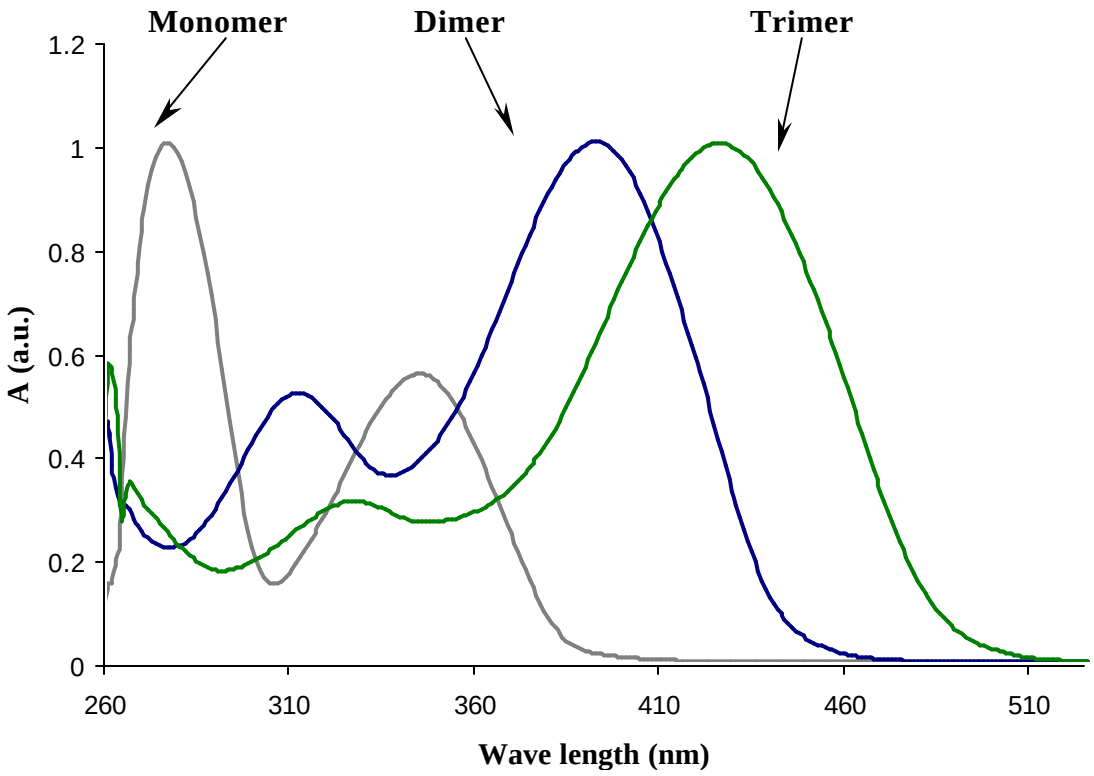

Fig. 2.5 UV/ visible absorption spectra (normalized) for monomer, dimer and trimer unit of 1,4-dimethoxy-2,5-divinylbenzene (in $CHCL_3$, 10^{-4} M).

The UV/visible absorption spectra showed (Fig. 2.5) a maxima at ~ 425 nm for the trimer, 394 nm for the dimer whereas the monomer showed ~ 276nm. The gradual red shift (monomer over dimer to trimer), indicates that oligomers formed and thus formation of an extended aromatic p- system. Photoluminescence spectroscopy results were also in line with the UV absorption data. The photoluminescence spectra showed (Fig. 2.6) a maxima ~ 482 nm for the trimer, ~ 442 nm for the dimer and ~ 392 nm for monomer. In both cases trends were same as reported by other groups.[68, 69] It is worth to note that there is only a relatively small overlap of the absorption end emisson in every oligomer.

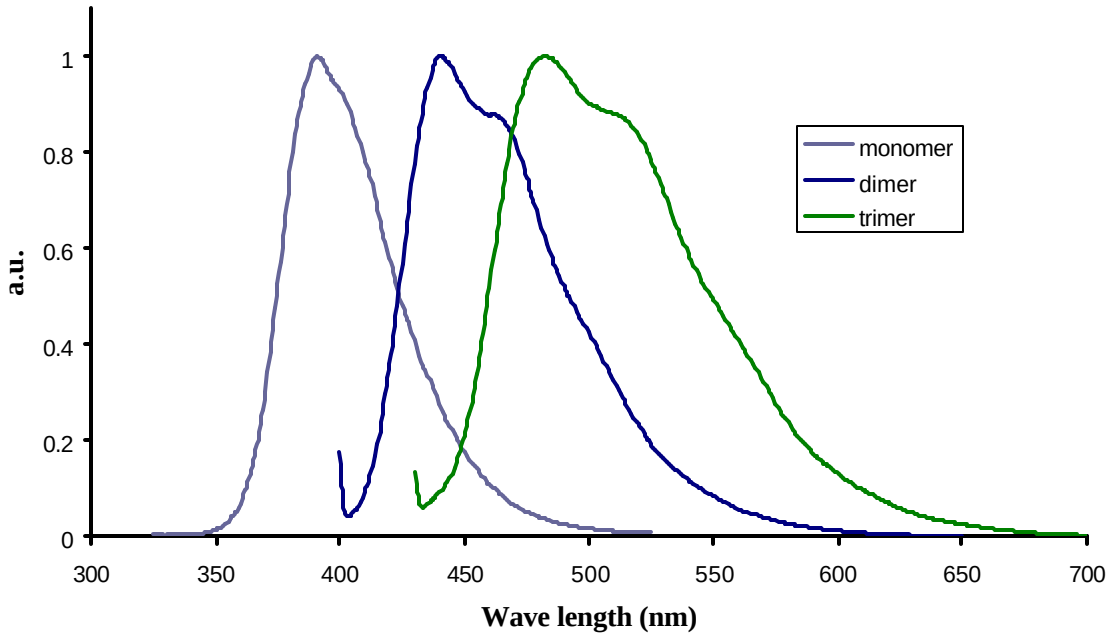

Fig. 2.6 Photoluminescence spectra (normalized) for monomeric, dimeric and trimeic unit of 1,4-dimethoxy-2,5-divinylbenzene (in $CHCL_3$, 10^{-8} M).

2.3 Conclusion and outlook

In conclusion, a novel facile synthetic method has been developed in order to synthesize dimeric and trimeric units of 1,4-dimethoxy-2,5-divinylbenzene in a targeted and optimised high-yield manner. Both NMR and FT-IR showed that products have all *trans* configuration at the vinylene. The short methoxy side chain caused pronounced differences in solublities, esspecial for oligomers larger than the trimer, thus allowing to mainly yielding trimer and dimer, which then could easily be isolated and purified. Major advantages of this approach are that the trimer or dimer can act as a "single-molecule system" with no structural defect Both dimer and trimer have the vinyl end functional groups, which can further be modified for future applications.A next step could include functionalizing the vinyl endgroups and/or performing exchange reactions at the side chains.

2.4 Experimental

General Information.

All of the experiments using air/moisture sensitive materials were carried out in a nitrogen filled Labconco protector glove box and/or by the use of dry argon filled dual manifold (inert gas/ vacuum) using standard Schlenk line techniques. All glassware was cleaned and dried for at least 16h in an oven at 120 ^{0}C prior to use.

Chemicals.

1,4-Dimethoxy benzene, methyltriphenylphosphonium bromide, ^{n}BuLi, TMEDA, and Grubbs-Hoveyda catalysts were obtained from Aldrich. Solvents e.g. tetrahydrofuran (THF), toluene, hexane, diethyl ether, DMF, dichloromethane and Na_2SO_4 were purchased from Fisher scientific. Except diethyl ether all solvents were dried and degassed by a "Pure Solv" solvent purification system (using activated alumina, copper catalyst, molecular sieves column.) by Innovative Technology Inc. before use. All other chemicals were used as received. Column chromatography was carried out on silica gel 60 (70-230 mesh) from EMD Chemicals Inc.

Instrumentation.

200 MHz ^{1}HNMR spectra were recorded in $CDCl_3$ on Varian Unity NMR instruments. $CDCl_3$ was used as an internal deuterium lock for ^{1}HNMR spectra. All of the peaks in the NMR spectra are reported in ppm.

UV-Visible absorption spectra were recorded using a Perkin Elmer Model 650 UV Spectrophotometer with 1-cm path length cells. The samples were prepared with HPLC grade chloroform ("Spectrasolv") in a sample cell.

Infrared spectra were recorded on a Tensor 27 Fourier Transformed Infrared spectrometer from Bruker optics using a Pike ATR accessory; data was processed and analyzed by OPUS software.

Photoluminescence spectra were recorded using a Horiba Jobin Yvon Fluoromax-3 spectrofluorometer with 1-cm path length cells. The samples were prepared with HPLC grade chloroform ("Spectrasolv") in a sample cell.

Synthesis of 1,4-dimethoxy-2,5-dialdehydebenzene(2)

6.76 g [49mmol] of 1,4-dimethoxy benzene was dissolved in 200 mL of dried hexane.22.1mL [148mmol] of TMEDA was added to it. The reaction mixture was cooled down to 0 ^{0}C. 59 mL [2.5 M in hexane, 148mmol] ^{n}BuLi was then drop wise added to it under continuous stirring. The reaction mixture was carried out at 35 ^{0}C for 48 h and then at room temp for 24 h. The reaction mixture was cooled down to 0 ^{0}C and 13.3mL [173mmol] anhydrous DMF was added to the reaction mixture. The reaction was continued for another 24 h at room temp. The reaction mixture was then added into a 1L HCl-ice bath. The precipitate was isolated, dissolved in dichloromethane and then washed with water for several times. The organic layer was separated and solvent was removed under vacuum. Finally the solid was washed with toluene and dried under vacuum.

^{1}H NMR (δ in ppm): 10.48 (s, 2H), 7.438 (s, 2H), 3.92 (s,6H).

Synthesis of 1,4-dimethoxy-2,5-divinylbenzene(3)

To a suspension of 26.6g (74.4mmol) methyltriphenylphosphonium bromide in 120mL of dry THF 26.8mL (2.5M in hexane) ^{n}BuLi was drop wise added. The mixture was stirred for 2h at room temp. Then 4.5g (12.4mmol) 1,4-dimethoxy-2,5-dialdehydebenzene was

slowly added to this mixture. The resulting mixture was then stirred for another 3h at room temperature and hydrolyzed with ice-cold water. The organic layer was collected and dried over Na_2SO_4. The solvent was removed and the residue was extracted with hexane. Finally the compound was purified by silica gel column chromatography, using hexane as an eluent.

^{1}H NMR (δ in ppm): 7.01(dd, 17.8Hz, 11.2Hz, 2H), 6.97 (s, 2H), 5.71(d, 17.8 Hz, 2H), 5.25 (d, 11.2 Hz, 2H), 3.82 (s, 6H).

Typical synthesis of oligomer/polymer

Synthesis of trimeric unit (4)

500 mg of 1,4-dimethoxy-2,5-divinylbenzene and 2 mol% of Grubbs-Hoveyda second generation catalyst was mixed and dissolved in 5mL of dry toluene/ dichloromethane. The resulting green color solution was heated at 50 ^{0}C for 3h. The by-product ethylene gas was removed intermittently by applying vacuum. The resulting red colored highly viscous mixture was poured in ice-cold methanol. The precipitate was filtered and dissolved in dichloromethane. Finally solvent was removed form the soluble fraction to get the 190mg of trimer (4).

^{1}H NMR (δ in ppm): 7.44 (s), 7.16(s), 7.14(s), 7.04(dd, 11.2Hz, 17.8 Hz), 7.01 (s), 5.73(d, 17.8 Hz), 5.26(11.2 Hz), 3.92(s), 3.88(s).

Synthesis of dimeric unit (5)

1.000 g of 1,4-dimethoxy-2,5-divinylbenzene and 2 mol% of Grubbs-Hoveyda second generation catalyst were dissolved in 4mL of dry toluene/ dichloromethane. The resulting green color solution was first stirred for 1h at room temperature and then heated at 48 ^{0}C overnight. The by-product ethylene gas was removed intermittently by applying

vacuum. The resulting solution was poured in ice-cold methanol after 18h. The precipitate was filtered and dissolved in dichloromethane (trimer). The methanol solution was concentrated and a yellow precipitate formed. The yellow precipitate was washed with cold methanol and then dissolved in toluene. Finally solvent was removed form the soluble fraction to get 80 mg of the above-mentioned dimer.

^{1}H NMR (δ in ppm): 7.41(s), 7.13(s), 7.04(dd, 11.2Hz, 17.6 Hz), 7.00 (s), 5.73(d, 17.6 Hz), 5.26(11.2 Hz), 3.87(s)

3 Synthesis of siloxane- and conjugated silane-PPV using Grubbs-type catalysts

3.1 Objective

The goal of this project was to design, synthesize, and characterize different silicon containing monomers and subsequently polymerize them via methathesis, particularly via ADMET. In order to synthesize the monomer a strategy was adopted in which *p*-chloro or *p*-bromo styrene were treated with magnesium metal in order to form the respective grignard reagents, followed by the addition of a dialkyl dichlorosilane as mentioned in literature by Kim et. al. [80]

ADMET polymerization has been employed for the synthesis of PPV type polymers because of the structural purity in the newly formed vinylene units in the final polymeric materials. However, typically Schrock type molybdenum or tungsten based catalyst have been reported, limiting the ease of preparation significantly due to stringent reaction conditions of these systems in regard to impurities and their functional group tolerance. In addition to this fact, silicon containing monomers do not undergo metathesis type reactions easily due to the electron-withdrawing effect of silicon and only a little information has been reported on effective homo metathesis.[76,77] By placing the silicon moiety between two styryl units, where silicon is at a "safe" distance from the terminal vinyl bonds, the adverse effect of silicon to ADMET is sufficiently reduced.

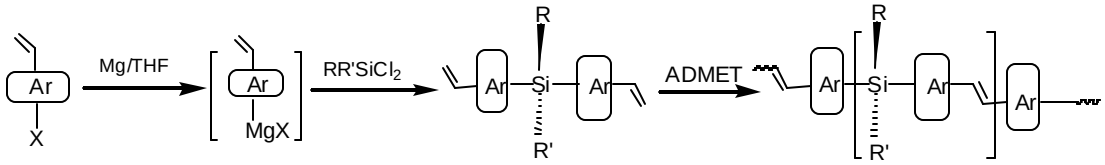

Scheme: 3.1. General synthetic plan for dialkyl SiPPV synthesis.

3.2 Results and discussions

3.2.1 Synthesis

3.2.1.1. Monomers

3.2.1.1.1 Grignard method

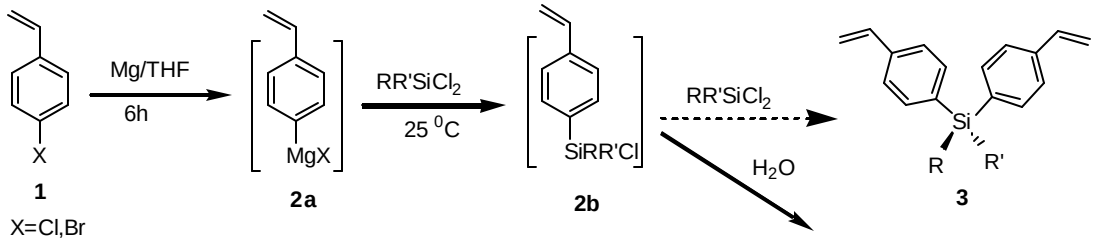

R	R'	% yield before purification	% yield of siloxane
Octyl	Octyl	55	36
Hexyl	Hexyl	54	37
Ethyl	Ethyl	52	41
Cyclohexyl	Methyl	58	51
Methyl	Methyl	65	*
		* silane and siloxane cannot be seperated	

Fig. 3.1. Synthesis of monomer 4 with different alkyl substituents

In order to make monomers [3, distyryl dialkylsilane] a simple synthetic route initially reported by Kim *et al.* was followed [fig 3.1].[80] The Grignard reagent **[2a]** was prepared in-situ from p-bromostyrene or p-chlorostyrene by reaction with flame-dried magnesium metal in anhydrous THF at an ambient temperature. The resulting Grignard reagent was then further reacted to afford the monomer **3** via a coupling reaction with dichloro dialkylsilane. During follow up processes, excess chlorosilanes were hydrolyzed by addition of 0.1M HCl. To our surprise we were not able to isolate the targeted distyryl dialkyl silanes (**3**), rather mainly distyryl dialkylsiloxanes (**4**). This is presumably due to the lower reactivity of chlorosilane with Grignard reagent after first substitution. A possible explanation is that after the first substitution of dicholorosilane an intermediate **2b** forms that is not reactive enough due to the aromatic substitution [preventing **2b** to

react further with **2a** to form **3**]. This fact was supported by detailed microstructure analysis, described in the characterization sections below. This method was used for different chloroalkyl silanes such as dioctyl-, methyl- cyclohexyl-, diethyl-, and dimethyl-dichlorosilanes. For long alkyl chain substitution, such as dioctyl, almost exclusively distyryl dialkyl siloxane was produced whereas for short chain such as methyl substitution [higher reactivity] a mixture of both silane and siloxane was observed which could not be separated.

As mentioned, we closely followed literature procedures; results from ^{1}H, ^{13}C NMR and other analysis were consistent with the published data. We only discovered the above mentioned siloxane compounds by performing careful ^{29}Si-NMR analysis after we could not explain the respective ADMET polycondensation results. These ^{29}Si-NMR spectra allowed us to distinguish between siloxane and silane. After the results from the ^{29}Si-NMR several more high-resolution NMR experiments, including quantitative ^{13}C-NMR, were carried out and yielded more evidence in this case.

3.2.1.1.2 Lithiation of diacetal of bromobenzaldehyde

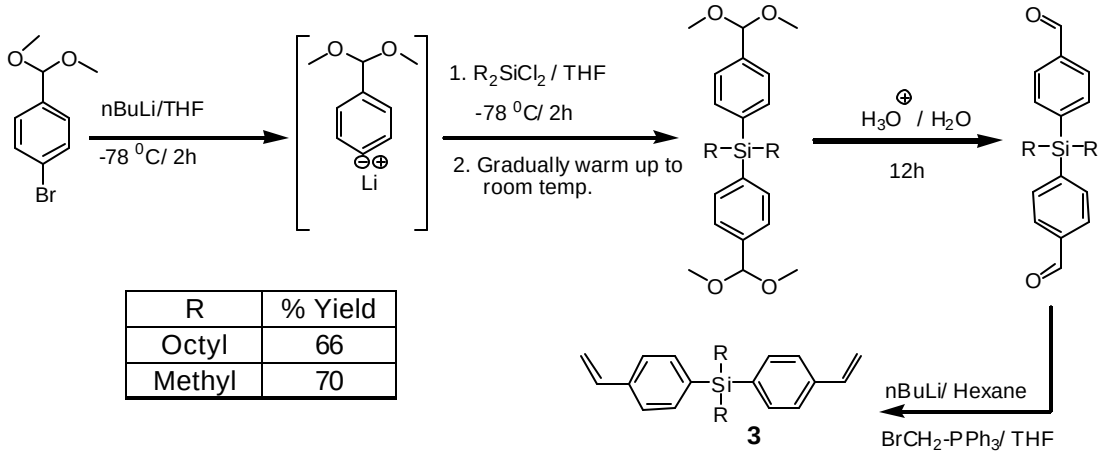

R	% Yield
Octyl	66
Methyl	70

Fig 3.2: Synthesis of monomers (**3**) with different alkyl substituents

In order to make the targeted distyryl dialkylsilane **(3),** a different strategy was adopted, where diacetal of bromobenzaldehyde was lithiated with butyl lithium at –78 ^{0}C followed by dropwise addition of dichloro dialkylsilane (fig. 3.2).[101] In order to ensure the completion of reaction, a small excess of the diacetal of bromobenzaldehyde was used. During follow up process, deacetylation was carried out by refluxing the reaction mixture in acidic medium, followed by neutralization, in order to afford dibenzaldehyde dialkylsilane. This intermediate was then further reacted to make distyryl dialkylsilane via a standard Wittig reaction. This method not only gave highly pure distyryl dialkylsilane but also resulted higher overall monomer yields.

3.2.1.1.3 Size analysis of monomers

Gel permeation chromatography was carried out (relative to polystyrene standards) for all monomers as show in fig.3.3. A narrowly distributed monomodal trace was observed for each case; indicating only one major product was obtained in each case [Traces of impurities as a high molecular weight fraction were observed for diethyl distyryl siloxane]. Dioctyl distyryl silane appeared at a slightly higher molar mass than dioctyl distyryl siloxane, which could be due to higher flexibility of siloxanes, as well as the diffence in specific interactions with the separation column material.

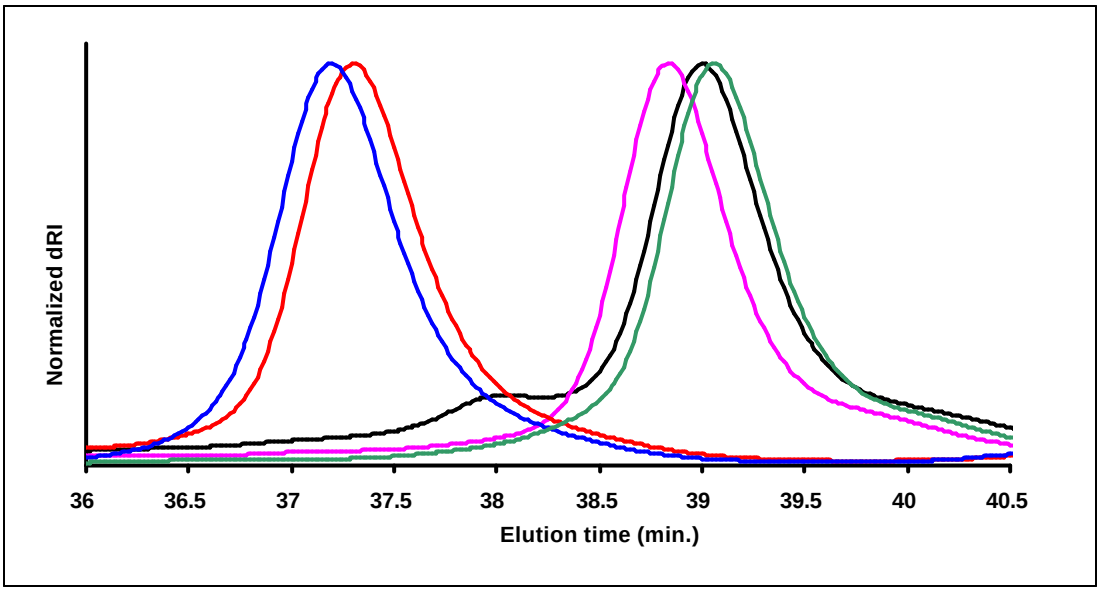

Monomer	Mn (Calculated)	Mn (Experimental)	PDI
Dimethyl distyryl silane	**264**	**288**	**1.02**
Dioctyl distyryl silane	**460**	**621**	**1.04**
Dioctyl distyryl siloxane	**731**	**629**	**1.01**
Diethyl distyryl siloxane	**366**	**301**	**1.04**
Methyl cyclohexyl distyryl siloxane	**474**	**313**	**1.02**

Fig. 3.3 Representative GPC traces of silane and siloxane monomers: dimethyl distyryl silane (—), dioctyl distyryl silane (—), dioctyl distyryl siloxane (—), diethyl distyryl siloxane (—) and methylcyclohexyl distyryl siloxane (—)

3.2.1.2 ADMET polycondensation

The ADMET polycondensation was carried out both for monomers of the types **(3)** and **(4)** with ruthenium based Grubbs- Hoveyda 2nd generation [(1,3-Bis-(2,4,6-trimethylphenyl)-2-imidazolidinylidene)dichloro(*o*-isopropoxyphenylmethylene)rutheniumin] ($C_{31}H_{38}Cl_2N_2ORu$) and Grubbs 2nd generation

type catalyst in order to understand the reaction limitations and to optimize the reaction conditions, temperature/ time of reaction/ amount of catalyst / and type of catalyst were varied.

3.2.1.2.1 Siloxanes systems

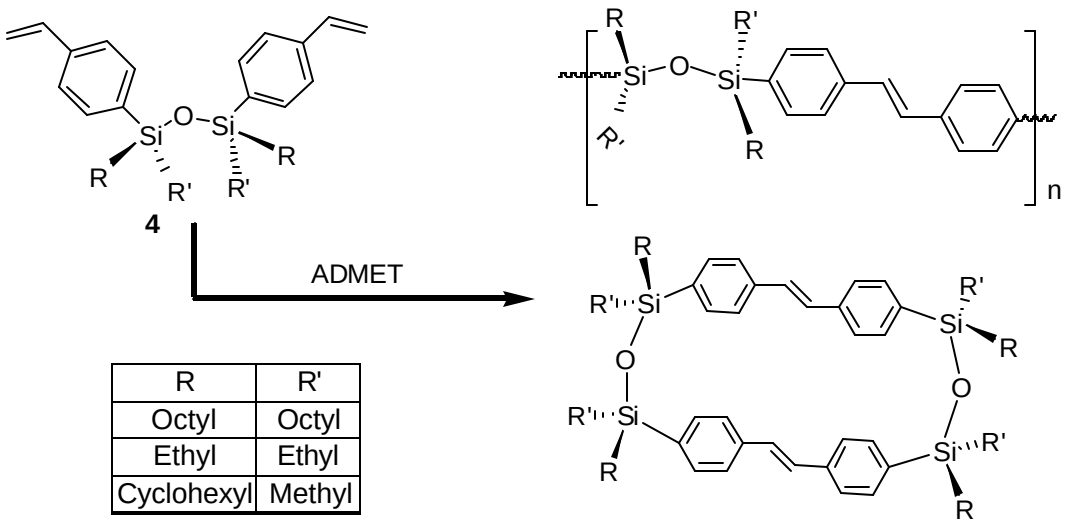

R	R'
Octyl	Octyl
Ethyl	Ethyl
Cyclohexyl	Methyl

[a] Reagents and conditions: [c] Grubbs 2nd generation catalyst or Grubbs-Hoveyda catalyst,toluene,0.1-18h. 45-50 ^{0}C

Scheme: 3.2 Synthesis of oligo/polymer (SiOPPV) from monomer (**4**)[a]

Initially, dioctyl substituted siloxane monomer **(4)** was used to synthesize polymers via ADMET. It was observed that there was almost no product formation at 35 ^{0}C (entry 1) when the ratio of catalyst: monomer remains same. The optimum reaction temperature was observed to be 48 ^{0}C with yields up to 89% of polymer (entry 4).

Table 3.1 Representative polymerization results of siloxane-based monomers (see table 3.2 for catalyst used)

Entry	Catalyst (Mol%)	Monomer (mg)	Time (h)	Temp (^{0}C)	Mass recovered (mg)	%Yield	Mn / PDI
ADMET of distyryl dioctylsiloxane monomer #							
1	10	190	18	35	163	N/A	Mainly monomer
2	10	300	18	40	267	N/A	Mainly monomer
3	4	600	18	40	570	N/A	Mainly monomer
4	2.5	360	18	48	320	89	1360/ 1.47
5	2.5^{+}	380	18	52	330	87	1400/1.25
6	2	500	60	30	425	N/A	Mainly monomer
7	1	300	18	50	260	87	1400/1.24
8	0.5	276	18	50	236	86	1410/1.25
9	2^{++}	250	18	50	220	88	Mainly monomer
#Solvent: Toluene [monomer concentration (0.13-0.32 M)]							
ADMET of distyryl methylcyclohexylsiloxane monomer#							
1(3)	1	255	18	50	232	91	940/1.02
2(4)	2.5	230	18	50	218.5	95	940/1.02
3(5)	2.5	220	12	50	202.4	92	800/1.02
4(6)	2.5	240	18	60	211	88	980/1.02
#Solvent: Toluene [monomer concentration (0.17-0.23 M)]							
ADMET of distyryl diethylsiloxane monomer#							
1(3)	2.5	230	18	50	209	91	610/1.59
2(4)	2.5	175	18	60	166	95	730/1.53
#Solvent: Toluene [monomer concentration (0.23-0.27 M)]							

The catalyst/ monomer ratio was varied from 0.5mol% (entry 8) to 10 mol% catalyst (entry 2) and it was observed that the reaction yield was highest at 2.5 mol% catalyst (entries 4,5) although 0.5mol% catalyst under comparable condition yields a considerable amount of product (entry 8). Generally most of the reactions were continued for more than 18 h but longer reaction times such as 60h (entry 6) with a low temperature did not yield a higher amount of product. It was also noticed that the Grubbs 1st generation catalyst did not work at all under these conditions, probably due to its low reactivity, whereas both Grubbs 2nd generation and Grubbs- Hoveyda 2nd generation catalysts produced similar results under the same conditions.

For other dialkyl substituted siloxane monomers (e.g methylcyclohexyl or diethyl) same results were observed as given in the table3.1. Dimethyl substituted siloxane was not subjected to polymerization because of low initial purity (a mixture of silane and siloxane) of monomer.

3.2.1.2.2 Size analysis of siloxane products

Gel permeation chromatography was carried out (relative to polystyrene standards) for all oligo/polymers as show in fig.3.4, 3.5, 3.6 and 3.7. A clear increase in molecular weight during the polymerization was observed in each case. It was found that in all siloxane based systems, regardless of polymerization conditions a narrowly distributed monomodal trace was observed; indicating only one major product was obtained [Traces of impurities as a high molecular weight fraction were observed for diethyl distyryl siloxane]

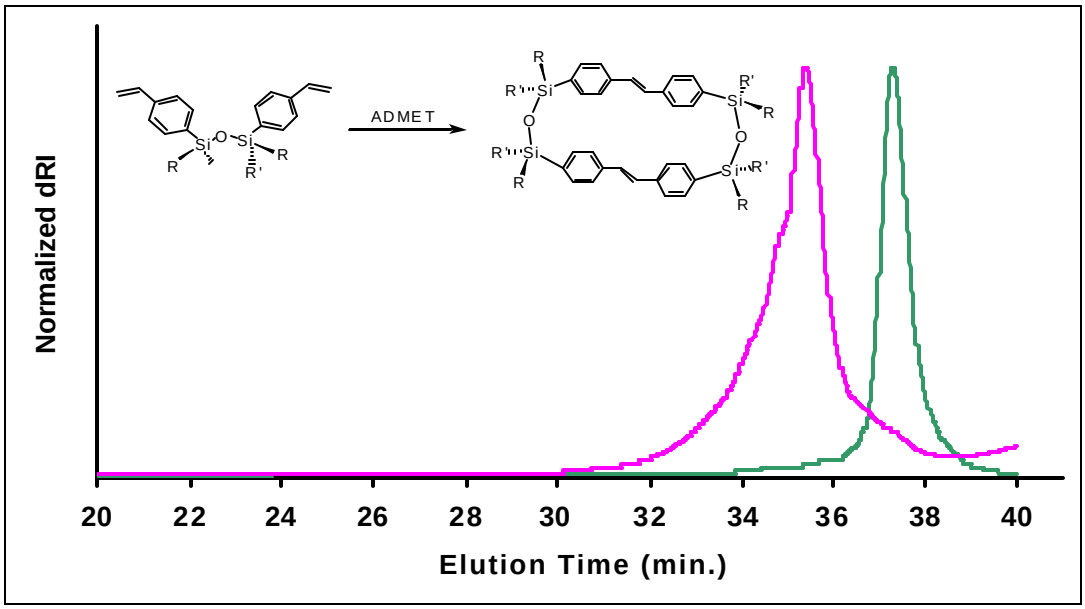

Fig. 3.4 Representative GPC traces for Dioctyl distyryl siloxane (—) and its oligo/polymer (—)

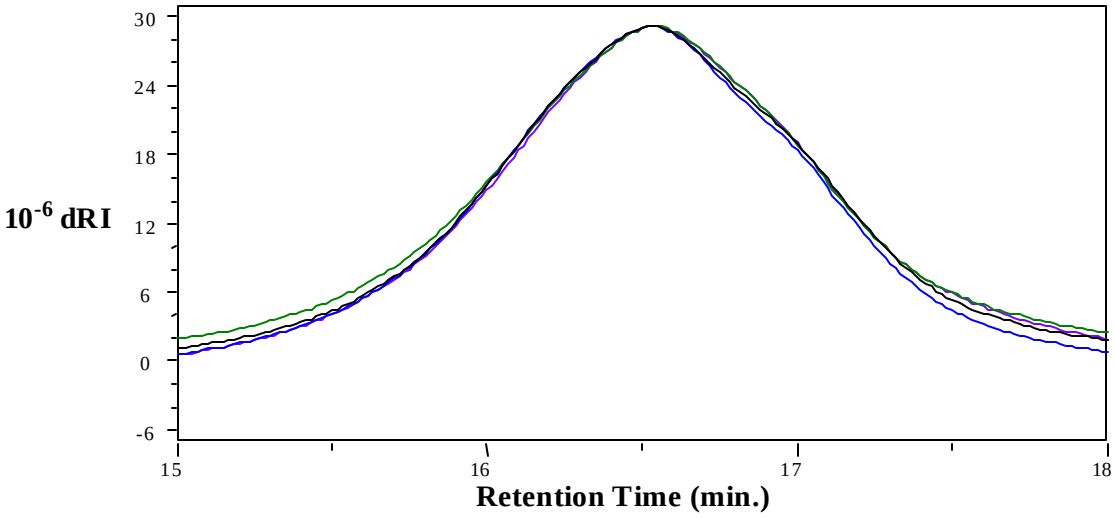

Fig. 3.5 GPC** traces for polymers (different batches) of dioctyldistyrylsilane.
Entry #5: (—) Entry #6: (—) Entry #7 : (—) Entry #8 : (—)
** A different column setup [HR1 and HR5E only] in GPC instrument was used

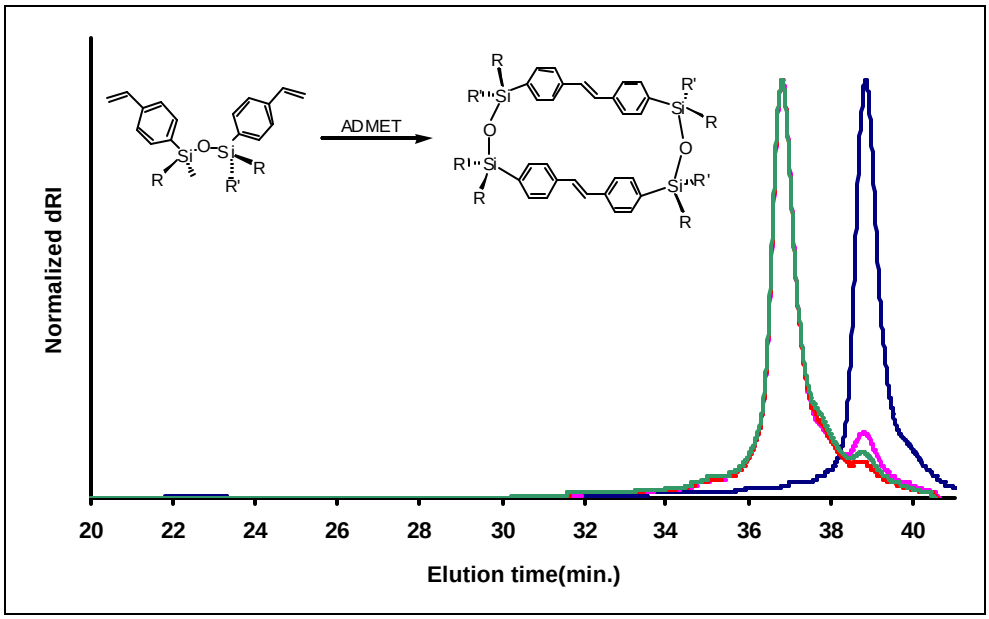

Fig. 3.6 Representative GPC traces for methylcyclohexyl distyrylsiloxane monomer: (—) and its oligo/polymer, Entry #4: (—), Entry #5 : (—),Entry #6 : (—)

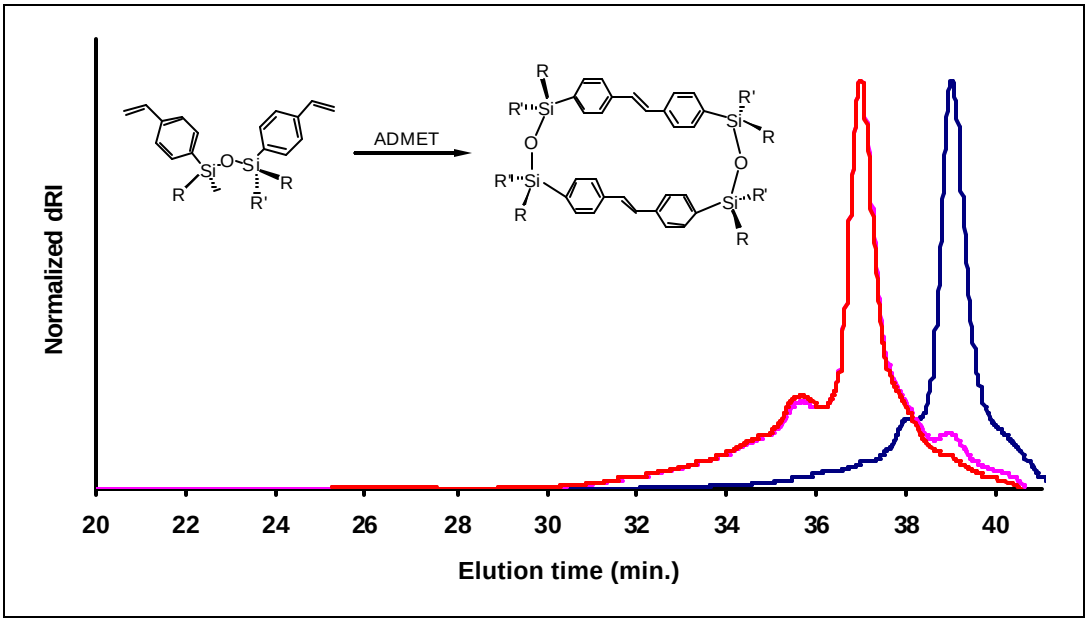

Fig. 3.7 Representative GPC traces for diethyl distyryl siloxane monomer: (—) and its oligo/polymer, Entry #3: (—), Entry #4: (—)

For all three siloxane-based systems as summarized in the polymerization table, the molar mass found indicated the formation of an exclusively dimeric unit. From the

microstructure analysis it was also observed that in the NMR there was no significant residual intensity from any vinyl groups present. This information indicates further that there was a formation of an exclusive cyclic species in all siloxane-based system. This is probably due to the presence of a highly flexible Si-O-Si linkage, which allows the back biting of terminal groups during polymerization. Several attempts to obtain absolute weights by means of mass spectrometry did not lead any conclusive results.

3.2.1.2.3 Silane systems

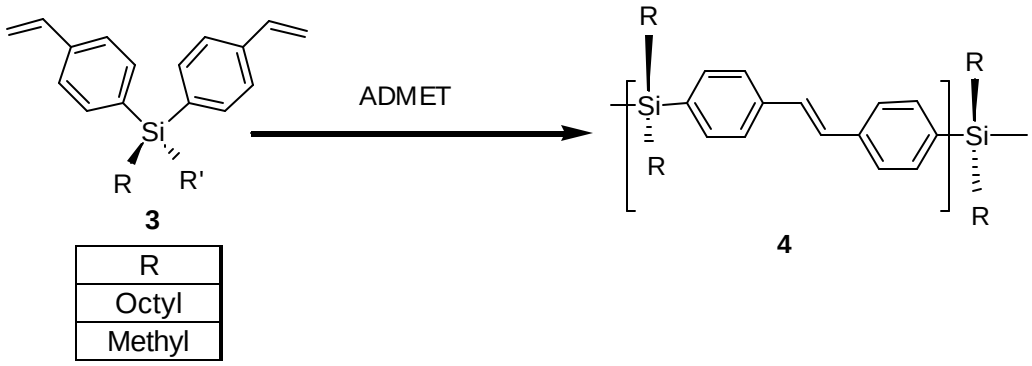

Scheme: 3.3 Synthesis of oligo/polymer (SiPPV) from monomer (**3**)

When dioctyl substituted silane monomers **(3)** were polymerized via ADMET under the same condition as the dialkyl substituted siloxane systems (**4**), the solutions became viscous after 6-8hr of reaction indicating the formation of higher molecular weight reaction products as supported by GPC. Table 3.2 summarizes representative ADMET results for monomers (**3**).

Table 3.2 Representative polymerization results of silane-based monomers

ADMET of distyryl dioctylsilane monomer#							
Entry	**Catalyst (Mol%)**	**Monomer (mg)**	**Time (h)**	**Temp (^{0}C)**	**Mass recovered (mg)**	**%Yield**	**Mn / PDI**
1	2^+	225	18	55	214	95	6050/1.73
2	2	225	10	55	203	90	3700/1.43
3	0.5	270	18	60	248	N/A	1530/1.00 [b]
4	1.5	220	18	65	196	89	5000/1.52
#Solvent: Toluene [monomer concentration (0.2-0.28 M)]							
ADMET of distyryl dimethylsilane monomer#							
1	2^+	250	18	50	225	90	2250/1.44**$**
#Solvent: Toluene [monomer concentration (0.25 M)]							

$GPC data representing only THF soluble fraction

+ **Catalyst: Grubbs 2nd generation catalyst.**

++ Catalyst: Grubbs 1st generation catalyst.

***In all other cases catalyst: Grubbs-Hoveyda 2nd generation catalyst**

[a] Reagents and conditions: [c] Grubbs 2nd generation catalyst or Grubbs-Hoveyda catalyst,toluene,0.1-18h. 45-50 ^{0}C. [b] trace amount of one oligomer (with mainly monomer),see Fig.3.8 (Entry #3)

3.2.1.2.4 Size analysis of silane products

For silane-based systems, very different results compared to the siloxane systems were observed as shown in fig.3.8 and 3.9. Varying molecular weights were observed for the ADMET products of dioctyl distyrylsilanes 3, depending on the reaction condition. At low catalyst concentration (entry-3) mainly monomer was observed. In all other cases Mn~4000-6000 g/mol could be observed. When reactions were stopped after only 2-3 h, mixtures of different oligomers were observed rather than higher molecular weight condensates, where as after longer reactions a relative smooth GPC traces was observed

with significantly higher molecular weights. When dimethyl

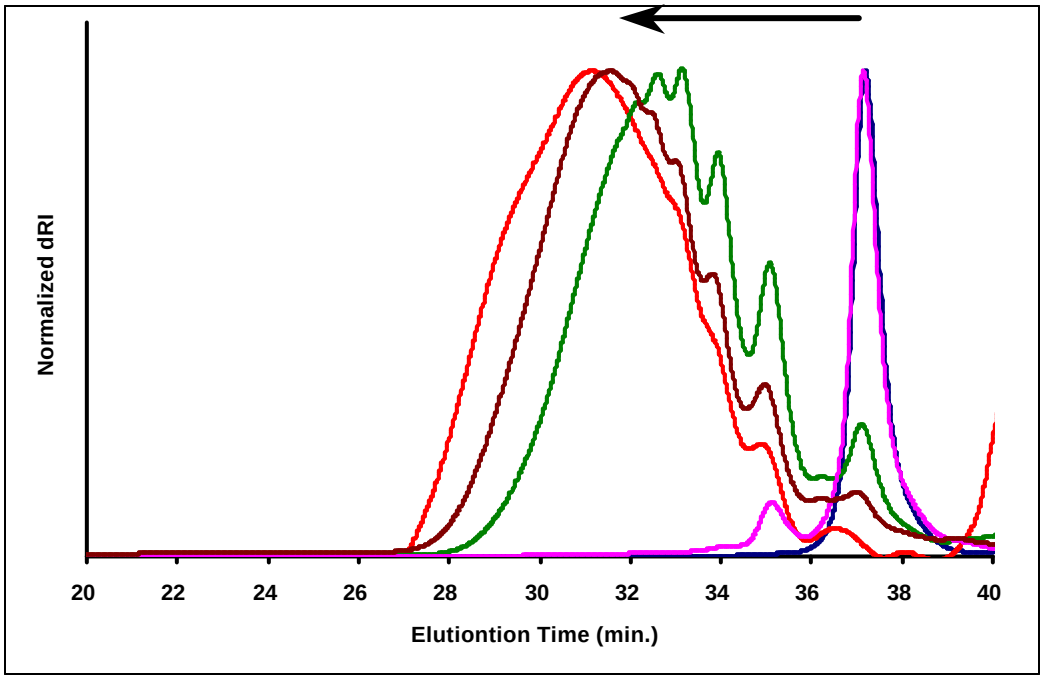

Fig. 3.8 GPC traces for monomer and oligo/polymeric unit of dioctyl distyryl silane monomer: (—) Entry #1: (—), Entry #2: (—), Entry #3: (—), Entry #4: (—)

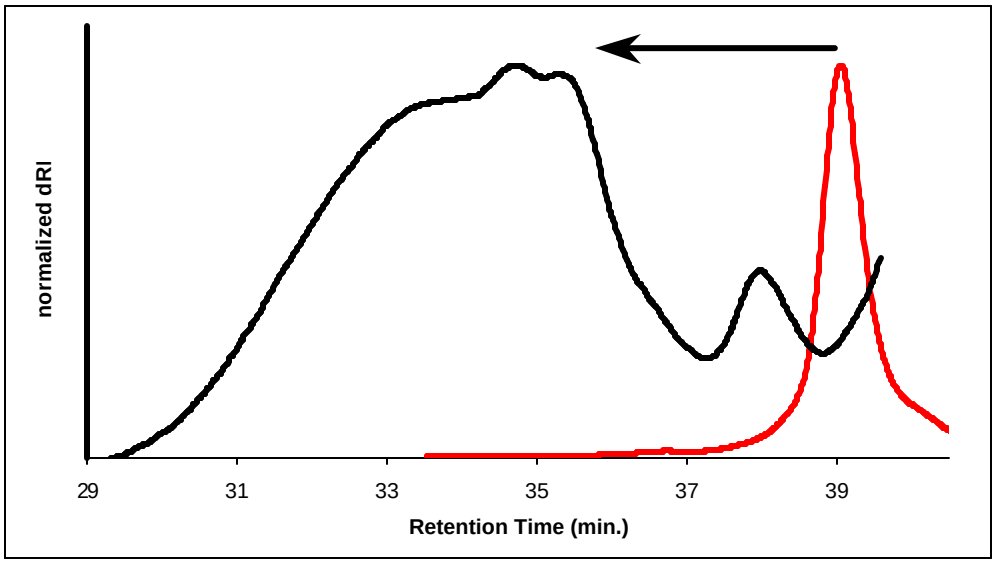

Fig. 3.9 Representative GPC traces for dimethyl distyryl silane monomer: (—) and its oligo/polymer (—) [Concentration of polymer in GPC was not measured, as the polymer has poor solubility in THF]

distyryl silane was polymerized, precipitation could be observed within a short reaction time of ~1h and the polymer displayed low solubility in common solvents due to the short alkyl chains on the silicon moiety.

3.2.2 Characterizations of materials

3.2.2.1 Monomers

The characterizations of both monomers were performed in regard to microstructure (NMR and FTIR) and size (GPC).

3.2.2.1.1 Microstructure analysis

3.2.2.1.1.1 NMR (^{1}H, ^{13}C, ^{29}Si)

The microstructures of all monomers were characterized by ^{1}H, ^{13}C and ^{29}Si NMR, together with the assignments and chemical shifts, are shown in the fig. 3.10 and table 3.3. Both siloxane and silane based systems are discussed together.

^{1}H-NMR resonances of -CH=C$\underline{H}_2$ the terminal vinyl group exhibit two doublets (1, 2 in fig. 3.10) with different coupling constants at ~ 5.8 and ~ 5.2 ppm respectively, corresponding to two vicinal protons (exo: J= ~17Hz, endo: J= ~ 11Hz), trans and cis respectively. The -C$\underline{H}$=CH_2 resonance was observed at around ~6.7 Hz. It is to be noted that almost the same chemical shifts (as mentioned above) were observed for all monomers, indicating “no observable effect” from the heteroatom component or its’ substitution.

The aromatic proton resonances (4 and 5 in fig.3.10) showed chemical shifts ranging from ~7.3-7.6 ppm, depending on the nature of the heteroatomic moiety. Aromatic

resonances in the siloxane-based monomers were shifted slightly down field compared to homologous silane-based monomers, probably due to the presence of the Si-O-Si linkage. In two comparable systems such as dioctyl substituted silane and siloxane monomers, the relative ratio of the integrated signals from the vinyl functions vs. the alkyl chains of siloxane system is twice as high as in the silane system. Proton resonance at ~0.57 ppm in the siloxane system indicates the presence of a methylene proton of long alklyl chain linked with connected to the Si in a -Si-O-, which is absent in silane system.

For the diethyl substituted siloxane monomer, a triplet proton resonance at 0.83ppm was observed for the terminal -C$\underline{H}_3$ of alkyl chain. The methylene proton resonance expected as a quartet, is found as a multiplet at 0.9-0.96 ppm due to Si-C-H coupling. For the methylcyclohexyl substituted siloxane monomer, a sharp singlet proton resonance at 0.34 ppm was observed for –Si-C$\underline{H}_3$. Two sets of methylene proton resonances (near to Si and far from Si), were observed at ~1.12 and ~1.7 ppm respectively as multiplets. Proton resonance for the Si-C-$\underline{H}$ from the cyclohexane ring was observed at 0.89 ppm. The relative integral ratios of all different protons were matched in accordance to the calculated values for each monomer (for detailed integral ratio of each monomer see experimental sections)

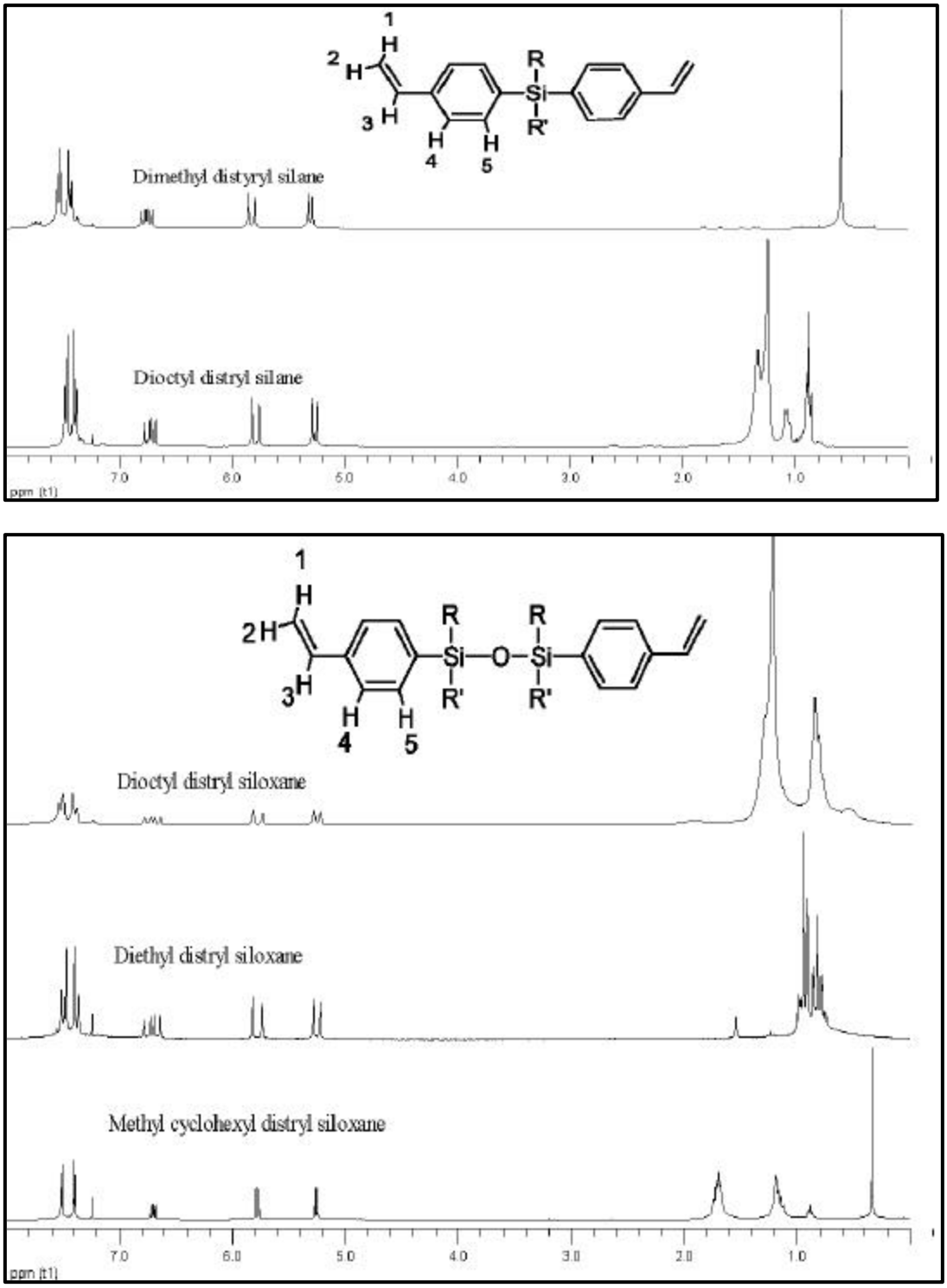

Fig. 3.10 Representative ^{1}H NMR of dialkyl distyryl siloxane/silanes

Table 3.3 ^{1}H NMR assignments of dialkyl distyryl siloxane/silanes

	R	R'	1	2	3	4-5	Alkyl chain (R)
Silane-monomer							
Distyryl dimethyl silane	CH_3	CH_3	5.82	5.30	6.75	7.6-7.44	0.6
Distyryl dioctyl silane	C_8H_{17}	C_8H_{17}	5.79	5.26	6.72	7.5-7.4	1.6-0.85
Siloxane-monomer							
Distyryl dioctyl siloxane	C_8H_{17}	C_8H_{17}	5.75	5.25	6.7	7.6-7.3	1.5-0.5
Distyryl diethyl siloxane	C_2H_5	C_2H_5	5.81	5.29	6.74	7.6-7.4	1.01-0.8
Distyryl methyl cyclohexyl siloxane	C_6H_{11}	CH_3	5.78	5.26	6.71	7.5-7.4	1.8-0.84, 0.34

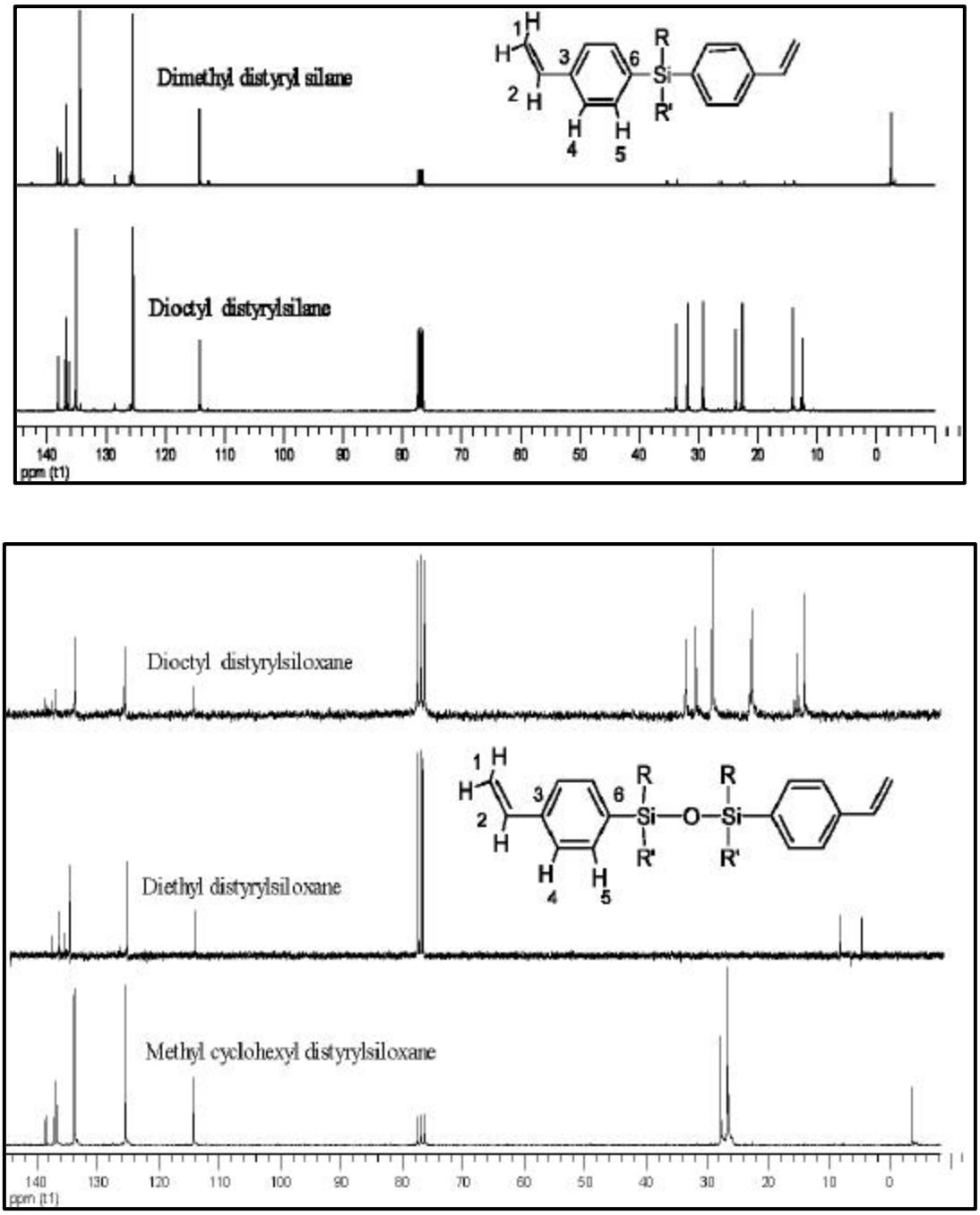

Fig. 3.11 Representative ^{13}C-NMR of distyryl dialkyl silane/siloxanes**.**

Table 3.4 ^{13}C-NMR (with assignments) of distyryl dialkyl silane/siloxanes

Silane-monomer								
	R	R'	1	2	3	4	5	6
Distyryl dimethyl silane	CH_3	CH_3	114.3	137.7	138.2	125.6	134.4	136.7
Distyryl dioctyl silane	C_8H_{17}	C_8H_{17}	114.2	136.9	138.1	125.5	135.1	136.4
	R	R'	Alkyl chain (R)					
Distyryl dimethyl silane	CH_3	CH_3	-2.4					
Distyryl dioctyl silane	C_8H_{17}	C_8H_{17}	33.7, 31.9, 29.2, 29.1, 23.7, 22.7, 14.1, 12.6					
Siloxane-monomer								
	R	R'	1	2	3	4	5	6
Distyryl dioctyl siloxane	C_8H_{17}	C_8H_{17}	114.4	137.4	138.5	125.6	133.7	136.8
Distyryl diethyl siloxane	C_2H_5	C_2H_5	114.5	137.1	138.4	125.8	135.4	136.1
Distyryl methyl cyclohexyl siloxane	C_6H_{11}	CH_3	114.3	137.1	138.5	125.5	133.8	136.8
	R	R'	Alkyl chain (R)					
Distyryl dioctyl siloxane	C_8H_{17}	C_8H_{17}	33.5, 31.9, 29.3, 29.2, 22.9, 22.7, 15.2, 14.1					
Distyryl diethyl siloxane	C_2H_5	C_2H_5	7.7,4.1					
Distyryl methyl cyclohexyl siloxane	C_6H_{11}	CH_3	27.7,26.7,26.6, -3.7					

^{13}C-NMR spectra for all siloxane and silane based monomers are shown in fig.3.11 and table.3.4 together with the respective assignments and exact chemical shifts. The carbon resonances associated with the terminal vinyl group –$\underline{C}$H=$\underline{C}$H$_2$ (1 and 2 in fig.3.11) were

observed at around 114.5 and 137.1 ppm and are found to be characteristic signals for all monomers. The aromatic carbon resonances (3,4,5,6 in fig.3.11) were observed at around 138.5, 125.5, 134 and 136.5 ppm resepctively with no major differences between silane and siloxane based monomers. Aliphatic carbons from the side chains of the heteroatom for different monomers were observed at around ~ 33 to –3.7 ppm depending on the chain length and structure. Carbon resonances for -Si-$\underline{C}H_3$ were observed at a negative chemical shift, whereas all other carbon resonance appeared as positive chemical shifts, relative to tetramethyl-silane (TMS).

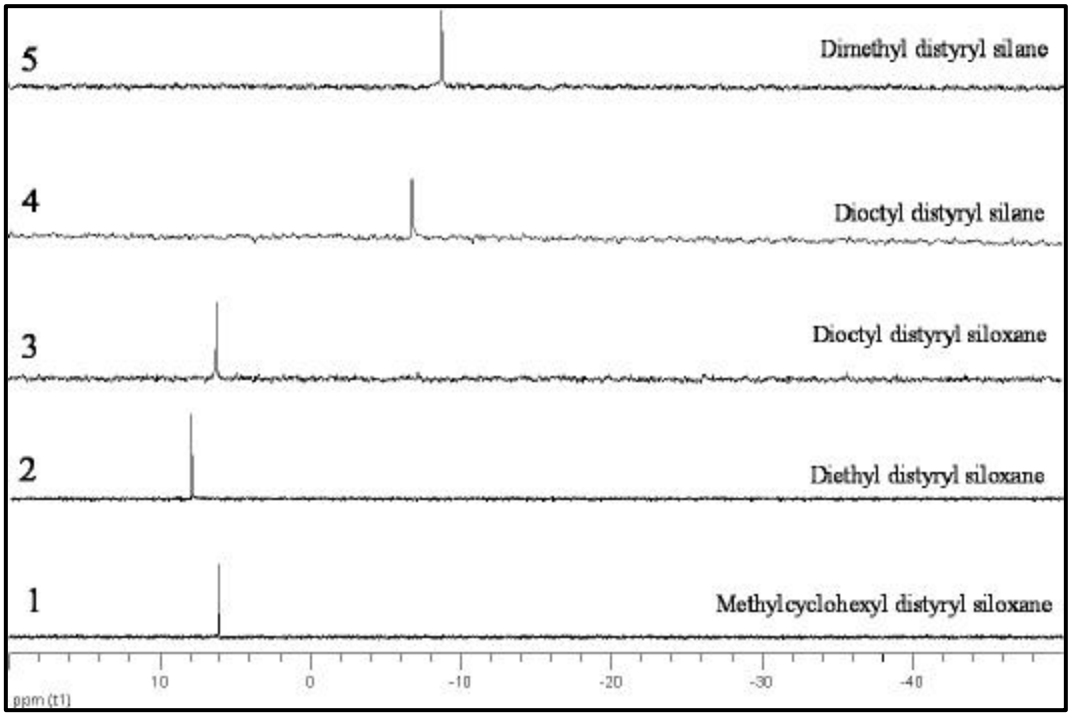

	Siloxane-monomers			**Silane-monomers**	
Spectrum #	**1**	**2**	**3**	**4**	**5**
Chemical shift (ppm)	**6.05**	**8.04**	**6.12**	**-6.84**	**-8.75**

Fig. 3.12 Representative ^{29}Si-NMR (with assignments) of distyryl dialkylsiloxane/ silanes.

^{29}Si-NMR unambiguously elucidates the difference between silane and siloxane system clearly. In fig.3.12, for all 3 siloxane systems the ^{29}Si resonance appears at ~8-9 ppm whereas in the silane cases, the ^{29}Si resonances were observed at ~ -6.8 to –8.7 ppm. A literature search for small molecule model compounds confirmed this analysis: The ^{29}Si resonances for $(CH_3)_2Si(C_6H_5)_2$ and $[(C_2H_5)_3Si]_2O$ are reported at –9.4 to –7.5 ppm and 9.11 ppm respectively.[102]

3.2.2.1.1.2 FTIR

FTIR spectroscopy provides (Fig 3.13(a) and (b)) further insight into of these monomers. C-H vibrations from aromatic, [stretching (~ 3010 cm^{-1}), in plane bending ((~ 1110 cm^{-1}) and out of plane bending (~ 827 and ~735 cm^{-1})] as well as aliphatic [asymmetrical (~ 2925 cm^{-1}), doublet asymmetrical and symmetrical of CH_3 (~ 2872 cm^{-1}), symmetrical (~ 2850 cm^{-1}), bending (~ 1465 cm^{-1}), CH_3 deformation (~1390 cm^{-1}), twisting (~1350-1150 cm^{-1}) and rocking (~ 690 cm^{-1})] were observed and systematically assigned.

Si-CH_2 [rocking (~1250 cm^{-1}), wagging (~1207 cm^{-1})], Si-phenyl [in plane bending (1117 cm^{-1}), stretching (~1105 cm^{-1})] signals were observed for all monomers. An additional broad absorption from Si-O-Si [linear stretching (~ 1075-1025 cm^{-1})] was also observed in the case of siloxane-based monomers [fig.3.13 (a)]. Terminal vinyl bonds show a sharp absorption from C=C stretching with conjugation ~1630 cm^{-1} as well as the out of plane deformation signals at ~ 987 and 906 cm^{-1} [fig. 3.13 (b) red marks].

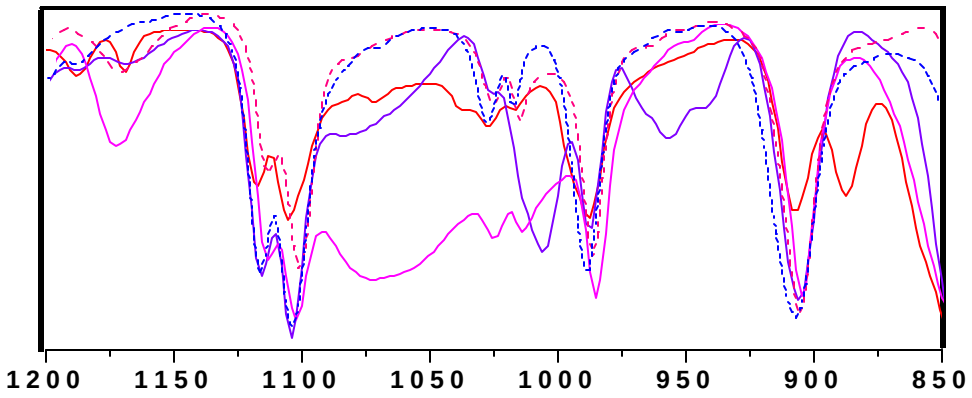

Fig. 3.13 (a) ATR-FTIR spectra (1200-650 cm^{-1}) of 1) Mecyclohexyl distyryl siloxane (—), 2) Diethyl distyryl siloxane (—), 3) Dioctyl distyryl siloxane, (—) 4) Dioctyl distyryl silane (---), 5) Dimethyl distyryl silane (---)

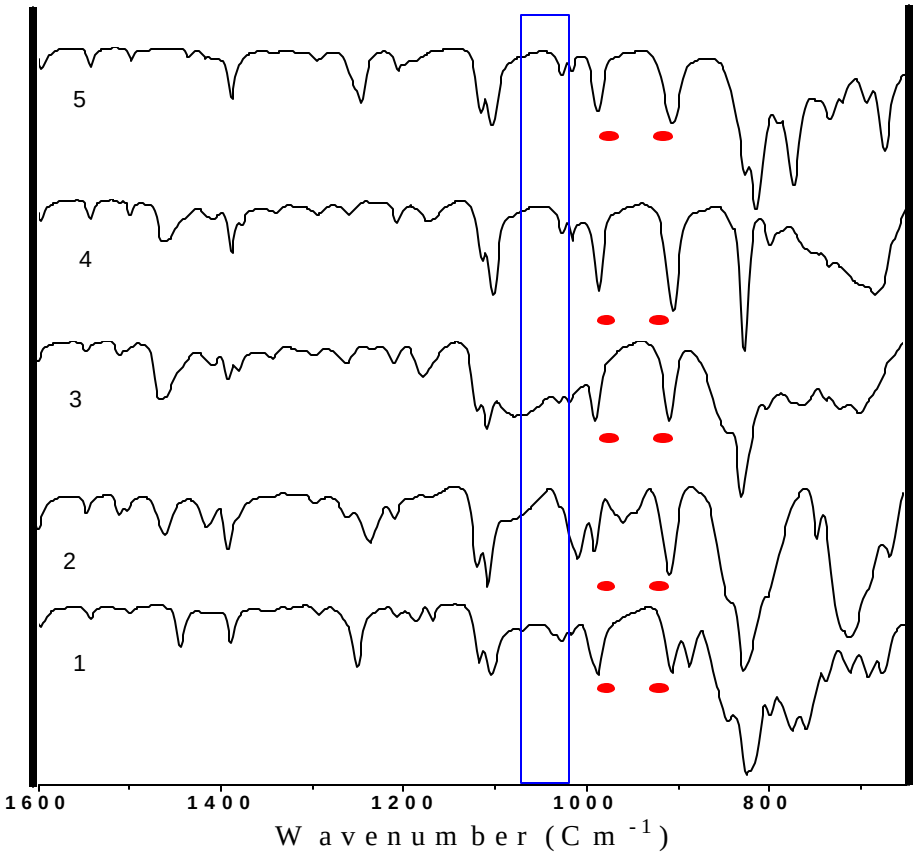

Fig. 3.13 (b) ATR-FTIR spectra (1600-650 cm^{-1}) of 1) Mecyclohexyl distyryl siloxane, 2) Diethyl distyryl siloxane, 3) Dioctyl distyryl siloxane, 4) Dioctyl distyryl silane, 5) Dimethyl distyryl silane

3.2.2.2 ADMET polycondensates

3.2.2.2.1 Microstructure Analysis

The characterizations of all oligomeric and polymeric ADMET condensates by means of NMR, ATR-FTIR, UV/vis, photoluminescence, and TGA (including a comparison with the corresponding monomers) were performed and are presented below.

3.2.2.2.1.1 NMR (^{1}H, ^{13}C, ^{29}Si)

The ^{1}H-NMR spectra for both silane and siloxane based oligo/polymers are shown in figures 3.14-16, together with the assignments (table 3.5) and chemical shifts.

The formation of product was marked by the appearance of resonance at around 7.1 ppm, indicating the formation of internal vinylene bonds (3). As the resonance of proton 3 appears, the resonance from the terminal vinyl functional group at ~ 5.2, 5.8 and 6.7 ppm, and characteristics of the monomers, gradually decreases over the course of a reaction. This resonance at 7.1 ppm is very close to the value for the internal vinylene signals for *trans*-stilbene.[103] Thus during polymerization, a new conjugated segment is formed which is structurally a *trans* stilbene unit. In the condensate, individual stilbene units are connected to each other by the heteroatomic linkage. No signal was observed at ~ 6.5 ppm (internal vinylene signals for *cis*-stilbene) indicating the absence of *cis* vinylene bonds. Resonances from the aliphatic protons of the silane/siloxane moiety were marked by broadening of peaks, relative to the respective monomers. In the oligo/polymers, residual signal intensity at ~5.2 and 5.7 ppm indicated the presence of unreacted monomer .

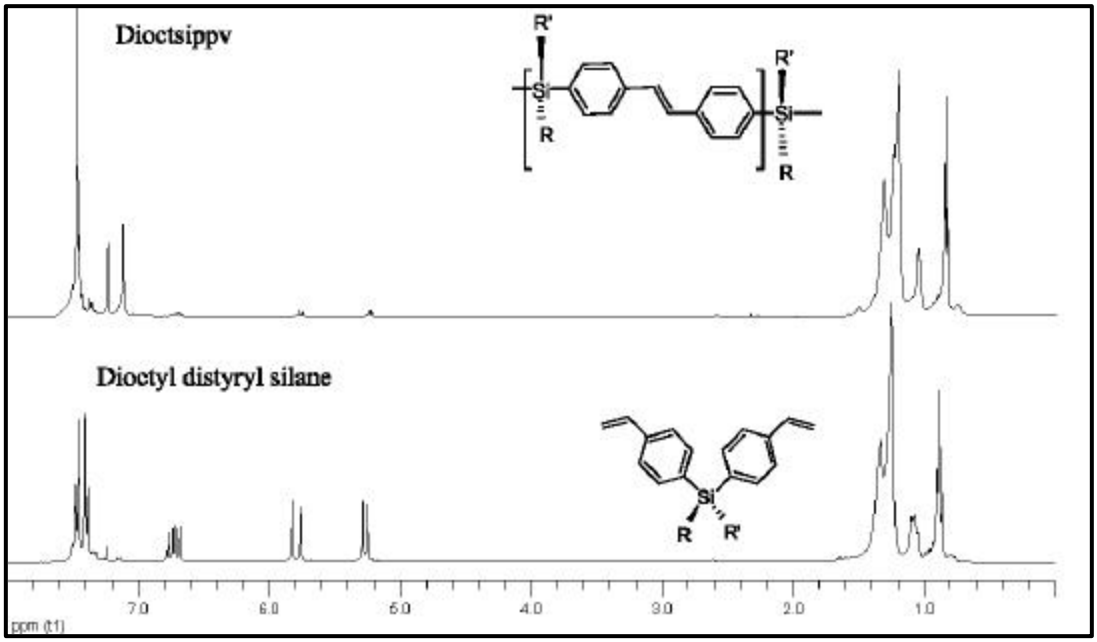

Fig. 3.14 Representative ^{1}H-NMR comparison between of monomer and oligo/polymer of dioctyl distyrylsilane

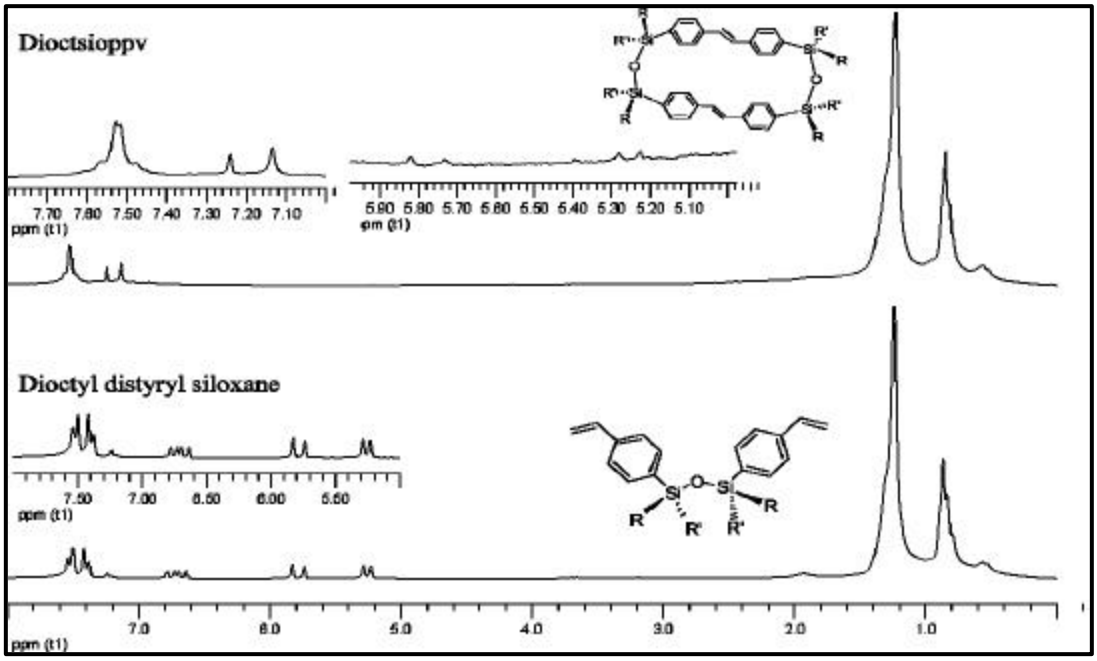

Fig. 3.15 Representative ^{1}H-NMR comparison between of monomer and oligo/polymer of dioctyl distyryl siloxane

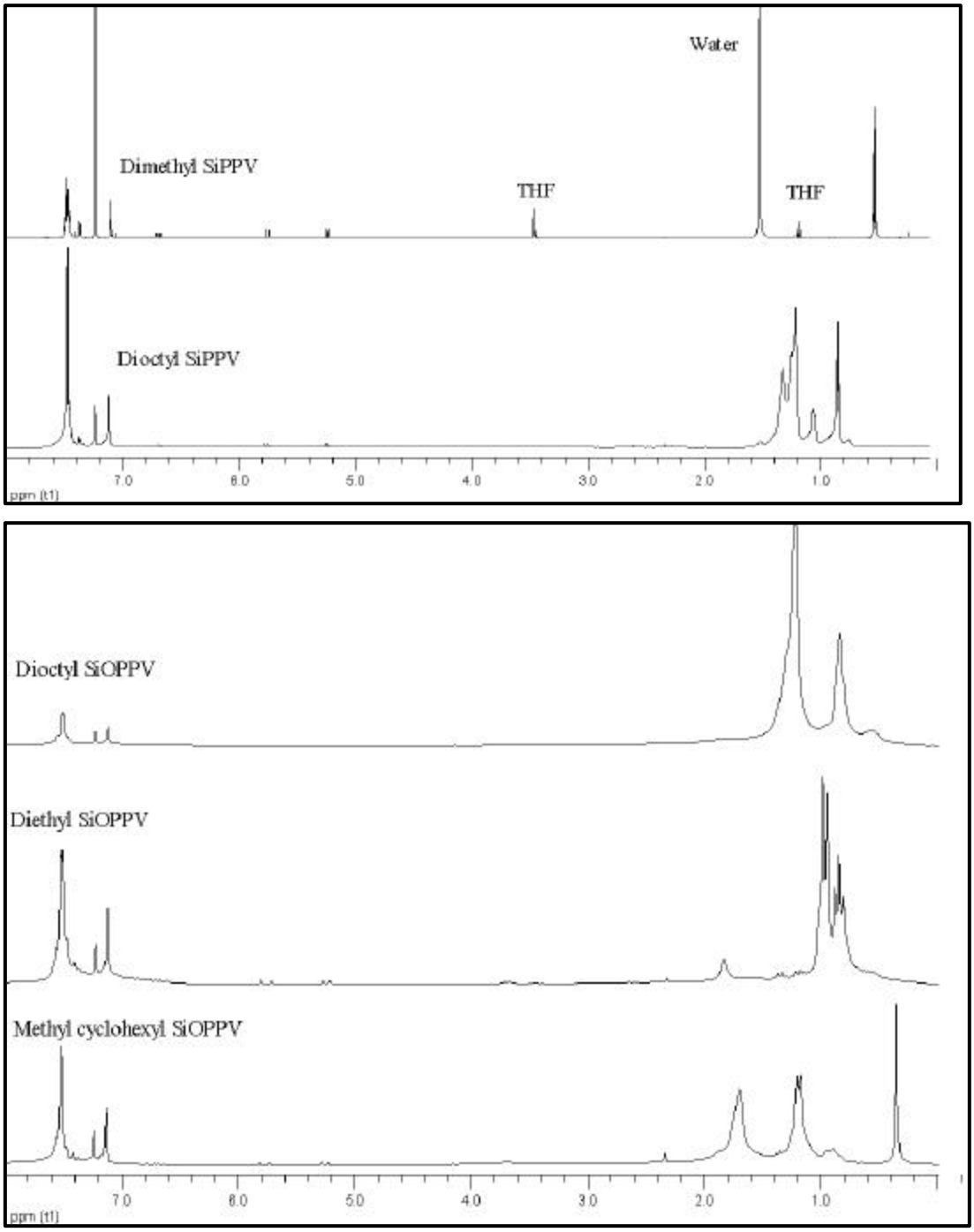

Fig. 3.16 ^{1}H NMR of dialkyl distyryl siloxane/silane oligo/polymers

However, in the case of dimethyl SiPPV, instead of monomer, some short oligomeric chain was found. As a result, additional Si-CH_3 and vinyl bond resonances were observed in the NMR (also supported by GPC traces).

Table 3.5 ^{1}H NMR assignments of dialkyl distyryl siloxane/silaneoligo/polymers

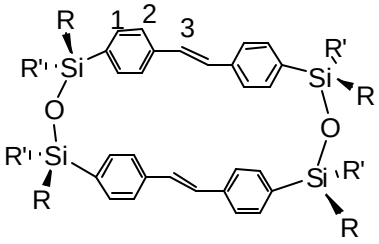

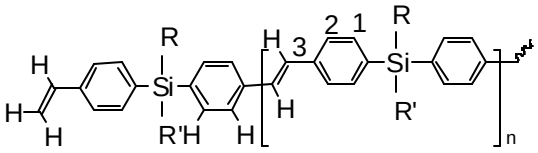

R,R'	Aromatic (1,2)	Trans vinylene bond (3)	Alkyl chain	
-CH_3	7.49-7.46 ppm	7.11ppm	0.54ppm	Silane
-C_8H_{17}	7.52-7.4ppm	7.13ppm	1.45-0.8 ppm	
-C_8H_{17}	7.7-7.4 ppm	7.14 ppm	1.6-0.5 ppm	Siloxane
-C_2H_5	7.65-7.48 ppm	7.15 ppm	1.1-0.85 ppm	
-CH_3 	7.65-7.45 ppm	7.14 ppm	2-1.5, 1.4-1.1, 0.9, 0.37 ppm	

Signals for the aliphatic protons in the silicon moiety were found not to be changed in comparison to monomers except for a broadening of peaks in the condensates. The resonances for the aromatic protons howeber shifted slightly downfield (from ~7.3-7.5 to ~7.5-7.6 ppm) as expected due to the formation of the conjugated stilbene segment.

It is important to note that for the silane-based ADMET condensates, resonances from vinyl bonds could easily easily be observed even for Mn ~6000 g/mol, whereas for siloxane-based products, almost no terminal vinyl bonds (traces from unreacted

monomer) were observed even for Mn ~1400 g/mol. This result indicates there is a probable formation of an exclusive "cyclic dimeric ring" in the case of the siloxane-based systems. This type of backbiting of vinyl bond is possible for the siloxane-based system due to the highly flexible Si-O-Si linkage, which is absent in the case of silane-based system.[13]C NMR data are shown in fig. 3.17, 3.18 and 3.19 with assignments (table 3.6)

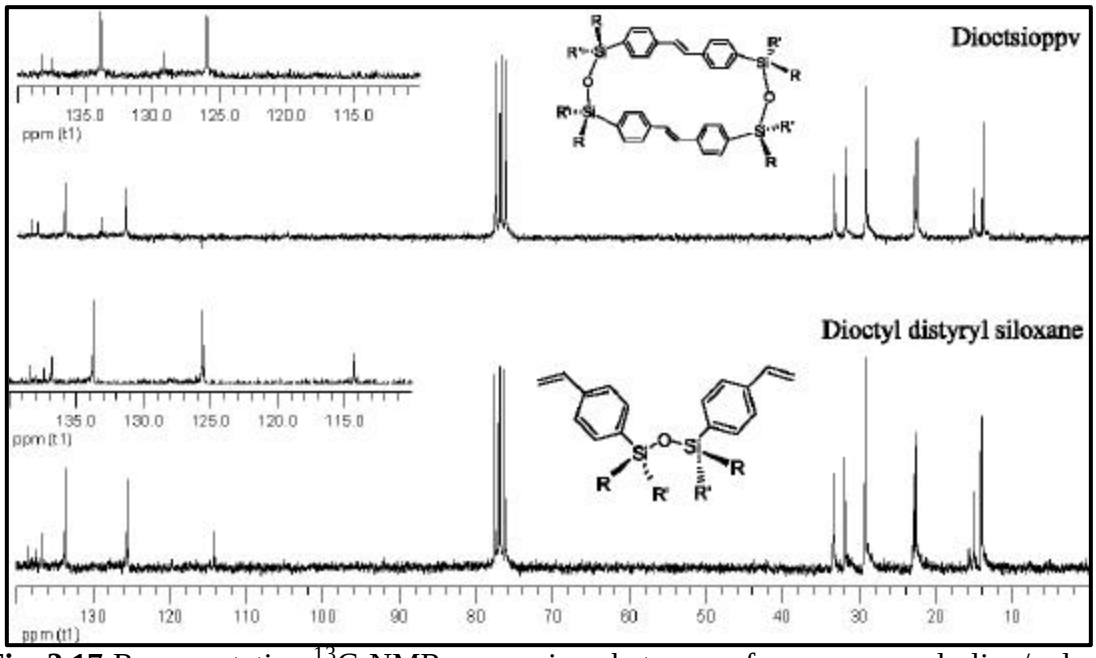

Fig. 3.17 Representative [13]C-NMR comparison between of monomer and oligo/polymer of dioctyl distyryl siloxane

and chemical shifts. These results are in line with [1]H-NMR results. The formation of the internal vinylene bond 5 was observed as a resonance appearing at around 128.8 ppm. As the resonance of 5 appears the resonance from the terminal vinyl functional group, characteristic of the monomers at ~136.8 and 114.5 ppm, gradually decreases over the course of reaction. This resonance (at around 129 ppm) is very close to the value for the internal vinylene signals for *trans*-stilbene. No major changes for aromatic (~139-126 ppm) and aliphatic carbons at the silicon moieties (~ 33-14 ppm) could be observed in in

any case from monomer to oligo/polymer). Some additional signals from the terminal groups and/or unreacted monomers were also observed for the silane systems (in line with ^{1}H-NMR results).

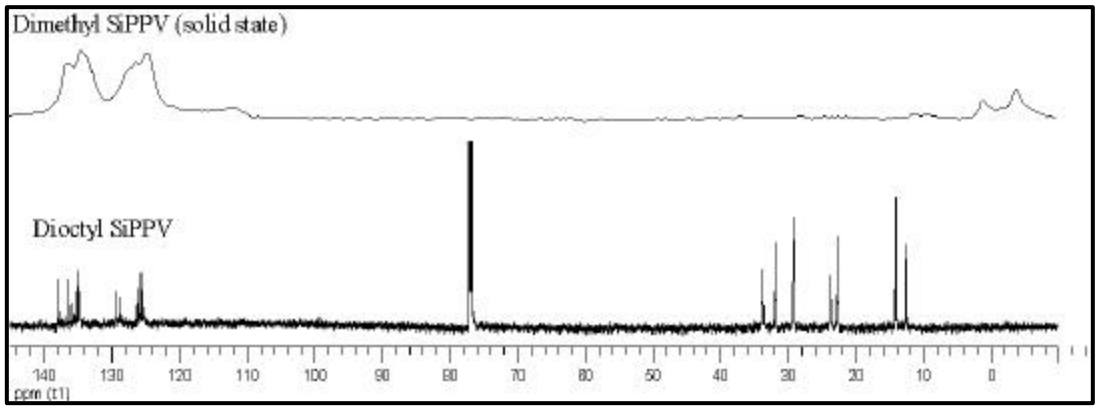

Fig. 3.18 Representative ^{13}C-NMR comparison between of monomer and oligo/polymer of dioctyl distyryl silane.

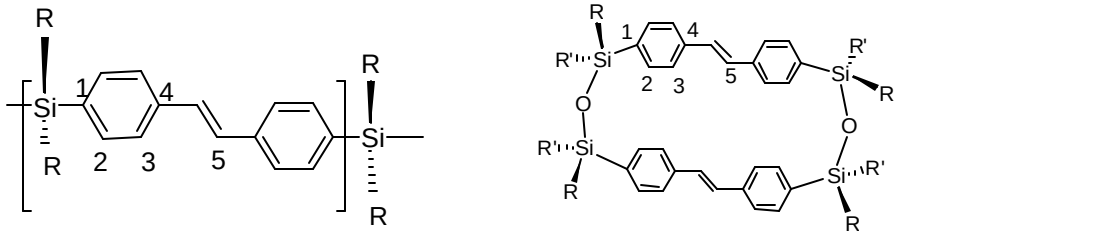

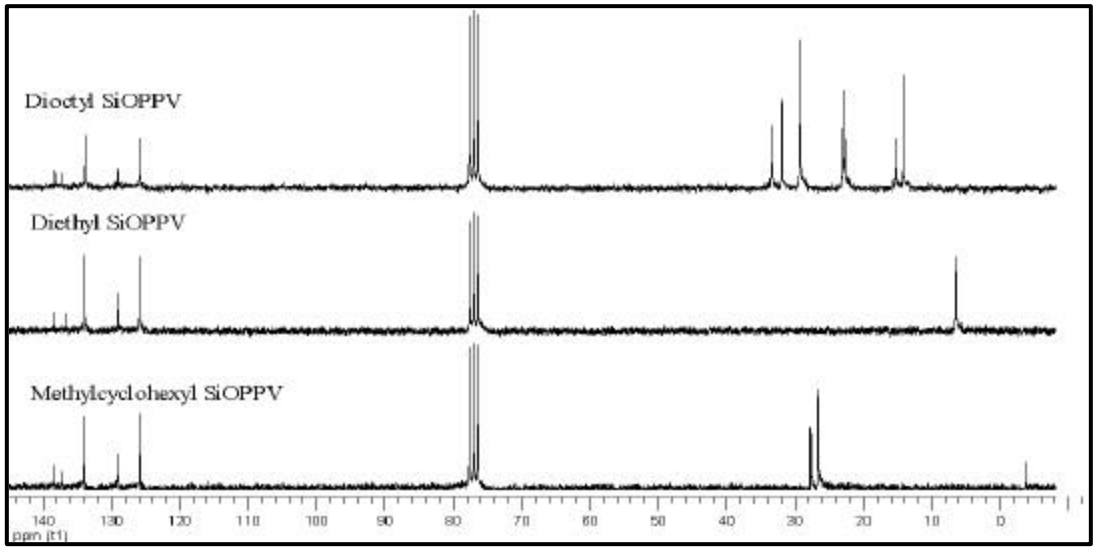

Fig. 3.19 ^{13}C NMR (assignments) of dialkyl distyryl siloxane/silane oligo/polymer

Table 3.6 ^{13}C NMR assignments of dialkyl distyryl siloxane/silane oligo/polymers
*Solid-state NMR data overlapped

Monomer	R	R'	1	2	3	4	5
DiOctSiPPV	C_8H_{17}	C_8H_{17}	136.3	135.2	125.8	137.9	129.0
DiMeSiPPV*	CH_3	CH_3	136.5	134.4	124.8	-	-

Monomer	R	R'	Alkyl chain (R)
DiOctSiPPV	C_8H_{17}	C_8H_{17}	33.7, 31.9, 29.2, 29.1, 23.7, 22.7, 14.1, 12.5
DiMeSiPPV*	CH_3	CH_3	-3.9

Monomer	R	R'	1	2	3	4	5
DiOctSiOPPV	C_8H_{17}	C_8H_{17}	137.4	133.8	125.9	138.2	129.1
DiEtSiOPPV	C_2H_5	C_2H_5	136.8	133.9	125.9	138.3	129.1
Mecylohexyl SiOPPV	C_6H_{11}	CH_3	137.1	134	125.9	138.3	129.1

	R	R'	Alkyl chain (R)
DiOctSiOPPV	C_8H_{17}	C_8H_{17}	33.5, 29.2, 22.9, 22.7, 15.8,15.2,14.1
DiEtSiOPPV	C_2H_5	C_2H_5	6.6, 6.4
Mecylohexyl SiOPPV	C_6H_{11}	CH_3	27.8, 26.8, 26.7, -3.6

^{29}Si-NMR of both oligomers andpolymers (figures 3.20-22) proved that there was no significant change in the Si-environment during the reaction as expected. ^{29}Si resonance for both silane and siloxane-based ADMET products were similar to the corresponding monomers. The presence of only one single ^{29}Si resonance further proved that there was no side reaction at the Si during polymerization. ^{29}Si resonance from unreacted monomer residue was difficult to observe due to relatively low concentration. Dimethyl SiPPV was investigated with solid-state ^{29}Si-NMR due to poor solubility in common solvents and hence the corresponding resonance signal is broader than the solution spectra.

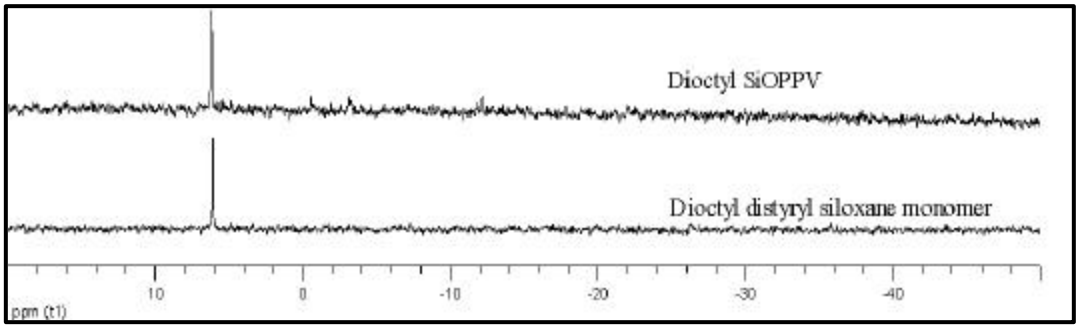

Fig. 3.20 Representative ^{29}Si-NMR comparison between of monomer and oligo/polymer of dioctyl distyryl siloxane**.**

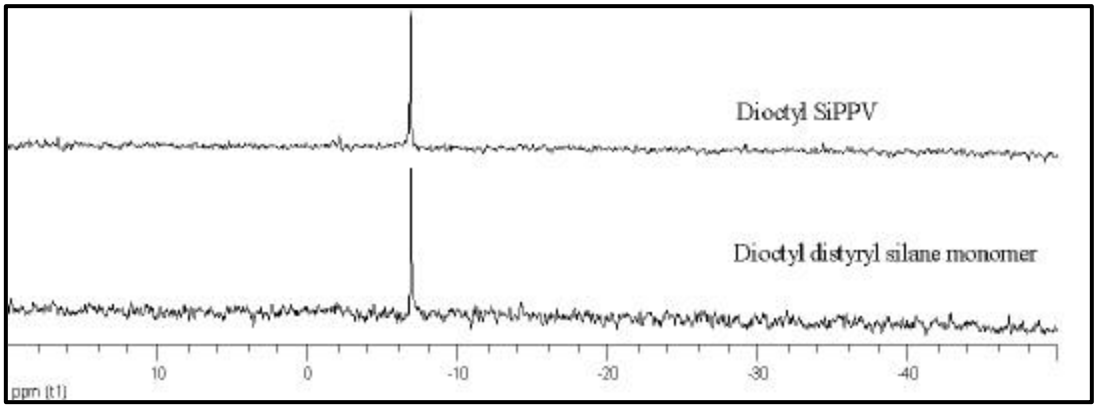

Fig. 3.21 Representative ^{29}Si-NMR comparison between of monomer and oligo/polymer of dioctyl distyryl silane**.**

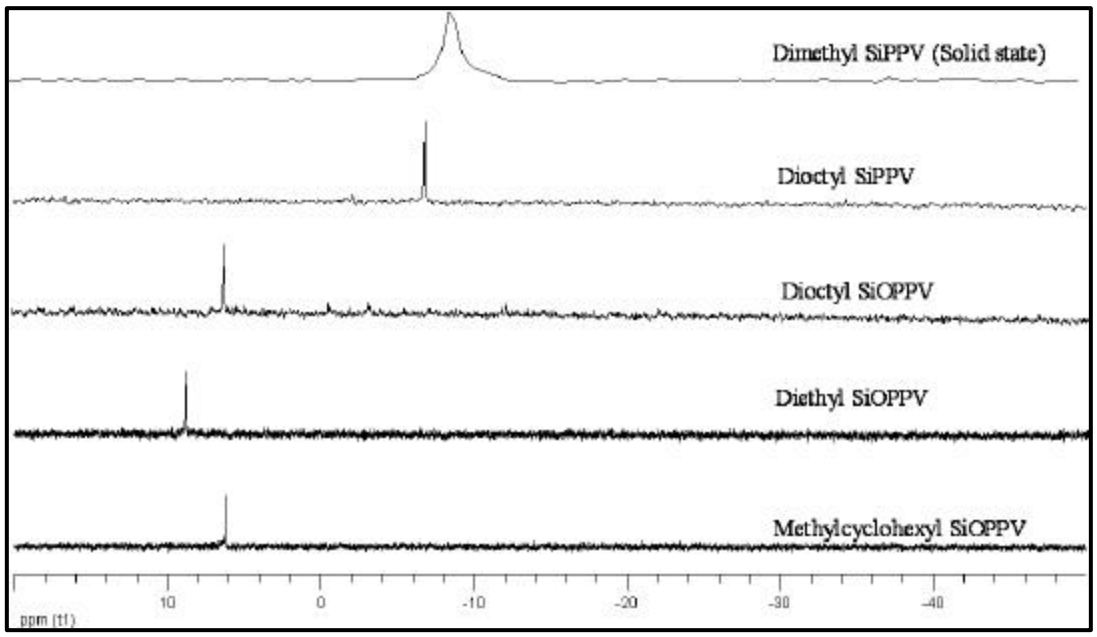

	SiOPPV			SiPPV	
Spectrum	**Mecyclohexyl SiOPPV**	**Diethyl SiOPPV**	**Dioctyl SiOPPV**	**Dioctyl SiPPV**	**Dimethyl SiPPV**
Chemical shift (ppm)	**6.22**	**8.84**	**6.21**	**-6.83**	**-9.68**

Fig. 3.22 ^{29}Si-NMR of dialkyl distyryl siloxane/silane oligo/polymers

3.2.2.2.1.2 FT-IR

FT-IR spectra of all polymers are shown in figures 3.23-25. Aromatic C-H vibrations for (out of plane bending mode) became broadened with reduced intensities in the ADMET products (~ 820 cm^{-1}) compared to the respective monomers (827 cm^{-1}) whereas aliphatic C-H rocking (~ 700 cm^{-1}) appeared more intense in the products than the monomers (~697 cm^{-1}). Si-CH_2 wagging vibrations (~1209 cm^{-1} for products and ~1207 cm^{-1} for monomers) were decreased after ADMET reaction, whereas Si-phenyl stretching vibrations (~1111 cm^{-1} for polymers and ~1105 cm^{-1} for monomers) were more intense.

Linear Si-O-Si stretching (~ 1075-1016 cm^{-1}) was observed for the siloxane-based systems, but not in the silane-based analogs. Furthermore, Si-Phenyl stretching vibration intensities (~1106 cm^{-1}) were almost negligible for all polymers. C=C stretching with conjugation for terminal vinyl bonds gave a sharp signal for monomers at ~1629 cm^{-1} but was negligible after ADMET, in contrast to the intensity for aromatic C=C stretching vibrations (~1598 cm^{-1}), which increased after ADMET (monomers at ~1597 cm^{-1}). Furthermore it was observed that C-H stretching at ~3088 cm^{-1} and out of plane bending vibration intensities (terminal vinyl bonds) at ~ 987 and ~906 cm^{-1} for monomers decreased significantly and a new vibration appeared at ~ 965 cm^{-1}, indicating formation of internal *trans* vinylene bond (out of plane bending mode) through polymerization. ADMET resulted in exclusively *trans* configured double bonds for this type of system due to steric factors in the intermediates of the catalytic cycle, yielding very defined microstructures.

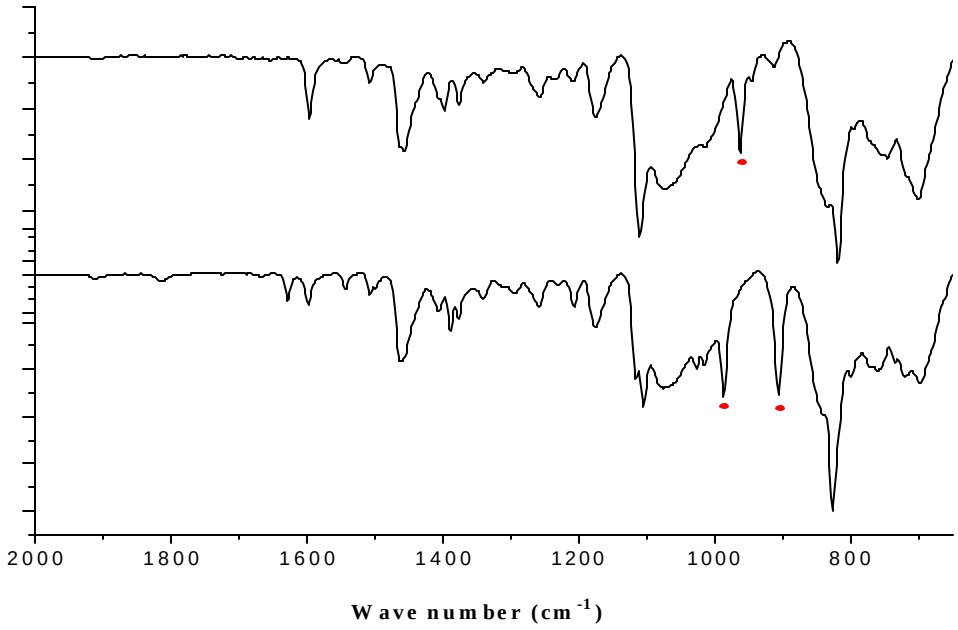

Fig. 3.23 ATR-FTIR spectra of monomer and polymer of dioctyl distyryl siloxane

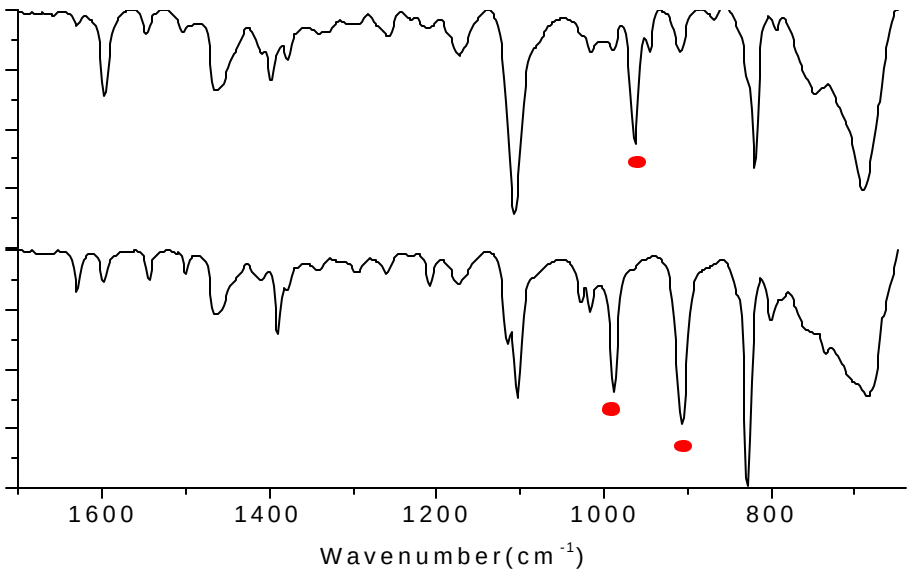

Fig. 3.24 ATR-FTIR spectra of monomer and polymer of dioctyldistyrylsilane

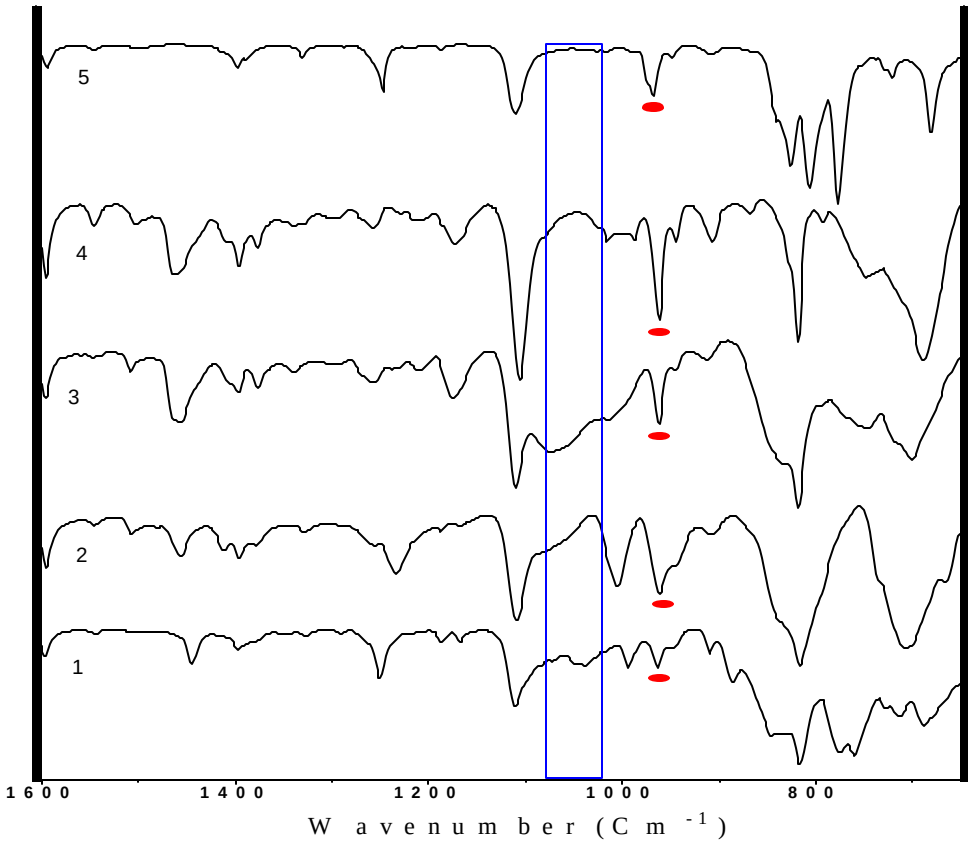

Fig. 3.25 ATR-FTIR spectra of 1) Mecyclohexyl SiOPPV, 2) Diethyl SiOPPV, 3) Dioctyl SiOPPV, 4) Dioctyl SiPPV, 5) Dimethyl SiPPV

3.2.2.2.1.3 Optical properties

The UV/vis absorption spectra were recorded and representative normalized absorption spectra of similarly concentrated solutions in hexanes are shown in fig.3.26. All monomers showed a similar absorption behavior, with an absorption maxima ~ 256-259 nm. Although all ADMET products showed a similar trend with maxima ~319-324 nm, slight changes in the absorption behavior were observed at lower wavelengths. A shoulder was also observed ~ 340 nm which was probably due to some aggregation. Concentration dependent absorption studies (not shown) confirmed this analysis. There was a ~ 63-65 nm red shift (monomer to oligomers/polymers) indicating the formation of *trans*-stilbene type units and thus an increase in conjugation length. Representative

normalized photoluminescence spectroscopy spectra are shown in fig. 3.27, and are in line with the UV/vis absorption data. The spectra were also carried out in hexane. All monomers showed a similar emission behavior with maxima ~ 306-307nm. Although all ADMET products showed the same trend with maxima ~359-366 nm, slight changes in emission behavior were observed at higher wavelength. In most cases, shoulders could be observed ~ 380 nm due to aggregation. Concentration dependent photoluminescence studies (not shown) confirmed this analysis. Overall, there was a ~ 52-60 nm red shift from monomer to respective oligomer/polymer, indicating the formation of *trans*-stilbene units and thus an increase in conjugation length.

It is worth to note that pure *trans*-stilbene has an absorption maxima ~295 nm and emission maxima ~347. These values correspond to a ~20-25 nm blue shift both for absorption and emission relative to the corresponding maxima of the ADMET products of the silane and siloxane systems, indicating an effective participation of the heteratomic centers in the conjugation

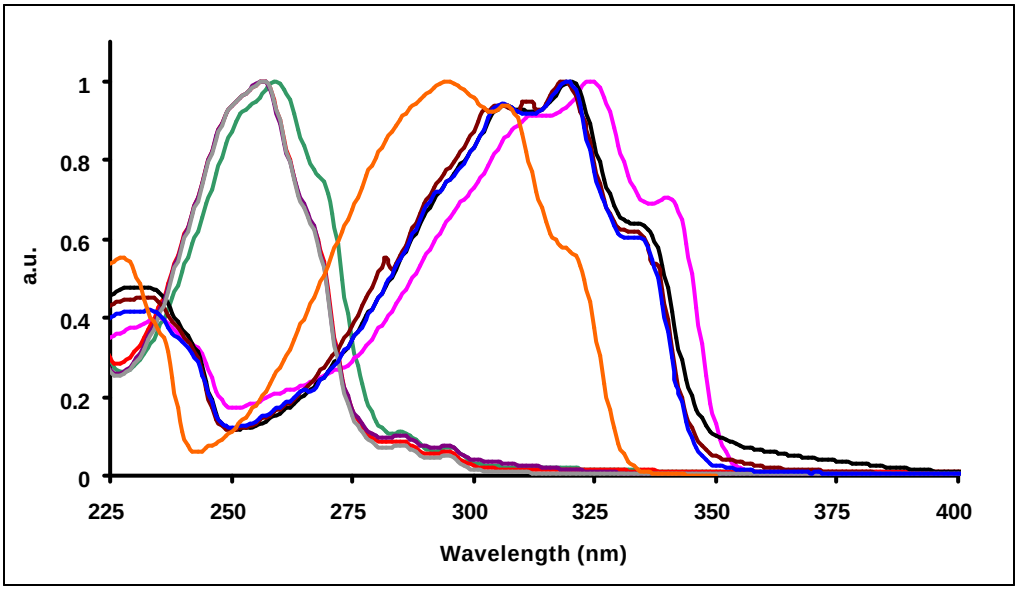

Fig. 3.26 Representative UV/visible absorption spectra (in hexane, concentration: 10^{-4} M) of dialkyl substituted silane/siloxane monomer, their oligo/polymer and trans- stilbene.

	R	R'	Absorption maxima (nm)	
			Monomer	Oligo/polymer
Silane	C_8H_{17}	C_8H_{17}	259(—)	324(—)
Siloxane	C_8H_{17}	C_8H_{17}	257(—)	320(—)
	C_2H_5	C_2H_5	256(—)	319(—)
	C_6H_{11}	CH_3	257(—)	319(—)
Trans-stilbene			295(—)	

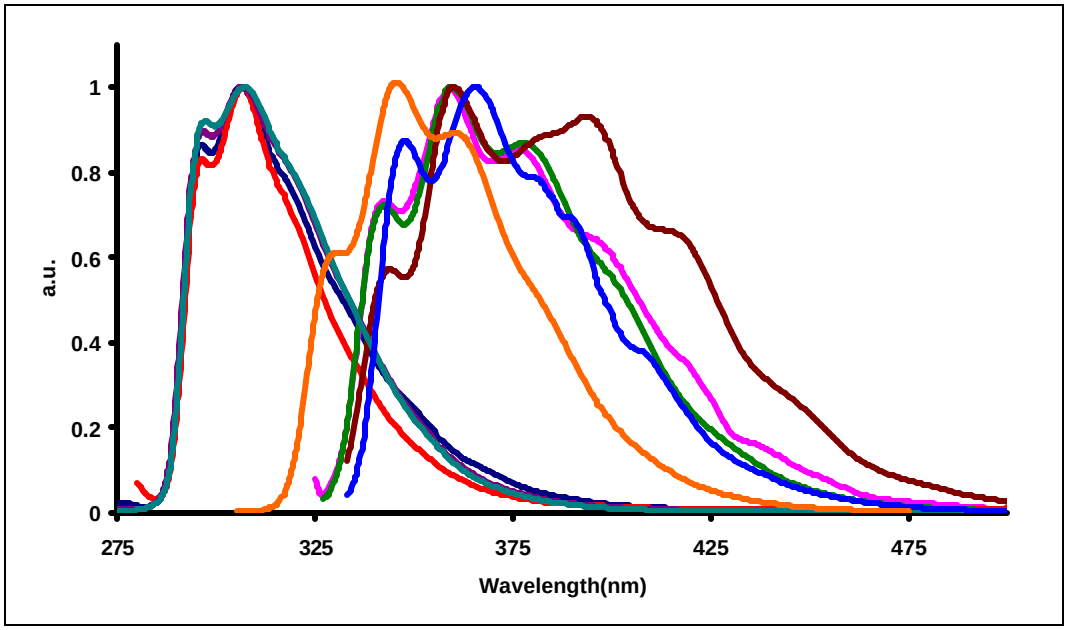

Fig. 3.27 Representative photoluminescence spectra (in hexane, concentration: 10^{-8} M) of dialkyl substituted silane/siloxane monomer, their oligomers/polymer and trans- stilbene. (Excitation wavelength = corresponding absorption maxima of compound)

	R	R'	Emission maxima (nm)	
			Monomer	Oligo/polymer
Silane	C_8H_{17}	C_8H_{17}	307(—)	366(—)
Siloxane	C_8H_{17}	C_8H_{17}	306(—)	360(—)
	C_2H_5	C_2H_5	306(—)	359(—)
	C_6H_{11}	CH_3	307(—)	359(—)
trans-stilbene			347(—)	

3.2.2.2.2 Thermal

Thermogravitymetric (TGA) analyses were carried out for the ADMET products under inert atmosphere (up to 600 ^{0}C) as shown in fig.3.28. For both dioctyl-substituted silane

and siloxane systems a comparable stability was observed.

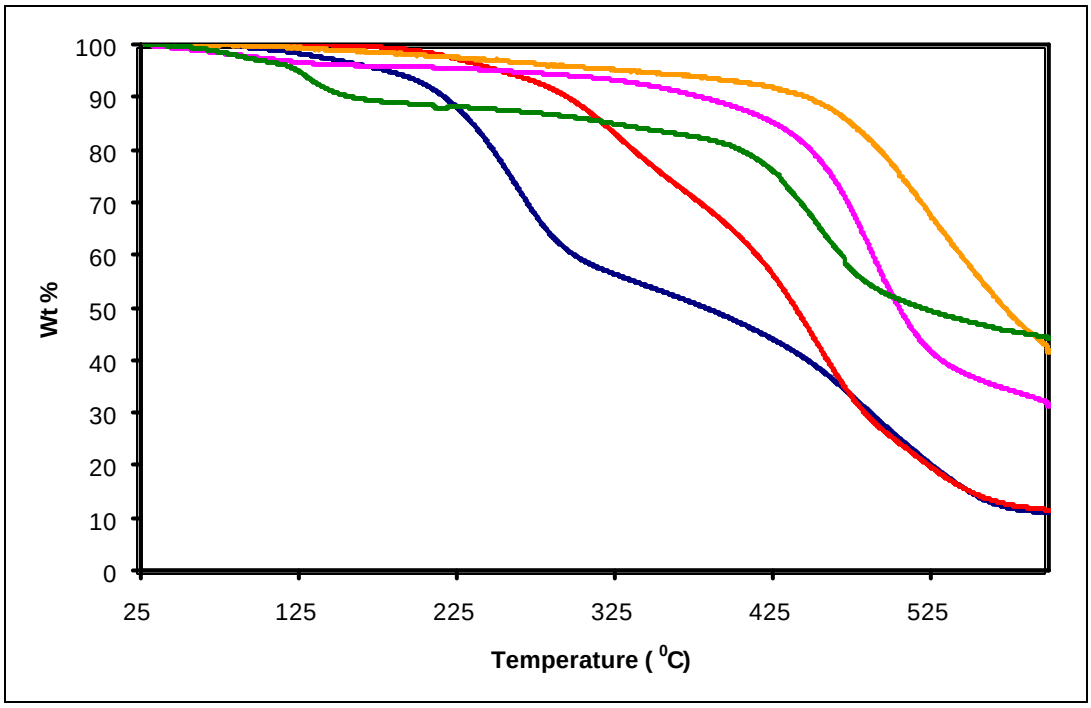

Fig. 3.28 Representative TGA thermogram of dialkyl substituted silane and siloxane oligo/polmers under inert atmosphere (scan rate 10 ^{0}C/ min.)

Oligo/polymer	**5% weight loss Temperature (^{0}C)**
DioctylSiPPV (—)	252
Dimethyl SiPPV (—)	333
DioctylSiOPPV (—)	253
DiethylSiOPPV (—)	180
MethylcyclohexylSiOPPV (—)	124

3.3 Conclusion and outlook

In conclusion, the synthesis of silicon containing poly(p-phenylenevinylene) via ADMET polymerization has opened a new way to generate blue light emitting polymers with the ability to avoid any structural impurities and thus improve the quality of the materials.

Synthesis of monomers via Grignard method yielded siloxane based systems. These monomers formed a cyclic structure upon ADMET, regardless of the reaction conditions, as indicated by detailed NMR and GPC investigations.

However, when monomers were made via lithiation of the diacetal of p-bromobenzaldehyde followed by subsequent reaction with dichloro silanes, silane based monomers were obtained as expected with relatively higher yields. Polymerization of the silane based monomers resulted in higher molecular weight polycondensates. The GPC traces reveal a typical polycondensate mixture with smaller oligomer fractions resolved individually.

As a future development in this area, study of the aggregation behavior and electrochemical properties of these materials may provide a further insight into the material properties and their potential applications.

3.4 Experimental

General Information.

All of the experiments using air/moisture sensitive materials were carried out in a nitrogen filled Labconco protector glove box and/or by the use of dry argon filled dual manifold (inert gas/ vacuum) using standard Schlenk line techniques. All glassware was cleaned and dried for at least 16h in an oven at 120 ^{0}C prior to use.

Chemicals.

Magnesium turnings, n-BuLi [2.5M in hexane], 4-bromobenzaldehyde dimethylacetal (98 %), triphenylphosphonium methyl bromide, sodium sulfate, sodium bicarbonate, sodium chloride, acetic acid and Grubbs-Hoveyda catalyst were obtained from Aldrich. *p*-

bromostyrene (98%) was obtained from Alfa Aesar and dichlorodioctylsilane was obtained form Gelest Inc. Magnesium turnings was flame dried under high vacuum prior to use. Solvents e.g. tetrahydrofuran (THF), toluene, hexane and diethyl ether were purchased from Fisher scientific. Except diethyl ether all other solvents were dried and degassed by "Pure Solv" solvent purification system (using activated alumina, copper catalyst, molecular sieves column.) by Innovative Technology Inc. before use. All other chemicals were used as received. Column chromatography was carried out on silica gel 60 (70-230 mesh) form EMD Chemicals Inc.

Instrumentation.

200 MHz, 300 MHz or 600 MHz ^{1}H NMR, 50 MHz, 75 MHz or 150 MHz ^{13}C NMR and 120 MHz ^{29}Si NMR spectra were recorded in $CDCl_3$ on Varian Unity NMR instruments. $CDCl_3$ was used as an internal deuterium lock for ^{1}H NMR, ^{13}C NMR and ^{29}Si NMR spectra. All of the signals in the NMR spectra are reported in ppm.

UV-Visible absorption spectra were recorded using a Perkin Elmer Model 650 UV Spectrophotometer with 1-cm path length cells. The samples were prepared with HPLC grade chloroform ("Spectrasolv") in a sample cell.

Infrared spectra were recorded on a Tensor 27 Fourier Transformed Infrared spectrometer from Bruker optics using a Pike ATR accessory; data was processed and analyzed by OPUS software.

Photoluminescence spectra were recorded using a Horiba Jobin Yvon Fluoromax-3 spectrofluorometer with 1-cm path length cells. The samples were prepared with HPLC grade chloroform ("Spectrasolv") in a sample cell.

Thermogravimetric Analysis was carried out on a Hi-Res TGA 2950 Thermogravimetric Analyzer from TA Instruments using platinum pan with a heating rate 10 ^{0}C/ min under continuous flow of nitrogen. Differential scanning calorimetric measurement was performed on a DSC Q100 V7.3 Build 249 Differential Scanning Calorimeter from TA Instruments using aluminum pan with a scanning rate 10 ^{0}C/ min under nitrogen flow (50ml/ min).

GPC analysis was carried out on an Alliance GPCV 2000 (Waters) instrument equipped with four Waters Styragel HR columns, i.e. HR-1, HR-3, HR-4, and HR-5E. HPLC grade THF was used as eluent, at a flow rate of 1.0 mL/min at 40 ^{0}C. Measurements are relative to a calibration with polystyrene standards and third order relative calibration curve was used to measure the molecular weight of unknown samples.

Synthesis of dibenzaldehyde dioctyl silane

40 mmol of 4-bromobenzaldehyde dimethylacetal was dissolved in 50 mL of dry THF. The temperature was lowered to –78 ^{0}C. 40mmol of ^{n}BuLi [2.5M in hexane, 16 mL] was slowly added. The reaction was stirred for 1.5h at –78 ^{0}C. 19.5 mmol of dichlorodioctylsilane in 5mL of THF were then added and the reaction was continued for 12h, and finally warmed up gradually to room temperature. The reaction mixture was concentrated, washed with brine and extracted twice with diethyl ether. The organic fractions were combined, dried over sodium sulfate and concentrated to a crude oil of the diacetal of dibenzaldehyde dioctylsilane.

This crude oil was then mixed with 20 mL of acetic acid and 25mL water and stirred for 5h at 40 ^{0}C. The resulting reaction mixture was neutralized with saturated sodium bicarbonate solution and then extracted with diethyl ether. The organic fractions were

further washed with brine, dried over sodium sulfate and concentrated to afford the dibenzaldehyde dioctylsilane as light yellow oil. Yield 85% [based on dichlorosilane used]

^{1}H-NMR ($CDCl_3$, ppm): 0.84 (t, *J*= 7Hz, 6H), 1.0- 1.3(m, 28H), 7.62(d, *J*=6.9 Hz, 4H), 7.82(d, *J*=6.9 Hz, 4H), 10.01(s, 2H). ^{13}C-NMR ($CDCl_3$, ppm): 192.49, 144.50, 136.8, 135.27, 128.7, 33.52, 31.82, 29.13, 29.05, 23.49, 22.61, 14.1,11.96. ^{29}Si-NMR ($CDCl_3$, ppm): -5.47

Synthesis of dibenzaldehyde dimethyl silane

The same procedure was followed as mentioned above for dibenzaldehyde dioctylsilane. The crude product was purified by recystallization from hexane-ethylacetate (4:1) mixture to obtain a crystalline material consisting of white needles . Yield 88% [based on dichlorosilane used]

^{1}H-NMR ($CDCl_3$, ppm): 0.62 (s, 6H), 7.65(d, *J*=7.88 Hz, 4H), 7.83(d, *J*=7.87 Hz, 4H), 10.01(s, 2H). ^{13}C-NMR ($CDCl_3$, ppm): 192.42, 145.61, 136.89, 134.66, 128.8, -2.84. ^{29}Si-NMR ($CDCl_3$, ppm): -6.6

Synthesis of dioctyl distyryl silane

To a suspension of 35mmol of triphenylphosphonium methyl bromide in 100mL of dry THF 30 mmol of n-BuLi [2.5M in hexane, 12mL] was slowly added at 0 ^{0}C. The reaction mixture was stirred for 3h. To this resulting solution 10 mmol of dibenzaldehyde dioctylsilane dissolved in 10 mL of dry THF were slowly added at 0 ^{0}C. The resulting mixture was stirred for 12h and then washed with brine. The organic phase was extracted with diethyl ether twice, dried over sodium sulfate and concentrated to yield a crude oil

of the dioctyl distyryl silane, which was purified by passing through a silica gel column using hexane as an eluent to obtain a colorless liquid. Yield 66 %

^{1}H-NMR ($CDCl_3$, ppm 0.9 (t, J= 7Hz, 6H), 1.0- 1.2(m, 4H), 1.2-1.5(m, 24H) 5.26(d, *J*=11.2Hz, 2H), 5.79(d, *J*= 17.7 Hz, 2H), 6.72 (dd, *J*= 11.2 Hz, 17.7Hz, 2H), 7.39(d, *J*=8.1 Hz, 4H), 7.47(d, *J*=7.8 Hz, 4H). ^{13}C-NMR ($CDCl_3$, ppm): 138.1, 136.9, 136.4, 135.1, 125.51, 114.2, 33.73, 31.9, 29.25, 29.15, 23.69, 22.66, 14.1, 12.55. ^{29}Si-NMR ($CDCl_3$, ppm): -6.84

Synthesis of dimethyl distyryl silane

Same procedure was followed as mentioned above for dioctyl distyryl silane to obtain a colorless liquid. Yield 66 %

^{1}H-NMR ($CDCl_3$, ppm 0.6(s, 6H), 5.30(d, *J*=10.8Hz, 2H), 5.82(d, *J*= 18.6 Hz, 2H), 6.75 (dd, *J*= 10.8Hz, 18.6Hz, 2H), 7.44(d, *J*=7.8 Hz, 4H), 7.54(d, *J*= 8.1 Hz, 4H). ^{13}C-NMR ($CDCl_3$, ppm): 138.21, 137.73, 136.74, 134.38, 125.57, 114.29,-2.42. ^{29}Si-NMR ($CDCl_3$, ppm): -8.75

Synthesis of dioctyl distyryl siloxane (3)

To a solution of (5.86g, 32 mmol) of *p*-bromostyrene in 70 mL of dry THF, flame dried magnesium turnings (1.54g, 64mmol) and a few iodine crystals of were added. The solution was refluxed under constant stirring. After 6h the reaction mixture was cooled to room temperature and transferred to another vessel using a pipette. Then a solution of 4.30g (16mmol) dichlorodioctylsilane in 20mL of dry THF was slowly added. The reaction mixture was stirred for 16 h at room temperature. After the reaction was complete, 0.1 M HCl solution was added to it dropwise until the formation of precipitate ceased. The suspension was quickly filtered and the filtrate was hydrolyzed with 200mL

of distilled water followed by extraction with 100mL of diethyl ether. The organic layer was collected, washed twice with 100mL of distilled water, and then dried over magnesium sulfate. Finally the solvent was removed under vacuum and the resulting crude product was purified by column chromatography (silica gel with hexane: methyl tert-butyl ether [95:5] as an eluent) to obtain **3** as a pale yellow liquid. The yield was 2.6g (36 %). ^{1}H-NMR ($CDCl_{3,}$ ppm): 0.52- 1.3(m, 34H), 5.25(d, *J*=11Hz, 2H), 5.75(d, *J*= 17.4Hz, 2H), 6.7(dd, *J*= 11Hz, 17.4Hz, 2H), 7.34-7.53(m, 8H). ^{13}C-NMR ($CDCl_{3,}$, ppm):138.49, 137.43, 136.8, 133.7, 125.6, 114.35, 33.48, 31.87, 29.21, 22.95, 22.65, 15.78, 15.18, 14.1 ^{29}Si-NMR ($CDCl_{3,}$ ppm): 6.12

Synthesis of diethyl distyryl siloxane

The same procedure was followed as mentioned above for dioctyl distyryl silane to obtain a colorless liquid. Yield 51%

^{1}H-NMR ($CDCL_{3,}$ ppm): 0.86 (m, 8H), 1.01 (t, *J*=7.8 Hz, 12H) 5.29(d, *J*=12Hz, 2H), 5.81(d, *J*= 24Hz, 2H), 6.74(dd, *J*= 12Hz, 24Hz, 2H), 7.42(d, *J*=7.8 Hz, 4H), 7.55(d, *J*= 8.4 Hz, 4H). ^{13}C-NMR ($CDCl_{3,}$ ppm): 138.4, 137.1, 136.1, 135.41, 125.8, 114.5, 7.7, 4.16 ^{29}Si-NMR ($CDCL_{3,}$ ppm): 8.04

Synthesis of methylcyclohexyl distyryl siloxane

The same procedure was followed as mentioned above for dioctyl distyryl silane to obtain a colorless liquid. Yield 41%

^{1}H-NMR ($CDCL_{3,}$ ppm): 0.34 (s, 6H), 0.87-0.91(m, 2H), 1.1-1.25 (m, 10H) 1.65-1.75(m, 12H) 5.26(d, *J*=11.6Hz, 2H), 5.78(d, *J*= 17.6Hz, 2H), 6.71(dd, *J*= 11.6 Hz, 17.6Hz, 2H), 7.4(d, *J*=8 Hz, 4H), 7.51(d, *J*= 8.04 Hz, 4H). ^{13}C-NMR ($CDCl_{3,}$ ppm): 138.25, 137.14, 133.97,129.1, 125.86, 27.75, 26.76,26.67,-3.62. ^{29}Si-NMR ($CDCL_{3,}$ ppm): 6.05

Typical Synthesis of oligo/poly(di-n-octyldiphenylsilyl phenylene vinylene) (OctSiPPV) (4).

360 mg (0.78 mmol) of dioctyldistyrylsilane and 2.5 mol% of Grubbs second generation catalyst was placed in an air free reaction tube and dissolved in 2mL of dry toluene. The reaction mixture was heated at 48 ^{0}C for 18h. Ethylene gas as a by-product was removed by applying vacuum intermittently. A viscous reaction mixture formed, which was cooled down to room temperature. To this resulting viscous mixture 5 mL of ethyl ether was added to kill the catalyst. The diluted solution was passed through a short silica gel column to remove the catalyst residue (using ethyl ether as an eluent). Finally, all volatiles were removed to yield 320mg of greenish-black polymer as a semi solid **(4)**. ^{1}H-NMR ($CDCL_{3,}$, ppm): 0.57-1.38(m), 5.26(d),5.78(d), 6.6-6.9(m), 7.13(s), 7.47-7.57(m). ^{13}C-NMR ($CDCL_{3,}$, ppm):138.2, 137.4, 133.84, 129.08, 125.91, 33.47, 31.88, 29.20, 22.96, 22.64, 15.79, 15.19, 14.09 ^{29}Si-NMR ($CDCL_{3,}$ ppm): 6.21

Synthesis of oligo/poly(dimethyl silyl phenylene vinylene) (MeSiPPV)

The same procedure was followed as mentioned above for oligo/poly(di-n-octyldiphenylsilyl phenylene vinylene). During the polymerization an off-white solid formed. The reaction mixture was poured over a large amount of ice-cold methanol and stirred for an hour. After that, polymer was filtered and dried in vacuum for 24h to obtain an off-white powder as product.

^{1}H-NMR ($CDCl_{3,}$ ppm) 0.53(s), 0.54(s), 5.24(d, *J*=10.85 Hz), 5.76(d, *J*= 17.6 Hz), 6.7 (dd, *J*= 10.85Hz, 17.6 Hz), 7.1(s), 7.48(m). ^{13}C-NMR (solid state, ppm): 136.47, 134.43, 124.8, 114.32, -3.93. ^{29}Si-NMR (solid state, ppm): -9.68

Synthesis of oligo/poly(dioctyl siloxane phenylene vinylene) (OctSiOPPV)

The same procedure was followed as mentioned above for oligo/poly(di-n-octyldiphenylsilyl phenylene vinylene) to obtain a greenish-black semi solid material as product.

^{1}H-NMR ($CDCl_3$, ppm): 0.52- 1.4(m), 7.13(s), 7.45-7.58(m, 8H). ^{13}C-NMR ($CDCl_3$, ppm): 138.2, 137.4, 133.8, 129.1, 125.9, 33.48, 31.88, 29.21, 22.95, 22.65, 15.78, 15.2, 14.1 ^{29}Si-NMR ($CDCl_3$, ppm): 6.12

Synthesis of oligo/poly(diethyl siloxane phenylene vinylene) (EtSiOPPV)

The same procedure was followed as mentioned above for oligo/poly(di-n-octyldiphenylsilyl phenylene vinylene) to obtain a greenish-black solid material as product.

^{1}H-NMR ($CDCL_3$, ppm): 0.86(t) 0.95-1.1(m) 7.41-7.58(d). ^{13}C-NMR ($CDCl_3$, ppm): 138.28, 136.75, 133.93, 129.1, 125.94, 6.57, 6.4 ^{29}Si-NMR ($CDCL_3$, ppm): 8.04

Synthesis of oligo/poly(methylcyclohexyl siloxane phenylene vinylene) (Mecyclohexyl SiOPPV)

The same procedure was followed as mentioned above for oligo/poly(di-n-octyldiphenylsilyl phenylene vinylene) to obtain a greenish-black semi crystalline material as product.

^{1}H-NMR ($CDCL_3$, ppm): 0.35 (s), 0.88-0.95 (br), 0.98-1.3 (m), 1.4-1.8 (m), 7.39(d, *J*=8 Hz, 4H), 7.13(s), 7.41-7.57(m). ^{13}C-NMR ($CDCl_3$, ppm): 138.3, 137.1, 134, 129.1, 125.9, 27.8, 26.8,26.7, - 3.6. ^{29}Si-NMR ($CDCL_3$, ppm): 6.05

Table 3.7 FTIR- monomer of dialkyl distyryl siloxane/silane

Methyl Sippv-M	Dioctyl Sippv-M	Dioctyl Sioppv-M	Diethyl Sioppv-M	Mecyclohex Sioppv-M	
3087	3089	3088	3089	3087	C-H Str. (CH=)CH_2
3062	3064	3063	3065	3063	C-H Str. (CH=)CR_2
3021/3008	3020/3009	3020/3008	3020 /3010	3020/3008	Ar. C-H Str.
2984/2957	2957	2956	2957	2956	Aliph. C-H Str. -doublet asymm. and symm. of -CH_3
	2923	2920	2913	2916	Aliph. Asymm. vib -CH_2-, Ar. overtone
2872	2872	2871	2877	2894	Aliph. C-H stretch. -doublet asymm. and symm. of -CH_3
	2854	2852		2845	Aliph. Symm. Vibr. -CH_2-
1813	1815	1815	1817	1815	Ar. overtone
1628	1631	1629	1630	1628	C=C str. with conjugation, Si-ph. C=C str. Vib.
1596	1599	1598	1599	1597	Ar. C=C Str. Vib.
1543	1545	1544	1545	1543	Ar. C-H OOP bending
1499	1501	1508	1509	1500	Ar. C=C Str. Vib.
1436	1467	1462	1460	1445	Aliph. C-H bending of -CH_2-, Aliph. C-H asymm. Deform, Ar. C=C Str. Vib.
1418/1408	1411	1406	1414	1418/1406	Si-CH_2 bending
1389	1391	1389	1391	1389	-CH_3 deform.
	1380	1377	1380		Aliph. -CH_3 symm. bending vib.
	1343	1341	1345	1344	Aliph. C-H twisting of -CH_2-
1295	1297	1295	1296	1292	-CH_3 symm. Str.
1247	1261	1259	1261	1251	Si-CH_2 rocking
	1231	1230	1236		Si-CH_2 deform.
1207	1209	1207	1210	1207	Si-CH_2 wagging
1188	1175	1176		1187/1169	
1116	1117	1116	1118	1117	Ph. C-H in plane bending
1104	1104	1105	1107	1105	Si-ph. Str. Vib.
		1075/1027	1080/1025	1071/1027	Linerar Si-O-Si str.
1027/1017	1029/1018	1016	1008	1017	-Si-C Str.
988	989	987	990	988	CH(=CH_2) OOP- deform.
906	908	906	908	907	CH(=CH_2) OOP- deform.
		840	840	887/846	Si-C Str.
827/815	830	827	827	825	1,4 Ph. C-H OOP bending
791/774	801	799/772		799/775	
	757	760		760	Aliph. C-H vib.
734	736	735	747	737/712	Ph. C-H OOP bending.
694/675	685	720/697	709	691/675	Aliph. C-H rocking

Table 3.8 FTIR- oligo/polymer of dialkyl distyryl siloxane/silane

Me sippv	Dioct sippv	Dioct sioppv	Diet sioppv	Mecy sioppv	
3061	3063	3064	3065	3065	C-H Str. (CH=)CR_2
3040/ 3014	3015	3017	3019	3019	Ar. C-H Str.
2956	2955	2955	2956	2960	Aliph. C-H Str..
	2921	2919	2912	2918	Aliph. Asymm. vib -CH_2- /Ar. overtone
2895	2870	2870	2877	2894	C-H stretch. -doublet asymm. and symm. of -CH_3 along with 2956.
	2852	2851	Overlap	2847	Aliph. Symm. Vibr. -CH_2-
1817	1806	1802	1809	1809	Ar. overtone
1628	1630	1635	1631	1631	C=C str. with conjugation,/ Si-ph. C=C str. Vib.
1595	1596	1597	1598	1598	Ar. C=C Str. Vib.
1547	1545	1548	1548	1547	Ar. C-H OOP bending
1505	1501	1508	1510	1484/1507	Ar. C=C Str. Vib.
1436	1467	1457	1460	1447	Aliph. C-H bending of -CH_2-, Aliph.C-H asymm. Deform, Ar. C=C Str. Vib.
1398	1397	1407/1398	1413/1399	1399	Si-CH_2 bending
1389				1389	-CH_3 deform.
	1377	1377	1381	1380	Aliph. -CH_3 symm. bending vib.
1330	1340	1340	1330	1345	Aliph. C-H twisting of -CH_2-,
1289	1298	1298		1293	-CH_3 symm. Str.
1248	1258	1258	1258	1252	Si-CH_2 rocking
	1230	1237	1236		Si-CH_2 deform.
1188	1209	1209	1190	1188	Si-CH_2 wagging
	1173	1175	1170	1170	
1112	1117	1111	1112	1113	Ph. C-H in plane bending
	1106				Si-ph. Str. Vib.
		1075	1082	1040/1072	Linerar Si-O-Si str.
1028 /1017	1029/ 1018	1016	1007	1028/1018	-Si-C Str.
989	989	998		996	CH(=CH_2) OOP- deform.
969 /948	963 /945	963 /946	964 /948	966 /946	t-vinylene OOP-deform.
906	907	913	910	911	CH(=CH_2) OOP- deform.
840	867	834	840	888	Si-C Str.
827/806	830	819	819	818	1,4 Ph. C-H OOP bending
777	801	795/772		777	
755		756		762	Aliph. C-H vib.
729/721	736	746	747/736	728/716	Ph. C-H OOP bending.
682	685	718/701	710/668	690	Aliph. C-H rocking

OOP = out of plane

4. Synthesis of homologous conjugated germane - and stannane -PPV

4.1 Objective

In Chapter 3, the synthesis and characterization of distyryl dialkyl silane and siloxane monomers and their polycondensation via ADMET were discussed. As an extension of that work, homologus other group-IV-element-containing monomers (i.e. Germane and Stannane) were synthesized in order to prove the scope of the synthetic approach, and to understand the sequential change and the effect of the heteroatomic moiety on the ADMET polymerization as well as on the properties of the target polymers. Thus the aim of this work was to design, synthesize and characterize distyryl dialkyl germane and stannane monomers, and subsequently polymerize them via ADMET. In order to synthesize the monomers a homologous approach to the one discussed in Chapter 3 for the case of Si was adopted; the diacetal of bromobenzaldehyde was lithiated with butyl lithium at –78 ^{0}C followed by dropwise addition of corresponding dichloro dialkyl germane or stannane, and subsequent workup.

4.2 Results and discussion

4.2.1 Synthesis of materials

4.2.1.1 Monomers

In order to make a homologous series of distyryl dialkylsilane/germane/stannane, the synthetic strategy described in Chapter 3 for the case of silane was used for all cases, in which the diacetal of bromobenzaldehyde was lithiated with butyl lithium at –78 ^{0}C, followed by dropwise addition of a corresponding dichloro dialkyl silane/germane/stannane (fig. 4.1). In order to ensure complete reaction, a small excess of

the diacetal was used. Deacetalization occured during the follow up process: The reaction mixture was refluxed with acid, followed by neutralization, in order to generate the respective dibenzaldehyde dialkyl silane/germane/stannane. This dialdehyde was converted into the corresponding divinyl monomer via a standard Wittig reaction. This method afforded pure homologous monomers in good yields.

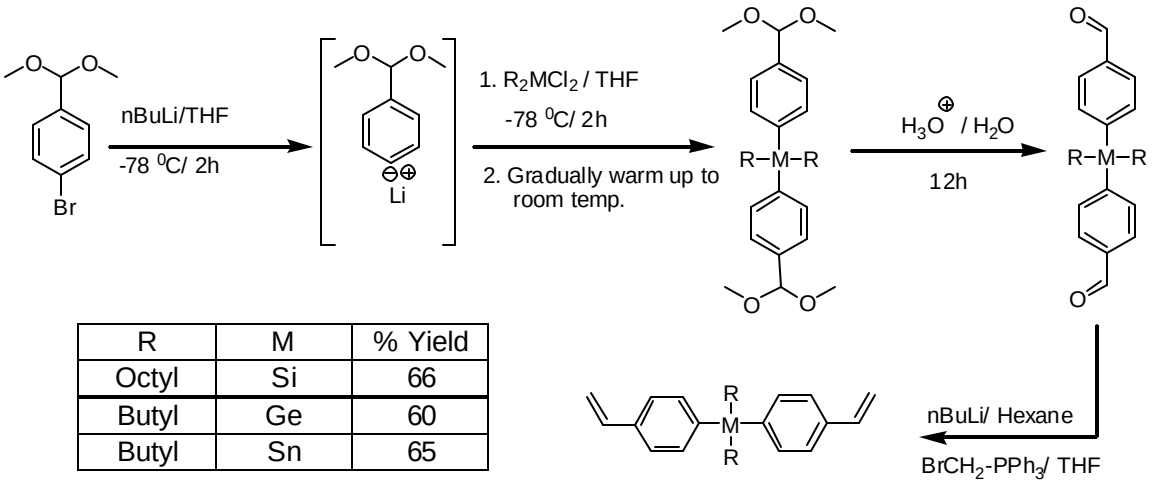

R	M	% Yield
Octyl	Si	66
Butyl	Ge	60
Butyl	Sn	65

Fig. 4.1 Synthesis of dialkyl distyryl Silane/ Germane /Stannane monomers

4.2.1.1.1 Size analysis of monomers

Gel permeation chromatography was carried out relative to polystyrene standards for all monomers as show in fig. 4.2. Narrowly distributed monomodal traces were observed for each case, indicating only one product was obtained in each case.

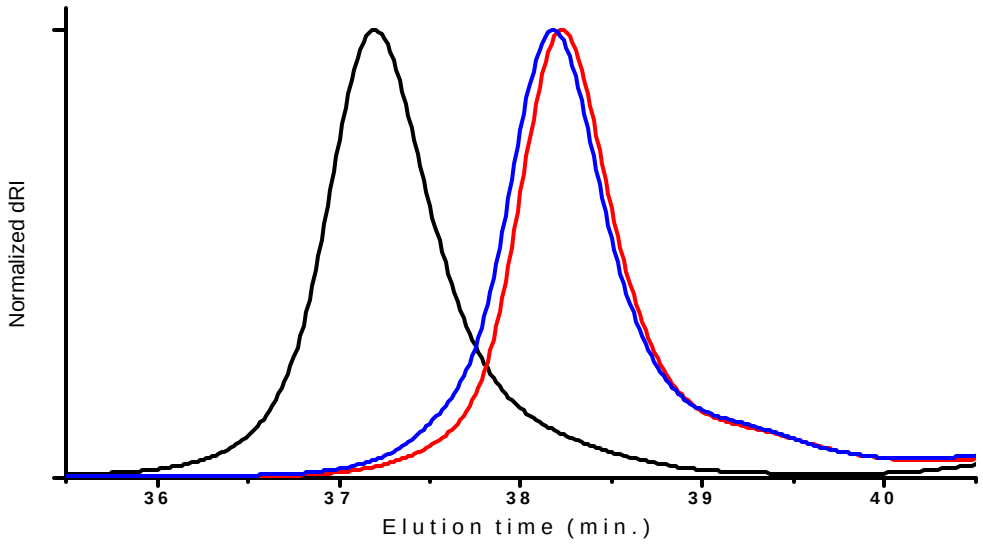

Fig. 4.2 GPC traces of distyryl dialkyl substituted silane (—)/ germane(—)/ stannane(—) monomers.

Monomer	Mn (Calculated)	Mn (Experimental)	PDI
Dioctyl distyrylsilane	**460**	**621**	**1.04**
Dibutyl distyrylgermane	**394**	**417**	**1.02**
Dibutyl distyrylstannane	**440**	**427**	**1.03**

4.2.1.2 ADMET polycondensation

The ADMET polycondensation was carried out with all monomers, using a ruthenium based Grubbs- Hoveyda 2nd generation or Grubbs 2nd generation type catalyst in toluene to afford structurally pure oligo/polymers as shown in fig. 4.3. In order to understand the reaction and to optimize the reaction conditions, temperature/ time of reaction/ amount of catalyst / and type of catalyst were varied. The by-product ethylene gas was removed by applying vacuum intermittently, driving the reaction towards the product side.

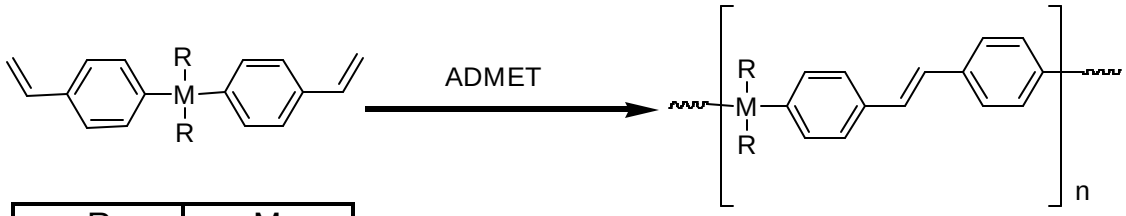

R	M
Octyl	Si
Butyl	Ge
Butyl	Sn

[a] Reagents and conditions: Grubbs 2nd generation catalyst or Grubbs-Hoveyda catalyst/toluene/10-18h/ 50-65 ^{0}C

Fig. 4.3 Synthesis of oligo/polymer from silane/germane/stannane monomers

The Si-containing polymers and their ADMET synthesis were discussed in detail in Chapter 3. Consequently, dibutyl substituted germane and stannane monomers were subjected to ADMET polycondensation under the above-mentioned conditions. In general, both germane and stannane followed the same trends as their silane homologs (see chapter 3). During the condensation, both the germane and stannane reaction mixtures became viscous after 6-8hr of reaction indicating the formation of high molecular weight mass as supported by GPC.

4.2.1.2.1 Size Analysis of products

GPC analyses were carried out for each sample and are summarized in figures 4.4-6. A clear increase in molecular weight during the polymerization was observed in each case. For the silane-based system data shown in fig. 4.4 and table 4.1 has also been discussed and presented in Chapter 3, but are used here to demonstrate the homologous nature of the series. Very similar characteristics were observed of the ADMET homologs with Ge and Sn. Varying molecular weights were observed for the ADMET products of germane or stannane monomers depending on the reaction conditions. For stannane, at low catalyst concentration (entry-8) mainly monomer was observed. In all other cases, Mn~1800-5000 g/mol could be observed. For the germane system, a similar trend was also observed with Mn ~ 2400-7710 g/mol.

Table 4.1 Representative ADMET polymerization results of distyryl dialkyl silane/germane/stannane monomers.

Entry	Catalyst (Mol%)	Monomer (mg)	Time (h)	Temp (^{0}C)	Mass recovered (mg)	%Yield	Mn / PDI
Representative table: ADMET of distyryl dioctylsilane monomer*							
1	2[+]	225	18	55	214	95	6050/1.73
2	2	225	10	55	203	90	3700/1.43
3	0.5	270	18	60	248	N/A	1530/1.00[a]
4	1.5	220	18	65	196	89	5000/1.52
***Solvent: Toluene [monomer concentration (0.2-0.28 M)]**							
Representative table: ADMET of distyryl dibutylgermane monomer**							
5	2.5	250	18	50	223	89	7710/2.56
6	2[+]	225	12	50	205	91	2400/1.49
****Solvent: Toluene [monomer concentration (0.19-0.25 M)],**							
Representative table: ADMET of distyryl dibutylstannane monomer***							
7	2	225	18	50	207	92	1810/2.01
8	0.5[+]	240	12	50	228	N/A	1070/1.007 [a]
9	2[+]	255	12	55	201	88	4910/1.82
*****Solvent: Toluene [monomer concentration (0.23-0.27 M)]**							
+ Catalyst: Grubbs 2nd generation catalyst.							
In all other cases Catalyst: Grubbs-Hoveyda 2nd generation catalyst							

[a] trace amount of one oligomer (with mainly monomer) was observed

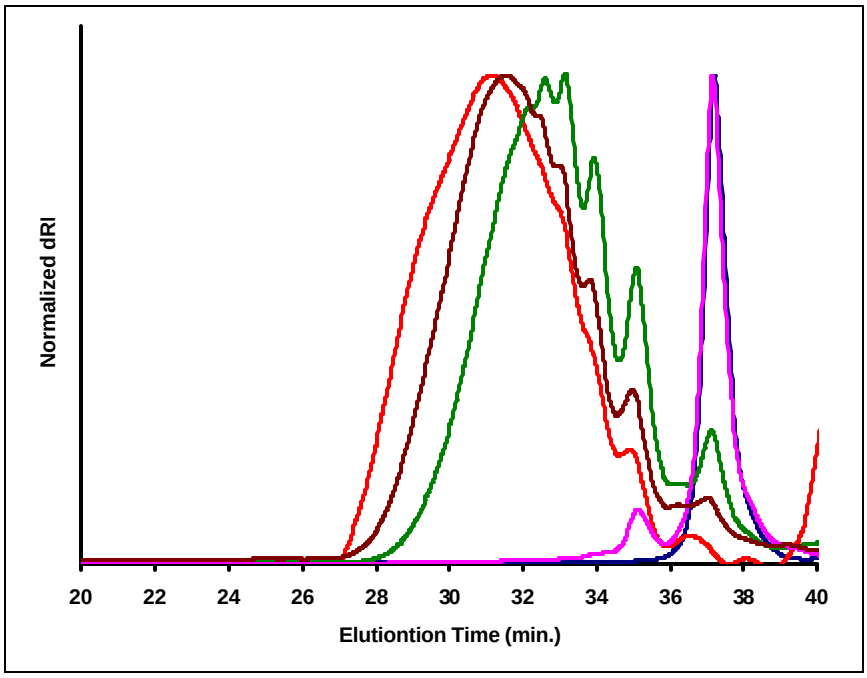

Fig. 4.4 GPC traces for dioctyl distyrylsilane monomer and its ADMET condensate mixture: (—) Set 1: (—) Set #2 : (—) Set #3 : (—) Set #4: (—) [see Chapter 3 also]

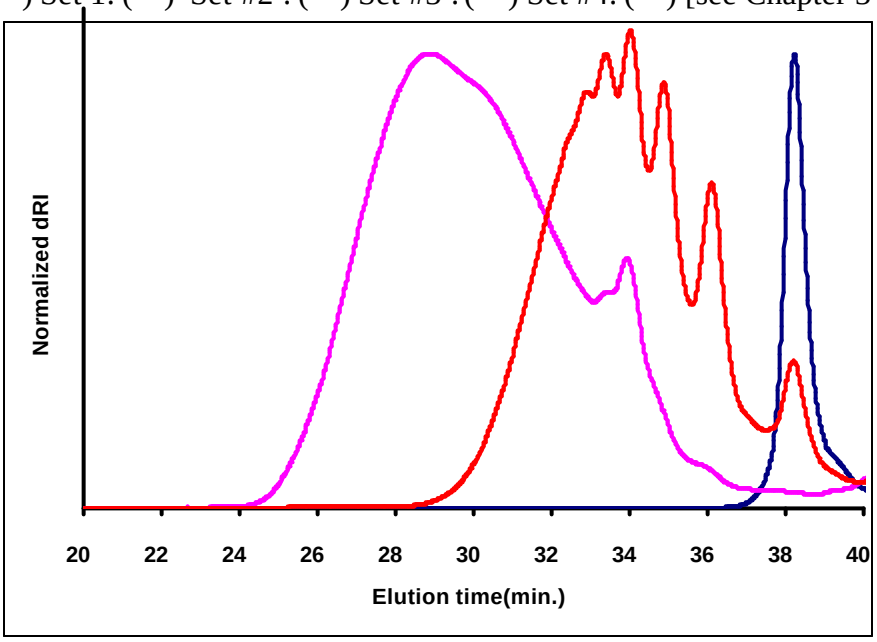

Fig. 4.5 GPC traces for dibutyl distyrylgermane monomer and its ADMET condensate mixture: (—) Set 1: (—) Set #2 : (—)

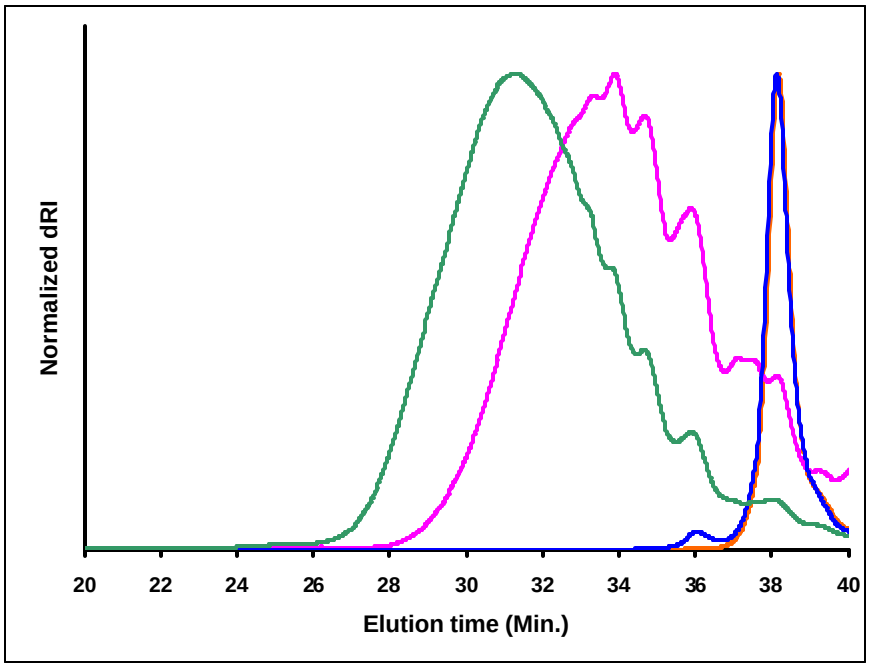

Fig. 4.6 GPC traces for dibutyl distyrylstannane monomer and its ADMET condensate mixture : (—) Set 1: (—)Set #2 : (—) Set #3 : (—)

4.2.2 Characterizations of materials

4.2.2.1 Monomers

Results from investigations into the microstrctures of the homologous monomer series are presented. The Si-homolog, also discussed in Chapter 3 is inserted into the discussion for reference and reasons of comparison.

4.2.2.1.1 Microstructure analysis

4.2.2.1.1.1 NMR (^{1}H, ^{13}C, ^{29}Si, ^{119}Sn)

Results from ^{1}H NMR analyses are presented together with the assignments and chemical shifts and shown in fig.4.7.

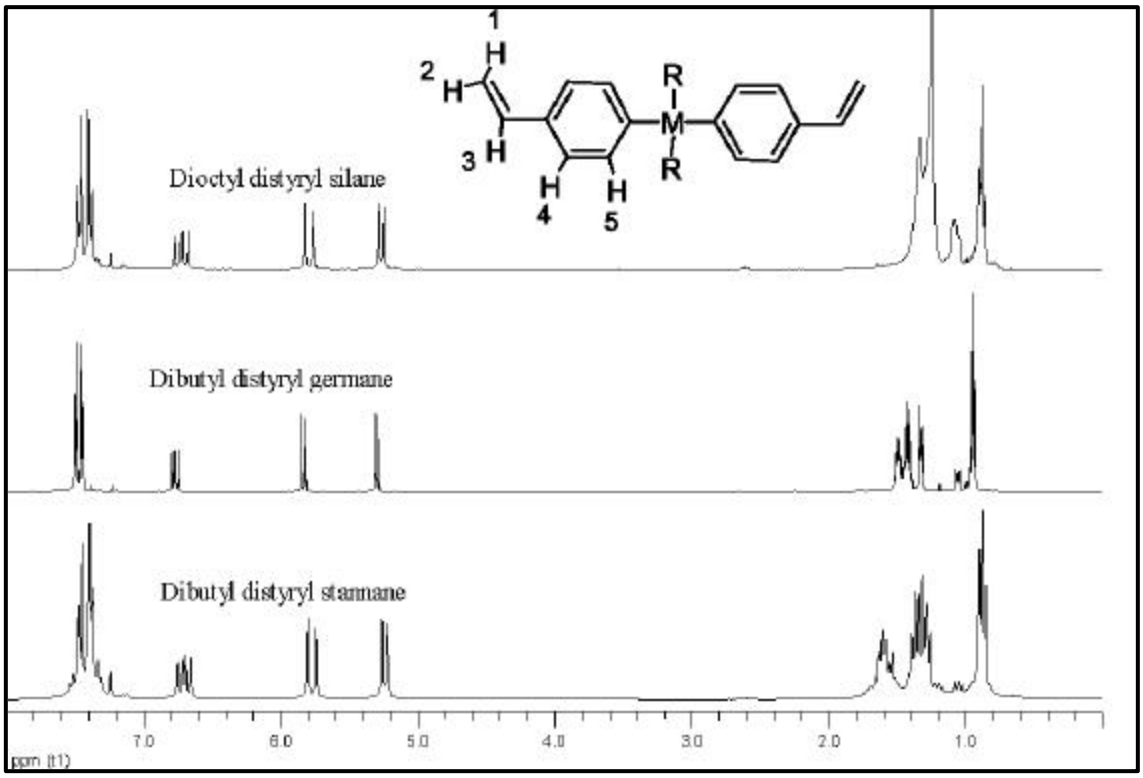

Monomer	R	M	1	2	3	4-5	Alkyl chain (R)
Distyryl dioctyl silane	C_8H_{17}	Si	5.79	5.26	6.73	7.5-7.4	1.6-0.85
Distyryl dibutyl germane	C_4H_9	Ge	5.84	5.31	6.78	7.5-7.45	1.53-0.93
Distyryl dibutyl stannane	C_4H_9	Sn	5.77	5.24	6.7	7.5-7.35	1.65-0.84

Fig. 4.7 ^{1}H-NMR (with assignments) of distyryl dialkyl silane/germane/stannane

^{1}H-NMR resonances for the terminal vinyl group, in all cases revealed two doublets (1, 2: with different coupling constants) at ~ 5.2 and ~ 5.7 ppm corresponding to two vicinal protons (exo, endo), cis and trans respectively. It is to be noted that, almost the same chemical shifts (~ 5.2, 5.8 and 6.7 ppm) were observed in all three cases, indicating no significant differences between the heteroatoms. The aromatic protons resonances in all

three cases were slightly different, ranging from 7.3-7.5 ppm, depending on the nature of the heteroatom. The alkyl side chains showed mainly 3 distinct resonances. The terminal methyl group showed a triplet at ~0.86 ppm. The methylene group adjacent to the heteroatom showed a multiplate at around ~1.6-1.3 ppm, which also overlapped with the multiplate resonances from the internal methylene signals (~1.4-1.2 ppm). The measured relative integral ratios of all different protons matched the calculated for each monomer.

^{13}C-NMR spectra for all monomers are shown in fig. 4.8 together with the respective assignments and chemical shifts. The carbon resonances associated with the terminal vinyl groups were observed at around ~136.8 ppm and ~114 ppm, characteristic signals for all monomers. The aromatic carbon resonances were observed at around ~138-125 ppm with no major changes amongst different heteroatoms. Depending on the chain length, aliphatic carbons (butyl or octyl) at the heteroatoms of different monomers were observed at ~ 33 to 10.3 ppm. A slight shift was observed for the methylene carbon connected to the respective heteroatom.

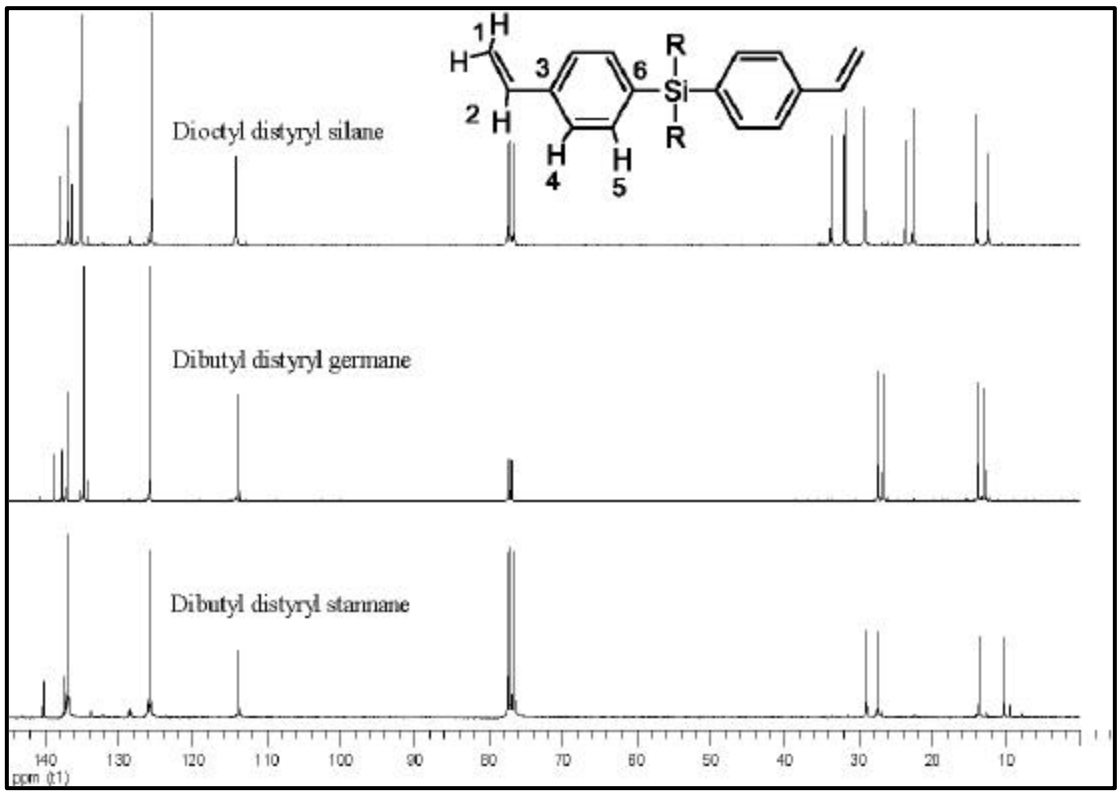

Monomer	R	M	1	2	3	4	5	6
Distyryl dioctyl silane	C_8H_{17}	Si	114.0	137.5	138.3	125.8	134.4	136.8
Distyryl dibutyl germane	C_4H_9	Ge	113.9	137.6	138.5	125.7	134.6	136.8
Distyryl dibutyl stannane	C_4H_9	Sn	113.9	1375	140.2	125.9	136.9	136.9

Monomer	R	M	Alkyl chain (R)
Distyryl dioctyl silane	C_8H_{17}	Si	33.7, 31.9, 29.2, 29.1, 23.7, 22.7, 14.1, 12.6
Distyryl dibutyl germane	C_4H_9	Ge	27.2, 26.5, 13.7, 13
Distyryl dibutyl stannane	C_4H_9	Sn	28.9, 27.3, 13.6, 10.3

Fig. 4.8 ^{13}C-NMR (with assignments) of distyryl dialkyl silane/germane/stannane

^{29}Si-NMR was carried out for the silane compounds and showed only one resonance for each monomer indicating one Si-species each, and was discussed in detail in Chapter 3. Homologous results were observed when performing ^{119}Sn-NMR on the corresponding systems, where only one resonance was observed for the monomer at ~ –70.8 ppm. Details of the spectra are shown in fig.4.12 and will be discussed further alongside the corresponding polymer (see Chapter 3.2.2).

4.2.2.1.1.2 FTIR

FTIR spectroscopy provides further insight into these homologous monomers as show in fig.4.9 The Si-containing monomers were discussed in detail in Chapter 3. For the germanium-based monomer, characteristic bands were observed for Ge-phenyl [stretching (~1087 cm^{-1})] and Ge-^{n}butyl [stretching (~870 and 883 cm^{-1})] along with trans/gauche (Ge-^{n}Butyl) stretching respectively at ~653 and 564 cm^{-1}. For the tin-based monomer, characteristic asymmetric/symmetric Sn-^{n}butyl stretching were observed at ~584/505 cm^{-1} respectively. Other observed major vibrationsfor these Ge – and Sn-based monomers follow the same trends as their Si-based counterparts, as indicated in table 4.2 and 4.3.

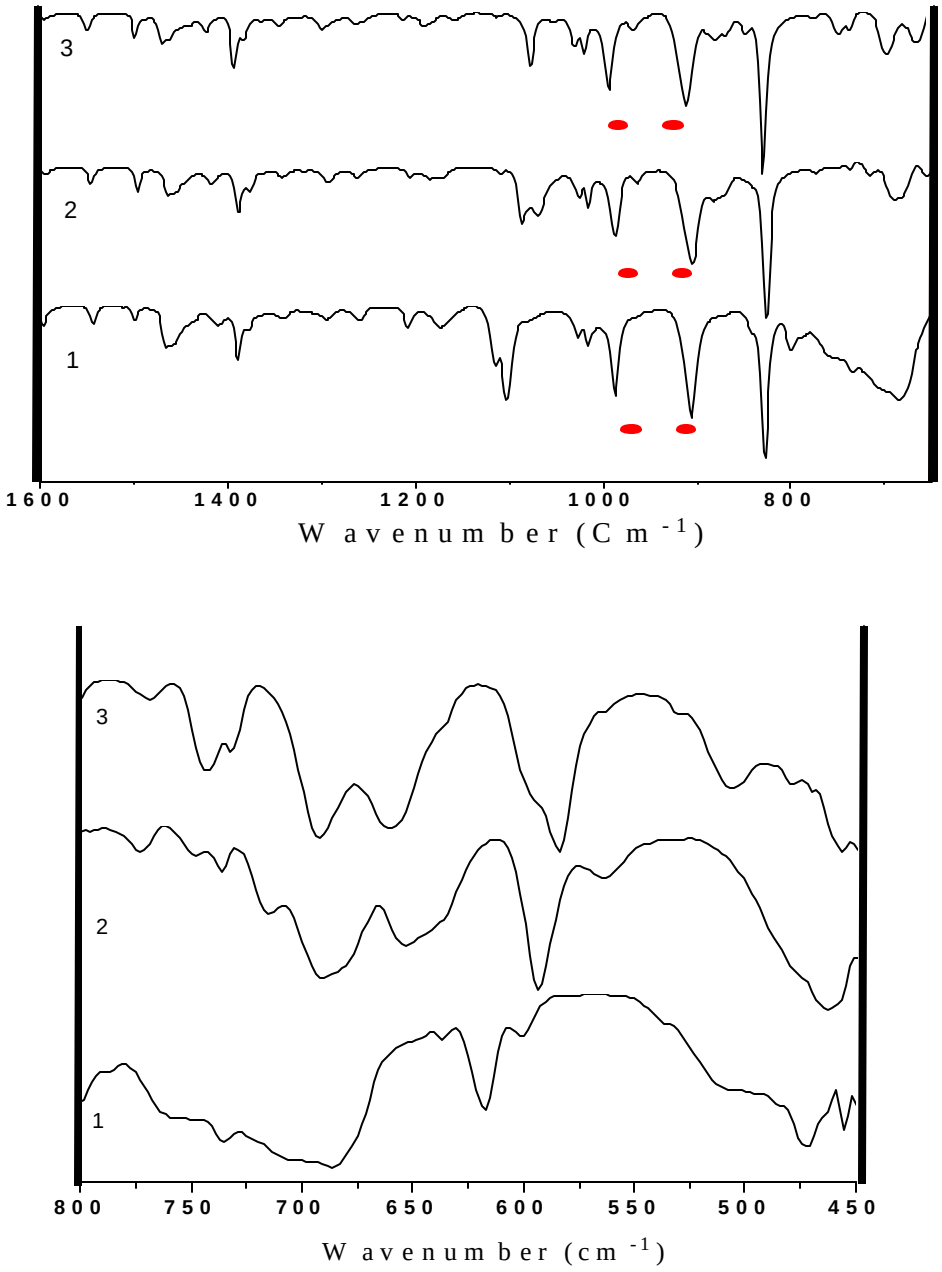

Fig. 4.9 FTIR spectra of distyryl dialkyl substituted silane (1) / germane (2) / stannane (3) monomers: (top) ATR-FTIR 1600-650cm^{-1}, (bottom): FTIR 800-450cm^{-1}**.**

4.2.2.2 ADMET polycondensates

4.2.2.2.1 Comments on solubility

All ADMET polycondensates showed significant solubility in common solvents e.g. hexanes, toluene, tetrahydrofuran, chloroform etc. due to presence of flexible silane/germane/stannane units in the main chain and respective alkyl side chains (intrinsic solvent).

4.2.2.2.2 Microstructure analysis

The characterizations of all oligo/polymers (and comparison with corresponding monomers) were performed by means of NMR, ATR-FTIR, UV/vis, photoluminescence, and TGA.

4.2.2.2.2.1 NMR (^{1}H, ^{13}C, ^{29}Si, ^{119}Sn)

The ^{1}H-NMR spectra for silane/germane/tin-based ADMET polycondensates are shown in fig. 4.10, together with the assignments and chemical shifts. The formation of polymer was marked by the appearance of a resonance at around 7.1 ppm, indicating the formation of internal vinylene bonds (3). As the resonance of 3 appeared the resonance from the terminal vinyl functional group, characteristic of monomers at around ~5.2, 5.7 and 6.7 ppm gradually decreased over the course of reaction. This resonance at 7.1 ppm is very close to the value for the internal vinylene signals for *trans*-stilbene as discussed for the Si-homolog above. Furthermore, there was no signal found at ~ 6.5 ppm indicating that there was no *cis* vinylene bond formed in the Ge and Sn cases either. Signals from the aliphatic protons of were slightly changed with a broadening of peaks. Resonance for the aromatic protons shifted slightly towards (~7.3-7.6 ppm to ~7.5-7.6 ppm) downfield as expected due to increased conjugation. It is important to note that in all cases, terminal

vinyl bonds (proton resonances at ~5.2, 5.7 and 6.7 ppm) were easily observed even for Mn ~7700g/mol.

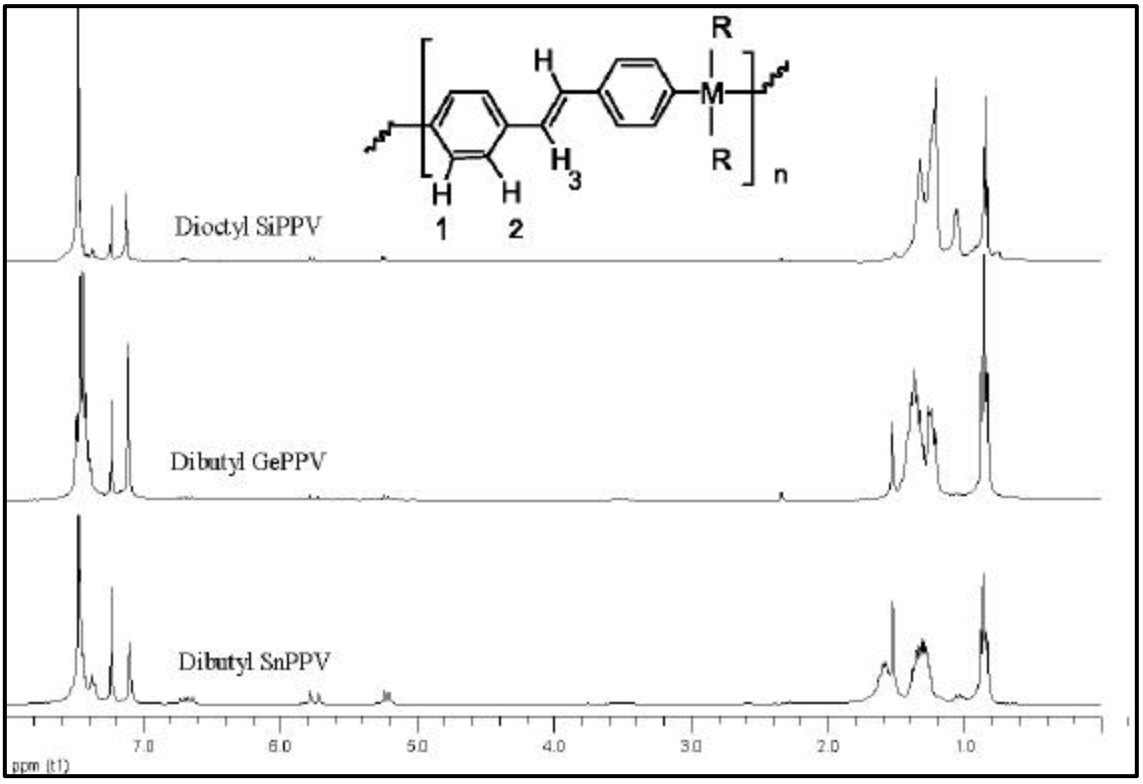

Monomer	R	M	1-2	3	Alkyl chain (R)
DiOctSiPPV	C_8H_{17}	Si	7.55-7.35	7.11	1.45-0.8
DiBuGePPV	C_4H_9	Ge	7.5-7.4	7.11	1.45-0.8
DiBuSnPPV	C_4H_9	Sn	7.6-7.4	7.10	1.65-0.8

Fig. 4.10 ^{1}H-NMR (with assignments) of distyryl dialkyl silane/germane/stannane oligo/polymers

^{13}C NMR data are shown in fig 4.11 with assignments and chemical shifts. These results are in line with the ^{1}H-NMR results. The formation of the internal vinylene bond (5) was observed as a resonance appearing at around ~128.8 ppm. As the resonance of (5) appeared the resonance from the terminal vinyl functional groups at ~136.8 and ~114.5

ppm, gradually decreased over the course of reaction. This resonance (at ~128.8 ppm) was very close to the value for the internal vinylene signals for *trans*-stilbene. No major differences for aromatic (~139-126 ppm) and aliphatic carbons (~ 33-10 ppm) between monomer and ADMET condensates were observed.

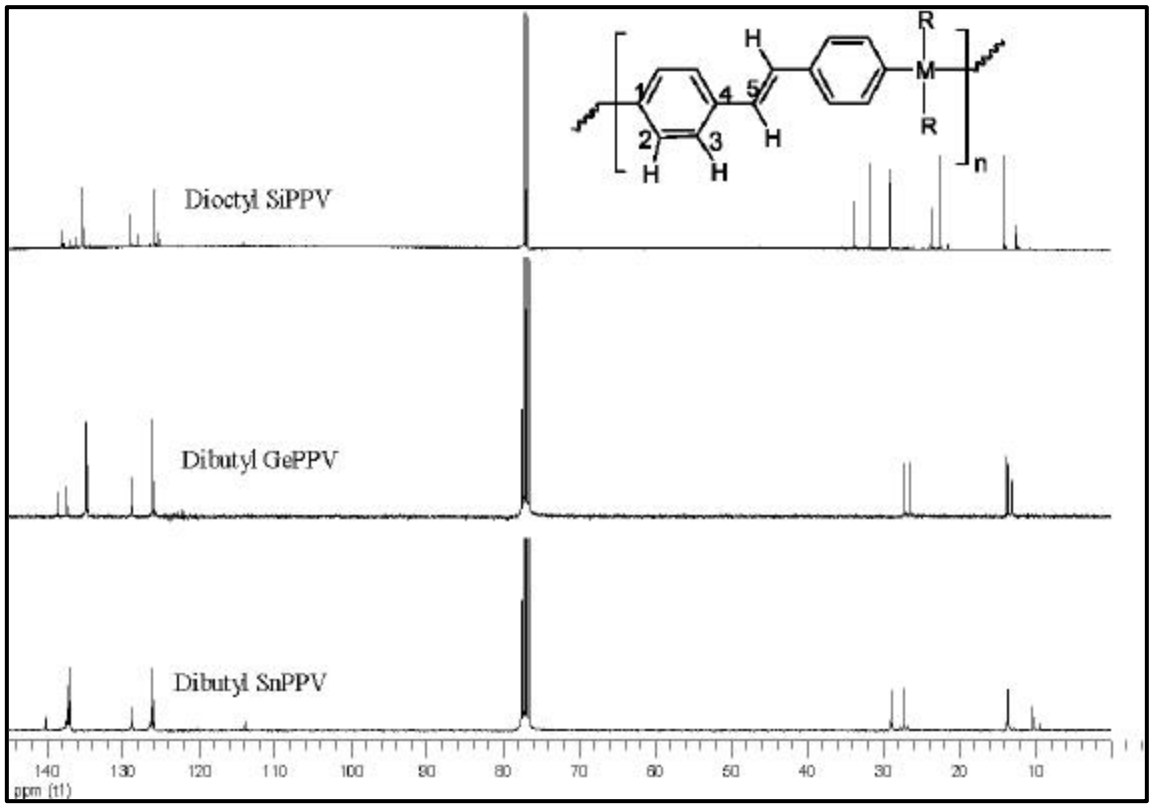

Monomer	R	M	1	2	3	4	5
DiOctSiPPV	C_8H_{17}	Si	136.3	135.2	125.8	137.9	129.0
DiBuGePPV	C_4H_9	Ge	137.4	134.8	126.0	138.5	128.8
DiBuSnPPV	C_4H_9	Sn	137.4	137.1	126.2	140.2	128.8

Monomer	R	M	Alkyl chain (R)
DiOctSiPPV	C_8H_{17}	Si	33.7, 31.9, 29.2, 29.1, 23.7, 22.7, 14.1, 12.5
DiBuGePPV	C_4H_9	Ge	27.2, 26.5, 13.7, 13.1
DiBuSnPPV	C_4H_9	Sn	28.9, 27.3, 13.6, 10.3

Fig. 4.11 ^{13}C NMR [with assignments] of distyryl dialkyl silane/germane/stannane ADMET products

^{119}Sn-NMR were carried out for all tin compounds and are shown in fig.4.12. Single resonances for both the dibutyl dibenzaldehyde stannane (~-69.6 ppm) and monomer (~-70.8 ppm) indicate the absence of other Sn species. ^{119}Sn-NMR resonances from the

ADMET condensates (~-70.5 ppm) were close to the corresponding monomers, with some broadening effect, probably due to C-Sn coupling. After polymerization, two tin resonances were observed indicating the presence of unreacted monomer residue.

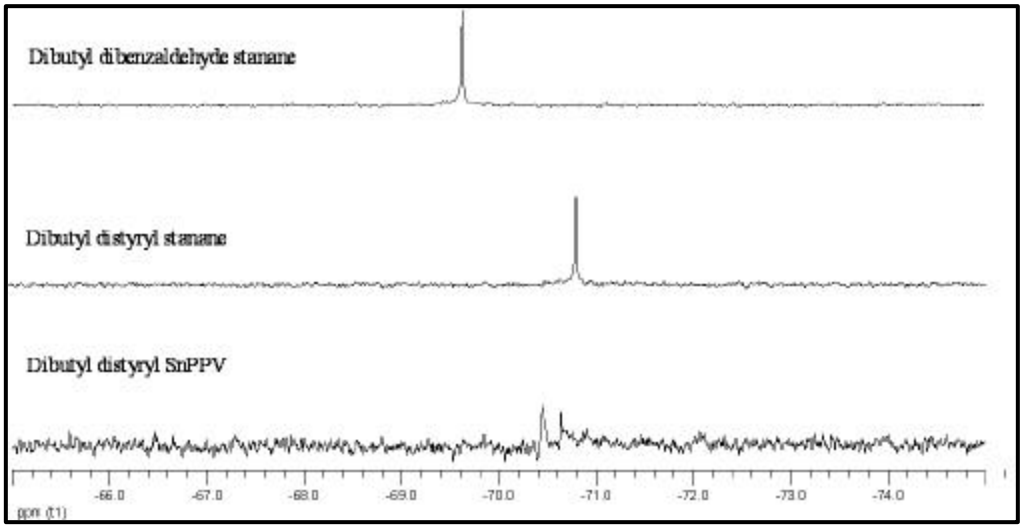

Fig. 4.12 ^{119}Sn-NMR of dibutyl dibenzaldehyde stannane, monomer and oligo/polymer of dibutyl distyryl stannane. [Tetramethyl tin (0 ppm) was used to calibrate the ^{119}Sn-NMR spectra]

For details in the Si-containing systems see earlier discussion.

4.2.2.2.2.2 FTIR

FTIR spectra of all polymers are shown in figures 4.13- 4.15. The Si-containing polymers were discussed in detail in Chapter 3. For germane-based polymers, characteristic bands for Ge-phenyl [stretching (~1090 cm^{-1})] and Ge-^{n}butyl [stretching (~873, 880 cm^{-1})] along with trans/gauche (Ge-^{n}Butyl) stretching respectively at ~654/559 cm^{-1} were observed. For tin-based polymer, characteristic asymmetric/symmetric Sn-^{n}butyl stretching respectively at ~593/503 cm^{-1} were observed. Other observed major vibrations

for these Ge and Sn-based systems follow the same trends as silane-based polymers, as indicated in tables 4.2 and 4.3.

Furthermore in all cases it was observed that out of plane bending vibration intensities (terminal vinyl bonds) at ~ 987 and ~906 cm^{-1} for monomers decreased significantly and a new signal appeared at ~ 965 cm^{-1}, indicating formation of internal *trans* vinylene bond (out of plane bending mode) during polymerization. ADMET results in *trans* configured double bonds for this type of system just as was described and discussed in earlier chapters.

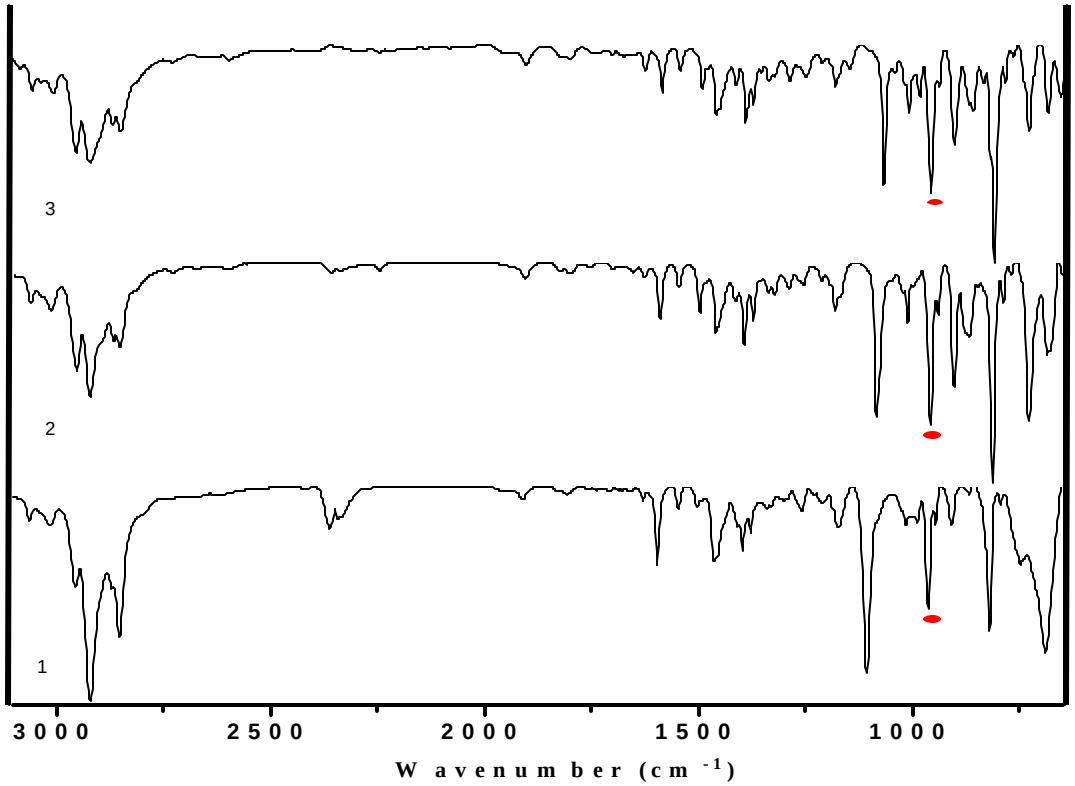

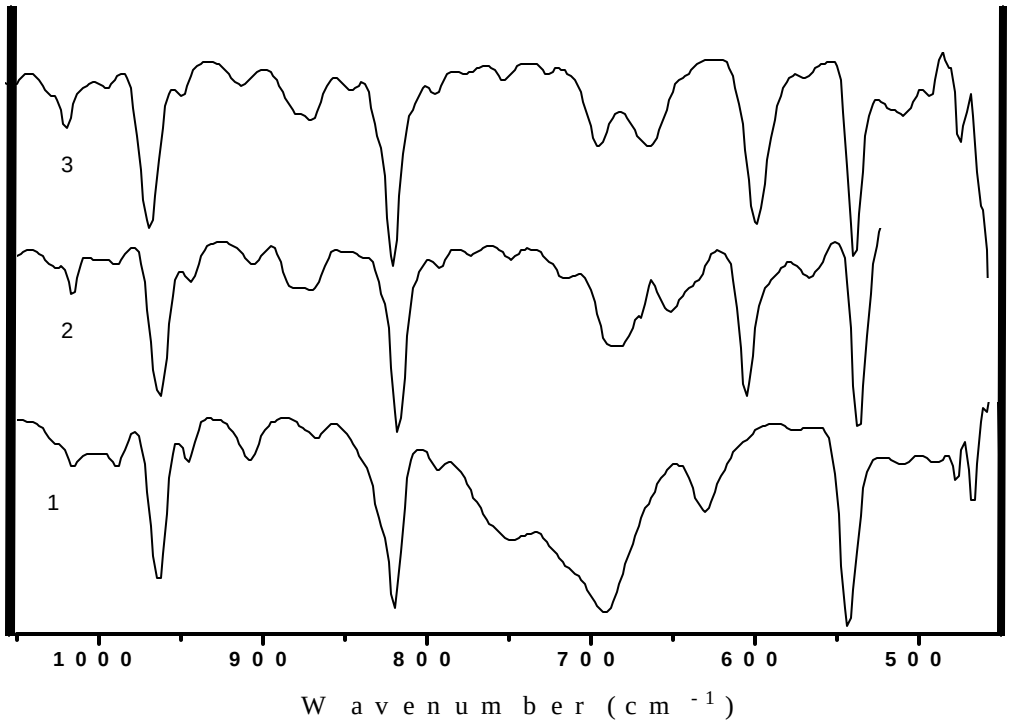

Fig. 4.13 FTIR of distyryl dialkyl silane (1) /germane (2) /stannane (3) oligo/polymers: (top) ATR-FTIR 3100-650cm^{-1}, (bottom): FTIR 1050-550cm^{-1}.

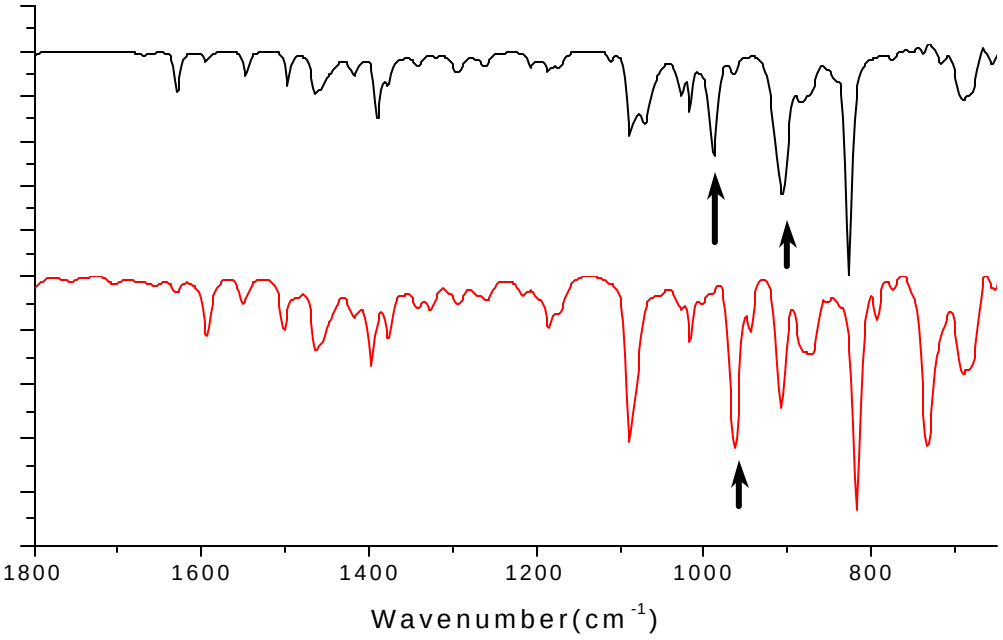

Fig. 4.14 Representative ATR-FTIR of DiButylGePPV monomer (black), polymer (red)

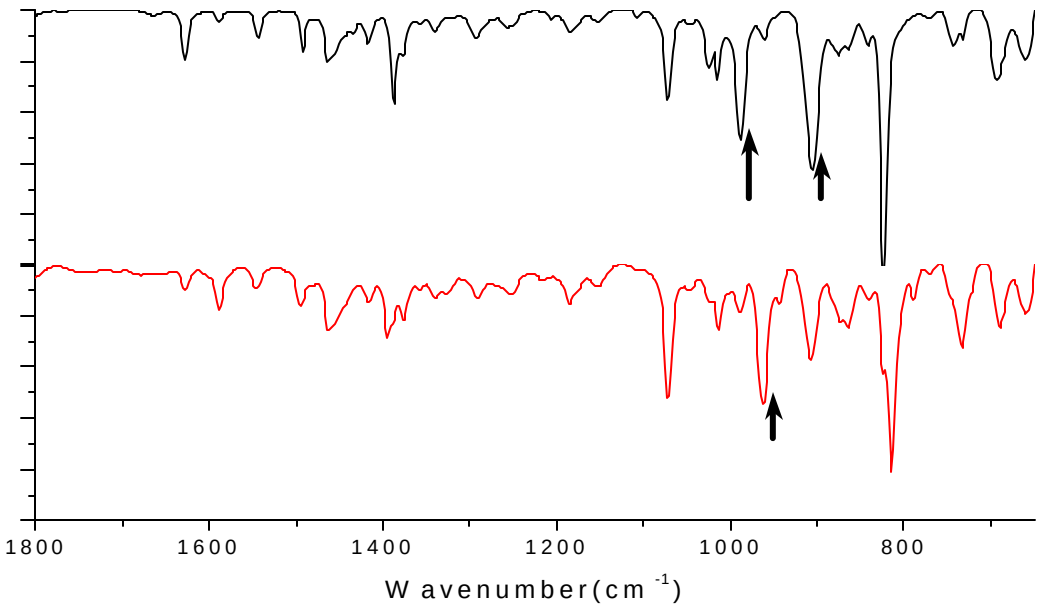

Fig. 4.15 Representative ATR-FTIR of SnPPV monomer (black) polymer (red)

4.2.2.2.2.3 Optical properties

The UV/vis absorption spectra were recorded and representative absorption spectra of similarly concentrated hexane solutions (normalized) are illustrated in fig.4.16. All monomers showed a similar absorption behavior, with a maxima ~ 257-259 nm. Although all ADMET condensates showed a similar trend with a maxima ~321-324 nm, slight differences in absorption behavior were observed at lower wavelengths. A shoulder was also observed ~ 340 nm which is probably due to some aggregation. Concentration dependent absorption studies (not shown) confirmed this analysis. There was a ~ 65 nm red shift (monomer to oligo/polymer) indicate the formation of *trans*-stilbene type units and thus an increase in conjugated length.

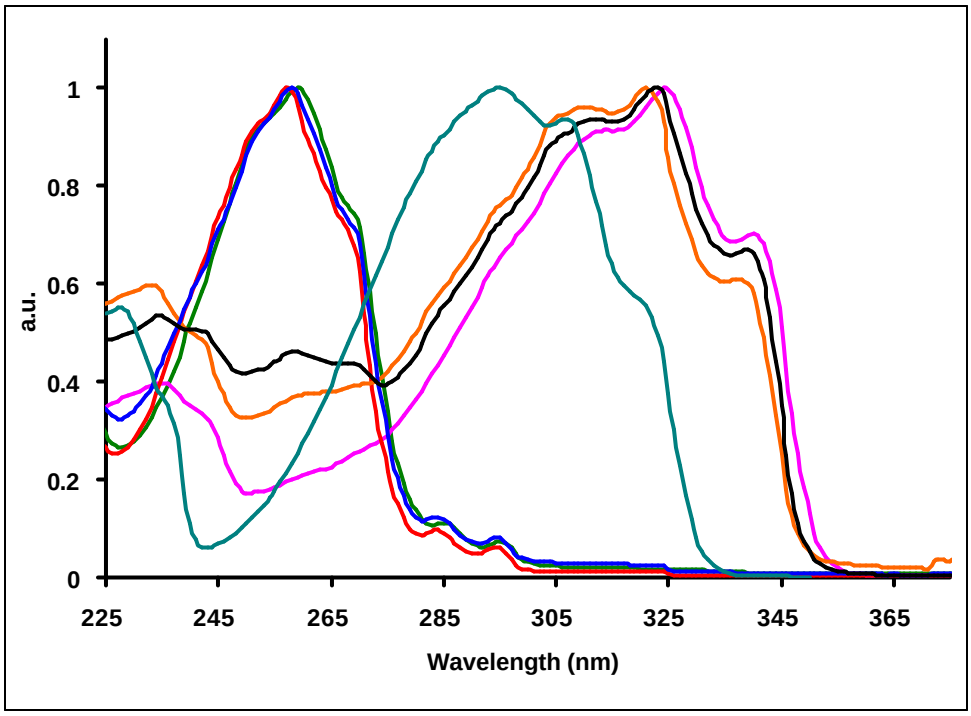

Fig. 4.16 Representative UV/visible absorption spectra (in hexane, concentration: 10^{-4} M) of dialkyl substituted silane/ germane/stannane monomer, oligo/polymer and trans-stilbene

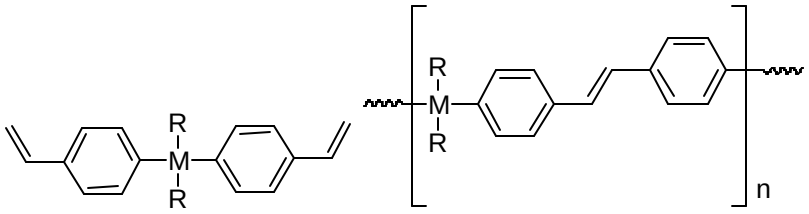

M	R	Maxima (nm)	
		Monomer	Oligo/polymer
Si	C_8H_{17}	259(—)	324(—)
Ge	C_4H_9	257(—)	321(—)
Sn	C_4H_9	258(—)	323(—)
Trans-stilbene		295(—)	

Representative photoluminescence spectroscopy results (normalized) are shown in fig. 4.17, and are in line with the UV/vis absorption data. The spectra were recorded as hexane solutions. All polymers showed a similar emission behavior, with a maxima ~ 306-307nm. Although all oligo/polymers showed a similar trend with a maxima ~363-366 nm, slight differences in emission behavior were observed at higher wavelengths. A shoulder was also observed ~ 380 nm which is probably due to some aggregation. A tail was also observed at higher wavelengths, also due to some aggregation. Concentration dependent photoluminescence studies (not shown) confirmed this analysis. Overall, there was a ~ 55-60 nm red shift from monomers to polymers indicating an increase in conjugation length. Absorption and emission showed minimal overlap. As discussed earlier, it is worth to note that *trans*-stilbene has absorption maxima ~295 nm and emission maxima ~347 nm. Thus the additional ~20-25 nm red shift (both in UV and PL) from *trans*-stilbene to the silane/ germane/ stannane systems indicates the effective participation of the heteratomic centers in the conjugation

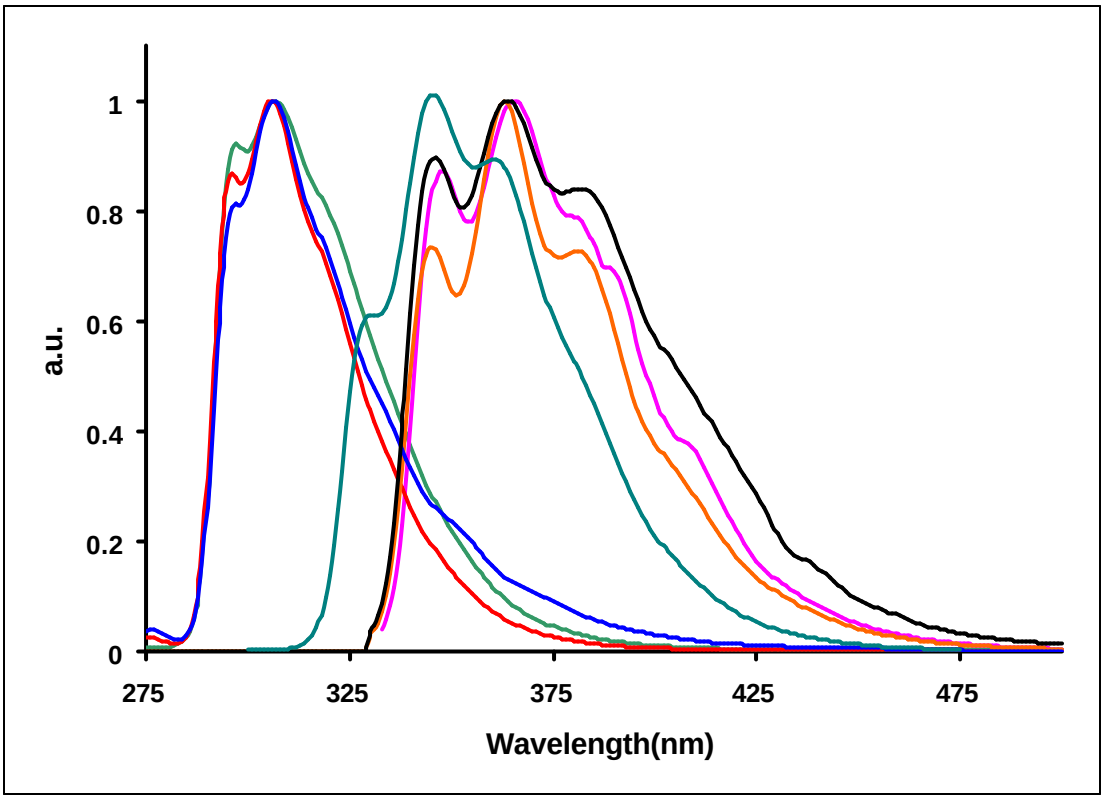

Fig. 4.17 Representative photoluminescence spectra (in hexane, concentration: 10^{-8} M) of dialkyl substituted silane/germane/stannane monomer, oligo/polymer and trans-stilbene (Excitation wavelength = corresponding absorption maxima of compound)

M	R	Maxima (nm)	
		Monomer	Oligo/polymer
Si	C_8H_{17}	306(—)	366(—)
Ge	C_4H_9	306(—)	363(—)
Sn	C_4H_9	307(—)	364(—)
Trans-stilbene		347 (—)	

Although a sequential increase in metallic character is expected from silane to germane to stannane based polymers, no significant differences in the absorption and emission spectra could be observed.

4.2.2.2.3 Thermal

Thermogravitymetric (TGA) analyses were carried out under inert atmosphere (up to 600 ^{0}C) and are shown in fig.4.18. In general, Ge substituted systems showed a relatively higher stability than Sn or Si based polymers.

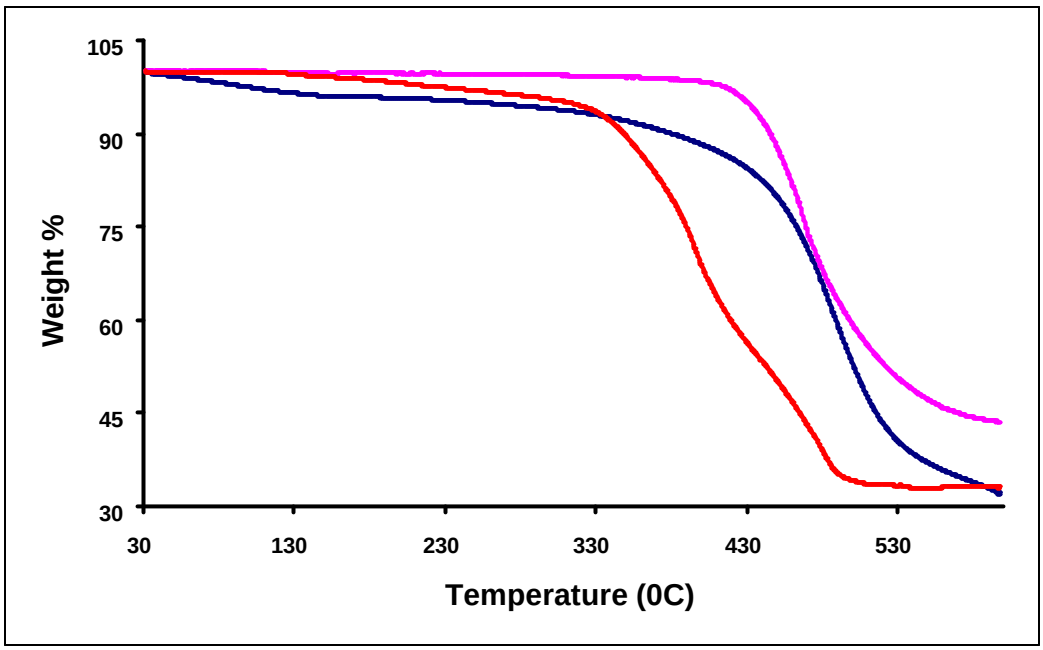

Fig. 4.18 Representative TGA thermogram of dialkyl substituted silane/germane/stannane oligo/polymers under inert atmosphere (scan rate 10 ^{0}C/ min.)

Oligo/polymer	5% weight loss Temperature (^{0}C)
DioctylSiPPV (—)	252
Dibutyl GePPV (—)	430
Dibutyl SnOPPV (—)	303

4.3 Conclusion and outlook

In conclusion, the synthesis of silicon/germanium/tin containing poly(p-phenylenevinylene) via ADMET polymerization has opened a new way to generate blue

light emitting polymers with the ability to avoid any structural impurities and thus improve the quality of the materials as indicated by NMR and GPC data.

Monomers were made from diacetal of p-bromobenzaldehyde, in all cases with high purity and moderately high yields. Polymerization of these monomers yielded higher molecular weight materials. Furthermore, analyses of GPC traces indicate the presence of individual short oligomeric components as a result of a typical polycondensation reaction.

4.4 Experimental

General Information.

All of the experiments using air/moisture sensitive materials were carried out in a nitrogen filled Labconco protector glove box and/or by the use of dry argon filled dual manifold (inert gas/ vacuum) using standard Schlenk line techniques. All glassware was cleaned and dried for at least 16h in an oven at 120 ^{0}C prior to use.

Chemicals.

BuLi [2.5M in hexane], 4-bromobenzaldehyde dimethylacetal (98 %), triphenylphosphonium methyl bromide, sodium sulfate, sodium bicarbonate, sodium chloride, acetic acid and Grubbs-Hoveyda catalyst were obtained from Aldrich. Dichlorodioctylsilane, dibutyldicholoro stannane, dibutyldicholoro germane were obtained form Gelest Inc. Solvents e.g. tetrahydrofuran (THF), toluene, hexane and diethyl ether were purchased from Fisher scientific. Except diethyl ether all other solvents were dried and degassed by “Pure Solv” solvent purification system (using activated alumina, copper catalyst, molecular sieves column.) by Innovative Technology

Inc. before use. All other chemicals were used as received. Column chromatography was carried out on silica gel 60 (70-230 mesh) form EMD Chemicals Inc.

Instrumentation.

200 MHz, 300 MHz or 600 MHz ^{1}H NMR, 50 MHz, 75 MHz or 150 MHz ^{13}C NMR, 120 MHz ^{29}Si NMR and 112 MHz ^{119}Sn NMR spectra were recorded in $CDCl_3$ on Varian Unity NMR instruments. $CDCl_3$ was used as an internal deuterium lock for ^{1}H NMR, ^{13}C NMR and ^{29}Si NMR spectra. All of the signals in the NMR spectra are reported in ppm.

UV-Visible absorption spectra were recorded using a Perkin Elmer Model 650 UV Spectrophotometer with 1-cm path length cells. The samples were prepared with HPLC grade chloroform ("Spectrasolv") in a sample cell.

Infrared spectra were recorded on a Tensor 27 Fourier Transformed Infrared spectrometer from Bruker optics using a Pike ATR accessory; data was processed and analyzed by OPUS software.

Photoluminescence spectra were recorded using a Horiba Jobin Yvon Fluoromax-3 spectrofluorometer with 1-cm path length cells. The samples were prepared with HPLC grade chloroform ("Spectrasolv") in a sample cell.

Thermogravimetric Analysis was carried out on a Hi-Res TGA 2950 Thermogravimetric Analyzer from TA Instruments using platinum pan with a heating rate 10 ^{0}C/ min under continuous flow of nitrogen. Differential scanning calorimetric measurement was performed on a DSC Q100 V7.3 Build 249 Differential Scanning Calorimeter from TA Instruments using aluminum pan with a scanning rate 10 ^{0}C/ min under nitrogen flow (50ml/ min).

GPC analysis was carried out on an Alliance GPCV 2000 (Waters) instrument equipped with four Waters Styragel HR columns, i.e. HR-1, HR-3, HR-4, and HR-5E. HPLC grade THF was used as eluent, at a flow rate of 1.0 mL/min at 40 ^{0}C. Measurements are relative to a calibration with polystyrene standards and third order relative calibration curve was used to measure the molecular weight of unknown samples.

Synthesis of dibenzaldehyde dioctyl silane

See chapter 3.4

Synthesis of dioctyl distyryl silane

See chapter 3.4

Synthesis of dibenzaldehyde dibutylgermane

40 mmol of 4-bromobenzaldehyde dimethylacetal was dissolved in 50 mL of dry THF. The temperature was lowered to –78 ^{0}C. 40mmol of ^{n}BuLi [2.5M in hexane, 16 mL] were slowly added. The reaction was stirred for 1.5h at –78 ^{0}C. 19.5 mmol of dichlorodibutyl germane in 5mL of THF were then added and the reaction was continued for 12h, and then gradually warmed up to room temperature. The reaction mixture was concentrated, washed with brine and extracted with diethyl ether twice. The organic fractions were combined, dried over sodium sulfate and concentrated to get a crude oil of the diacetal of dibenzaldehyde dibutylgermane.

This crude oil was then mixed with 20 mL of acetic acid and 25mL water and stirred for 5h. The resulting reaction mixture was neutralized with saturated sodium bicarbonate solution and then extracted with diethyl ether. The organic fraction was further washed

with brine, dried over sodium sulfate and concentrated to afford the dibenzaldehyde dibutylgermane as light yellow oil. Yield 85% [based on dichlorogermane]

^{1}H-NMR ($CDCl_3$, ppm): 0.84 (t, *J*= 6.7Hz, 6H), 1.25- 1.45(m, 12H), 7.59(d, *J*=7.86 Hz, 4H), 7.82(d, *J*=7.72 Hz, 4H), 9.99(s, 2H). ^{13}C-NMR ($CDCl_3$, ppm): 192.39, 147.06, 136.4, 134.82, 128.82, 33.52, 26.95, 26.21, 13.55, 12.77.

Synthesis of distyryl dibutylgermane

To a suspension of 35mmol of triphenylphosphonium methyl bromide in 100mL of dry THF 30 mmol of n-BuLi [2.5M in hexane, 12mL] was slowly added at 0 ^{0}C. The reaction mix was stirred for 3h. To this resulting solution 10 mmol of dibenzaldehyde dibutylgermane dissolved in 10 mL of dry THF was slowly added at 0 ^{0}C. The resulting mixture was stirred for 12h and then was with brine solution. The organic phase was extracted with diethyl ether twice, dried over sodium sulfate and concentrated to get a crude oil of the distyryl dibutyl germane, which was purified by passing through a silica gel using hexane as an eluent. Yield 60 %

^{1}H-NMR ($CDCl_3$, ppm 0.95(t, *J*=7.2Hz, 6H), 1.0- 1.53(m, 12H), 5.31(d, *J*=10.87Hz, 2H), 5.84(d, *J*= 17.61 Hz, 2H), 6.77 (dd, *J*= 10.87Hz, 17.61Hz, 2H), 7.46(d, *J*=7.98 Hz, 4H), 7.5(d, *J*= 8.01 Hz, 4H). ^{13}C-NMR ($CDCl_3$, ppm): 138.53, 137.61, 136.86, 134.62, 125.74, 113.91,27.17,26.44,13.68,13.07

Synthesis of dibenzaldehyde dibutylstannane

40 mmol of 4-bromobenzaldehyde dimethylacetal was dissolved in 50 mL of dry THF. The temperature was lowered to –78 ^{0}C. 40mmol of ^{n}BuLi [2.5M in hexane, 16 mL] were slowly added. The reaction was stirred for 1.5h at –78 ^{0}C. 19.5 mmol of dichlorodibutyl stannane in 5mL of THF were then added and the reaction was continued for 12h, and

then gradually warmed up to room temperature. The reaction mixture was concentrated, washed with brine and extracted with diethyl ether twice. The organic fractions were combined, dried over sodium sulfate and concentrated to get a crude oil of the diacetal of dibenzaldehyde dibutyl stannane.

This crude oil was then mixed with 20 mL of acetic acid and 25mL water and stirred for 5h. The resulting reaction mixture was neutralized with saturated sodium bicarbonate solution and then extracted with diethyl ether. The organic fraction was further washed with brine, dried over sodium sulfate and concentrated to afford the dibenzaldehyde dibutyl stannane as light yellow oil. Yield 85%

[Calculation based on dichlorostannane]

^{1}H-NMR ($CDCl_3$, ppm): 0.86 (t, *J*= 7.3 Hz, 6H), 1.36(m, 4H), 1.6(m, 8H), 7.64(d, *J*=7.64 Hz, 4H), 7.81(d, *J*=7.97 Hz, 4H), 9.99 (s, 2H). ^{13}C-NMR ($CDCl_3$, ppm): 192.58, 149.57, 137.16, 136.37, 128.83, 33.52, 28.76,27.21 13.47, 10.57.

^{119}Sn-NMR ($CDCl_3$, ppm): -69.62

Synthesis of distyryl dibutylstannane

To a suspension of 35mmol of triphenylphosphonium methyl bromide in 100mL of dry THF 30 mmol of n-BuLi [2.5M in hexane, 12mL] was slowly added at 0 ^{0}C. The reaction mix was stirred for 3h. To this resulting solution 10 mmol of dibenzaldehyde dibutyltin dissolved in 10 mL of dry THF was slowly added at 0 ^{0}C. The resulting mixture was stirred for 12h and then concentrated in vacuum. Hexane was added to the residual paste, and the mixture was passed through a mixture of celite and magnesium sulfate powder. The filtrate was washed with brine solution, extracted with diethyl ether twice, dried over sodium sulfate and concentrated to get a crude oil of the distyryl dibutyltin, which was

further purified by passing through a silica gel chromatography using hexane as an eluent. Yield 65 %

^{1}H-NMR ($CDCl_3$, ppm): 0.86 (t, *J*=7.14 Hz, 6H), 1.05-1.65 (m, 12H), 5.24(d, *J*=10.85 Hz, 2H), 5.77(d, *J*= 17.59 Hz, 2H), 6.7 (dd, *J*= 10.85 Hz, 17.59 Hz, 2H), 7.38(d, *J*=6.45 Hz, 4H), 7.46(d, *J*=7.4 Hz, 4H), ^{13}C-NMR ($CDCl_3$, ppm): 140.18, 137.52, 137.15, 136.92, 125.87, 113.88,28.9,27.32,13.62,10.31. ^{119}Sn-NMR ($CDCl_3$, ppm): -70.8

Typical Synthesis of oligo/poly(di-n-octyldiphenylsilyl phenylene vinylene) (OctSiPPV) (4).

See chapter 3.4

Synthesis of oligo/poly(dibutyl germyl phenylene vinylene) (BuGePPV)

Same procedure was followed as mentioned above for oligo/poly(di-n-octyldiphenylsilyl phenylene vinylene) to obtain a greenish-black semi solid material as product. See chapter 3.4

^{1}H-NMR ($CDCl_3$, ppm): 0.86(s, 7.2 Hz), 1.13-1.63(m), 7.12(s), 7.35-7.51(m). ^{13}C-NMR (solid state, ppm): 138.5, 137.4, 134.8, 128.8, 126, 27.2, 26.5, 13.7, 13.

Synthesis of oligo/poly(dibutyl stanyl phenylene vinylene) (BuSnPPV)

Same procedure was followed as mentioned above for oligo/poly(di-n-octyldiphenylsilyl phenylene vinylene) to obtain a greenish-black semi solid material as product. See chapter 3.4

^{1}H-NMR ($CDCl_3$, ppm): 0.86 (t, *J*=7.14 Hz), 1.21-1.41(m), 1.47-1.65(m), 5.22(d, *J*=10.89 Hz), 5.75(d, *J*= 17.59 Hz), 6.67 (dd, *J*= 10.85 Hz, 17.59 Hz), 7.1(s), 7.45-7.6(m). ^{13}C-NMR ($CDCl_3$, ppm): 140.2, 137.4, 137.1, 128.8, 126.2, 28.9, 27.3, 13.6, 10.3. ^{119}Sn-NMR ($CDCl_3$, ppm): -70.45, -70.64

Table 4.2 FTIR monomer and polymer of dibutyl distyryl germane

DibuGeppv-M	DibuGeppv	
3087		**C-H Str. (CH=)CH_2**
3061	**3064**	**C-H Str. (CH=)CR_2**
3020/3007	**3017**	**Ar. C-H Str.**
2956	**2957**	**Aliph. C-H Str..**
2925	**2927**	**Aliph. Asymm. vib -CH_2- /Ar. overtone**
2872	**2871**	**C-H stretch. -doublet asymm. and symm. of -CH_3 along with 2956.**
2855	**2856**	**Aliph. Symm. Vibr. -CH_2-**
1814		**Ar. overtone**
1667/1629	**1630**	**C=C str. with conjugation.**
1595	**1595**	**Ar. C=C Str. Vib.**
1546	**1551**	**Ar. C-H OOP bending**
1497	**1503**	**Ar. C=C Str. Vib.**
1463	**1464**	**Aliph. C-H bending of -CH_2-, Aliph./C-H asymm. Deform, Ar. C=C Str. Vib.**
1418	**1419**	
1389	**1398**	**-CH_3 deform.**
1377	**1378**	**Aliph. -CH_3 symm. bending vib.**
1341	**1341/1328**	**Aliph. C-H twisting of -CH_2-,**
1294	**1294**	**-CH_3 symm. Str.**
1262	**1261**	
1206		
1185	**1186**	
1110		**Ph. C-H in plane bending**
1087	**1090**	**Characteristics band for phenylgermenium comp.**
1026/1016	**1017**	**Aliph. C-C deform.**
988		**CH(=CH_2) OOP- deform.**
964	**945**	**Aliph. C-H deform**
	964	**t-vinylene OOP-deform.**
906	**908**	**CH(=CH_2) OOP- deform.**
883/870	**880/873**	**Characteristics band for n-butylgermenium comp.**
827	**820**	**1,4 Ph. C-H OOP bending**
	794	
773	**775**	
737/715		**Ar. C-H OOP bending.**
691	**690**	**Aliph. C-H rocking/ vib.**
653	**654**	**Trans (Ge-Butyl) streching**
593	**607**	
564	**569**	**Gauche (Ge-Butyl) streching**
462	**539**	

OOP = out of plane

Table 4.3 FTIR monomer and polymer of dibutyl distyryl stannane

DibuSnppv-M	DibuSnppv	
3087		C-H Str. (CH=)CH_2
3057	3056	C-H Str. (CH=)CR_2
3007	3008	Ar. C-H Str.
2957	2956	Aliph. C-H Str..
2926	2925	Aliph. Asymm. vib -CH_2- /Ar. overtone
2871	2870	C-H stretch. -doublet asymm. and symm. of -CH_3 along with 2956.
2852	2851	Aliph. Symm. Vibr. -CH_2-
1812		Ar. overtone
1665/1628	1628	C=C str. with conjugation
1589	1588	Ar. C=C Str. Vib.
1543	1546	Ar. C-H OOP bending
1492	1495	Ar. C=C Str. Vib.
1463	1462	Aliph. C-H bending of -CH_2-, Aliph./C-H asymm. Deform, Ar. C=C Str. Vib.
1417	1417	
1387	1394	-CH_3 deform.
	1376	Aliph. -CH_3 symm. bending vib.
1358	1358	
1340	1339	Aliph. C-H twisting of -CH_2-,
1293	1290	-CH_3 symm. Str.
1257	1253	
1206	1215	
1185	1185	
1152	1152	
1117		Ph. C-H in plane bending
1107		
1072	1071	
1046	1046	
1024/1014	1013	Aliph. C-C deform.
988		CH(=CH_2) OOP- deform.
961	943	Aliph. C-H deform
	962	t-vinylene OOP-deform.
907	906	CH(=CH_2) OOP- deform.
875	864	
841	840	1,4 Ph. C-H OOP bending
824	814	
769	789	
743	747	
732	720	Ph. C-H OOP bending.
692/660	689/658	Aliph. C-H rocking/ vib.
584	593/563	Sn-C assym. Str.
505	533/ 503	Sn-C ssym. Str.

5. Synthesis of conjugated polyazines using PPV building blocks

5.1 Objective

In this project we report on the efficient polycondensation of dialdehyde functional OPV building blocks with hydrazine via polyazine formation under mild conditions, affording soluble and processable materials. The products are rigid-rod type polymers featuring extended π- conjugated electron systems with integrated azine units and symmetrical side chain substitution at the OPV building blocks. The electronic character of the aromatic block can be tuned easily (i.e., size and type of aromat, different side chains). Specifically, the optimization of the coupling reactions of hydrazine with 2,5-diheptyloxy-1,4-diformylbenzene **1** and a homologous *alpha-omega*-aldehyde-functional trimeric diheptyloxy-OPV **2** (IUPAC: 2,5-Bis(heptyloxy)-1,4 -bis[2,5-bis(heptyloxy)-4-formyl-phenylene vinylene]benzene) are presented (scheme 5.1). **1** and **2** were synthesized in analogy to literature.[34] The polymer products **P1** and **P2** were analyzed in regard to size, microstructure, optical and electrochemical properties.

5.2 Results and discussion

5.2.1 Synthesis of polymers

Scheme 5.1 summarizes the general approach and representative synthetic conditions. Typically, **1** or **2** were combined with equimolar amounts of hydrazine (hydrazine as a 1.0 M solution in THF). The polymerizations were carried out in various solvents, i.e., chloroform, THF, benzene, toluene, and dichloromethane, at ambient (25 ^{o}C) or slightly elevated temperatures (up to 50 ^{o}C) in the case of **P2**, as illustrated in Table 5.1. Usually precipitate appears 2-3 h after the reaction starts. After an appropriate reaction time,

acetone was added to “deactivate” unreacted hydrazine and “cap” any amine chain ends. Volatiles were then removed under vacuum.

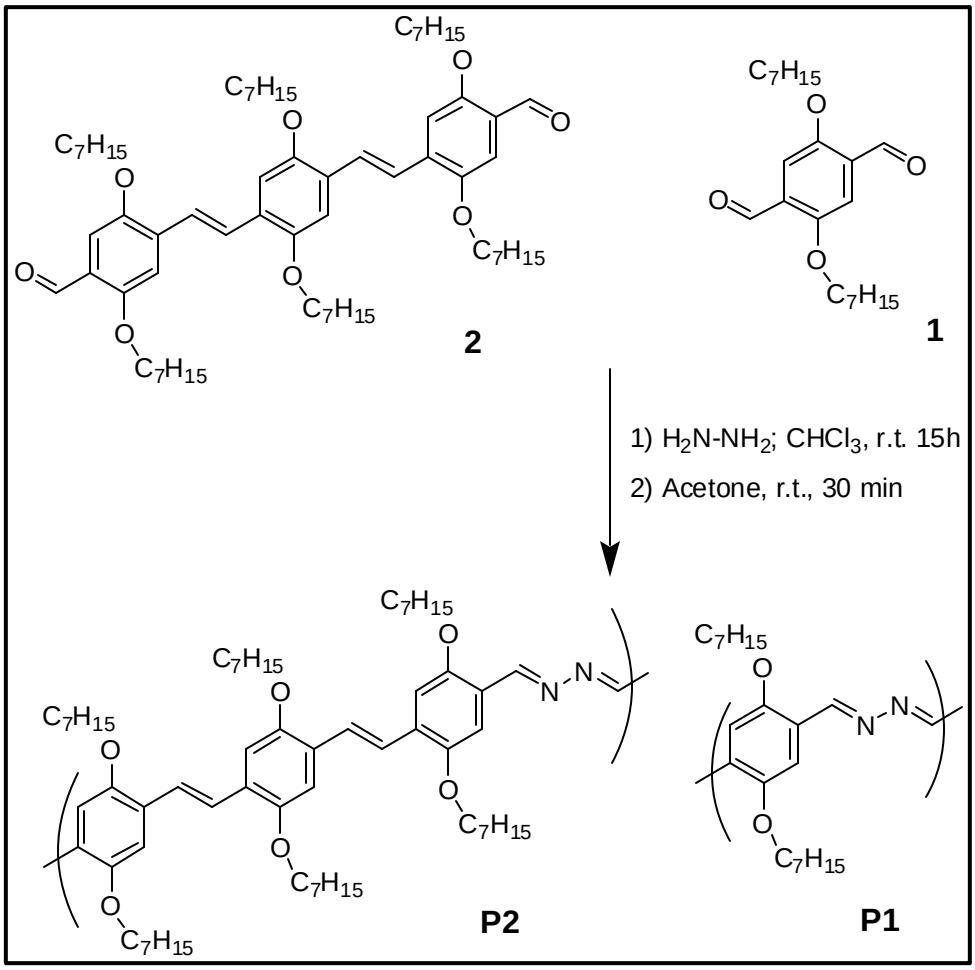

Scheme: 5.1. Synthesis of polyazines P1 and P2

In the case of **P1**, ~10-15 % by weight insoluble residues were obtained when using $CHCl_3$ or $CDCl_3$ as the main reaction solvent (Table 5.1, # 1-3). Molecular weight analysis was carried out via size exclusion chromatography (SEC) in THF, thus all presented molecular weights are representative only of the THF soluble fraction of the products (lower product solubility in THF). Reactions in benzene, toluene, THF, or dichloromethane as (Table 5.1, # 4-7) resulted in less soluble products **P1**, rendering SEC no longer meaningful. This observed behavior is counter-intuitive in the case of the

reaction in THF (Table 5.1, # 7), where the overall molecular weights were expected to be lower. In the case of the isolated product mixtures of **P2** (Table 5.1, # 8-10), the insoluble residues were less, i.e., ~5-10% by weight.

Table 5.1. Representative Syntheses of P1 and P2

Polymer	#	Conditions [§] Solvent/t [h]/ T [^{0}C]	Yield[1] [%]	M_n [2], M_n/ M_w
P1	1	$CHCl_3$/5/25	92	1418, 1.3
	2	$CHCl_3$/3/25[*]	96	1135, 1.2
	3	$CDCl_3$/3/25[**]	92	1251, 1.3
	4–7	benzene, toluene, CH_2Cl_2,THF/ 12/25	93-94	n.a.
P2	8	CH_2Cl_2/THF (1/1 v/v) /16/25	92	8701, 2.4
	9	$CHCl_3$/16/25	90	10468, 1.8
	10	THF/24/50	95	10324, 2.3

[§][**1**,**2**]/[hydrazine]=0.10M/0.10M,1.0M hydrazine in THF; [*] [1]/[hydrazine]=0.15M/0.10M; [**] [1]/[hydrazine]=0.030M/0.030M; [1] Isolated Mass; [2] THF-soluble fractions, relative to polystyrene standards; n.a. not applicable (insoluble in THF)

Also, the solubility of **P2** in THF was significantly higher than in the case of **P1**, making the presented molecular weights and distributions more representative. The increased solubility can be attributed to more flexible side chains per repeat unit.

Figures 5.1 and 5.2 summarize representative SEC- traces of the THF-soluble fractions of **P1** and **P2**, together with SEC- traces of the monomers **1** and **2** (**P1** traces normalized to the signal from the dimer fraction at ~36.5 min). The molecular weights M_n of the THF-soluble fractions of **P1** and **P2** typically are in the range of ~ 1,100-1,400 g/mol and ~8,700-10,500 g/mol respectively, relative to polystyrene standards. Longer reaction times lead to increase M_n's. Also, reactions in $CHCl_3$ resulted in higher molecular

weights compared to CH_2Cl_2 (Table 5.1, #8 versus #9). Even after 10 min of reaction time SEC traces of **P1** indicate significant product formation.

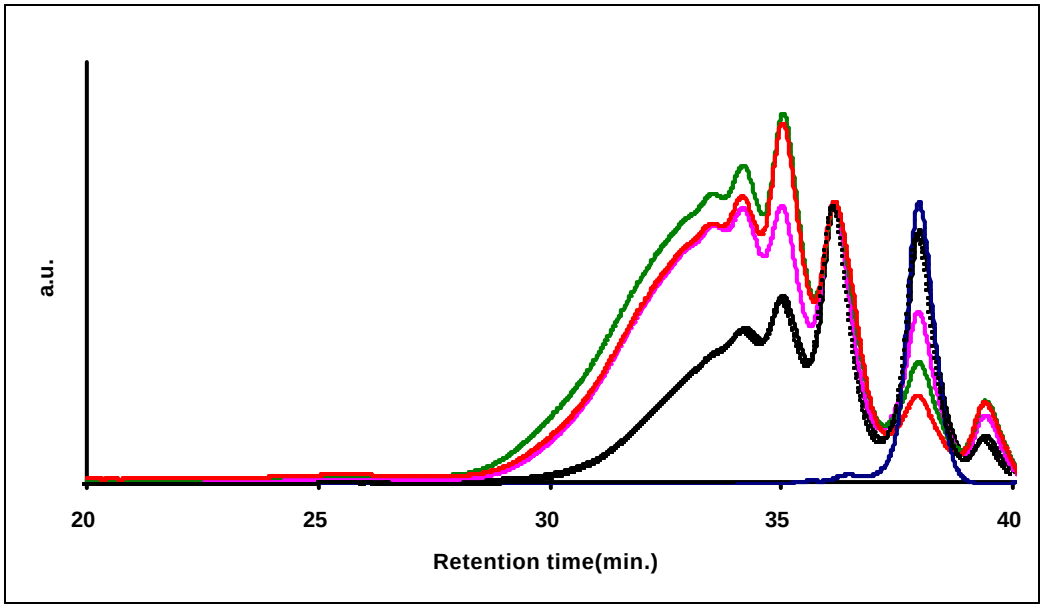

Fig. 5.1 GPC–Traces: 1(-) and P1 (Table 1, # 3) at different reaction times: 10 min (-), 30 min (-), 80 min (-), 170 min (-); B: 2(-) and P2 (Table 1): entry #'s 8(-), 9(-), 10 (-).

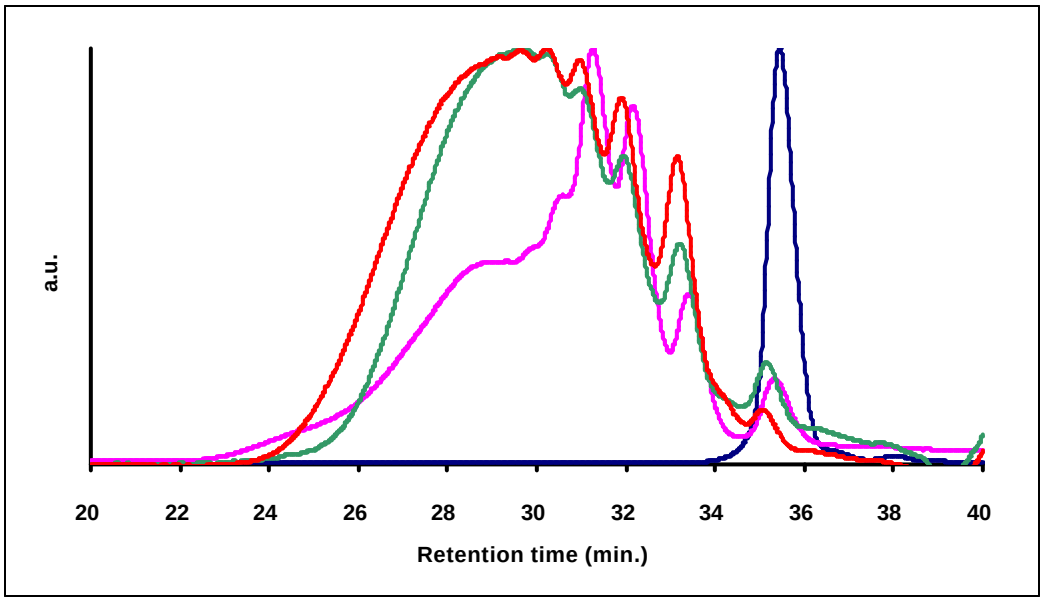

Fig. 5.2 GPC–Traces: 2(-) and P2 (Table 1): entry #'s 8(-), 9(-), 10 (-).

5.2.2 Characterization of materials
5.2.2.1 Microstructure analysis
5.2.2.1.1 NMR (^{1}H, ^{15}N)

^{1}H-NMR spectra (fig. 5.3) of the **P1** reaction mixtures exhibit characteristic resonances for the azine at ~9.05 ppm and aromatic protons at ~ 7.7 ppm almost immediately upon combination of the monomers. ^{15}N-NMR spectrum (gHMBC) (fig.5.4) confirms the presence of only one nitrogen species with a single resonance at ~ 376 ppm, corresponding to the *s*-trans conformer with respect to the C=N-N=C linkage, and yielding an efficiently delocalized electron system. We always observe residual signal intensity from aldehyde-protons in the spectra of **P1** and **P2**. These signals at ~10.5 ppm are due to unreacted monomers **1** and **2** in the condensation mixtures (also observed in the SEC traces of **P1** and **P2**, at ~38 min and ~35.5 min respectively). No chain-end specific aldehyde protons could be assigned via NMR. In the case of **P2** (fig 5.5), the

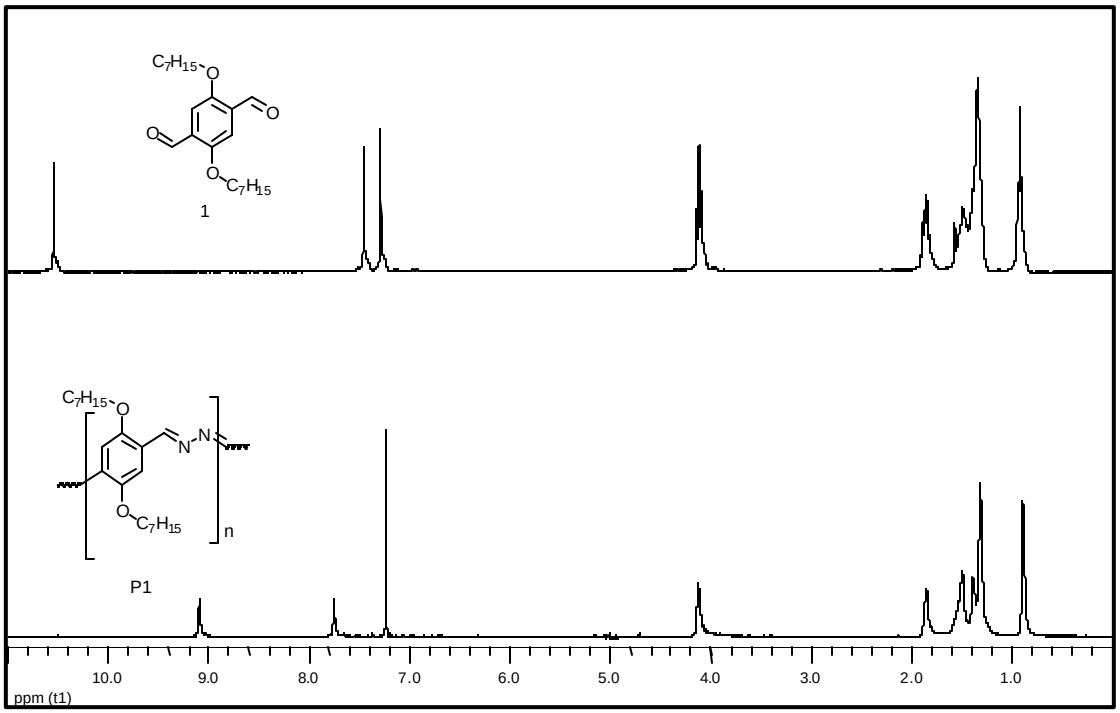

Fig. 5.3 Representative ^{1}H-NMR spectra of **1**(top) and **P1** (bottom)

azine proton resonance is observed at ~9.15 ppm, also corresponding to the *s*-trans conformation. This is corroborated by ^{15}N-NMR (fig 5.6) with one single resonance at ~373 ppm. Integration of the NMR – signals confirms the presence of two azine protons per repeat unit in **P1** and **P2**.

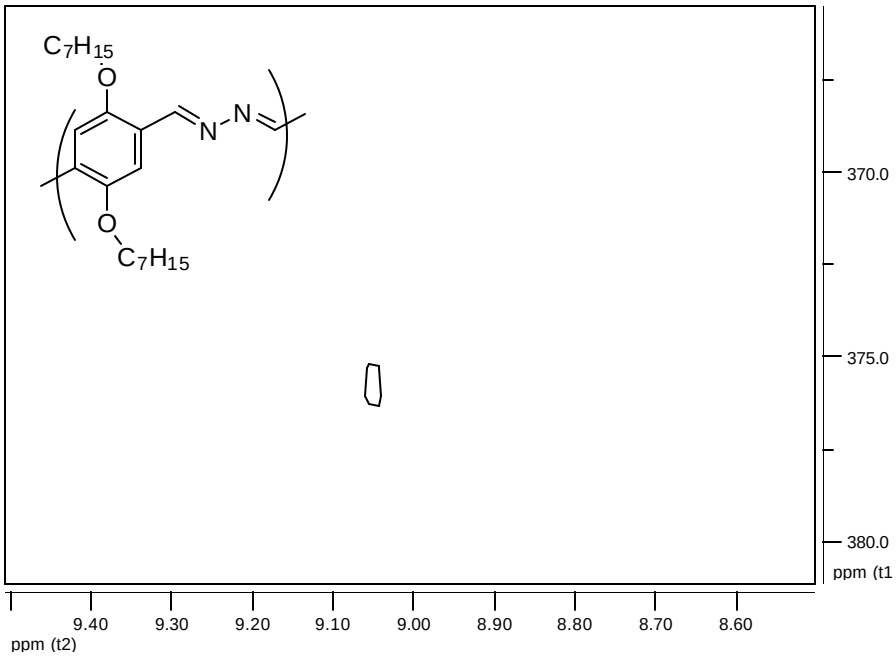

Fig. 5.4 Representative 2D ^{1}H-^{15}N-NMR-spectra of **P1**

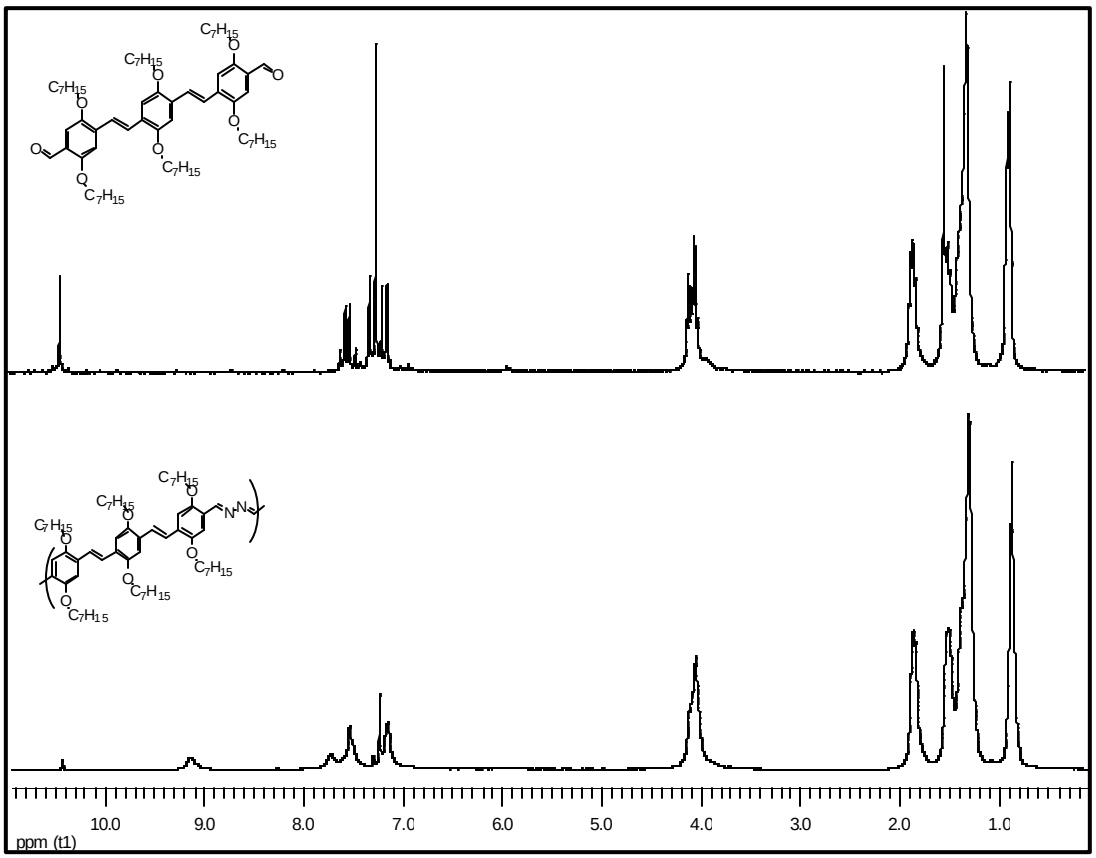

Fig. 5.5 Representative ^{1}H-NMR spectra of **1**(top) and **P1** (bottom)

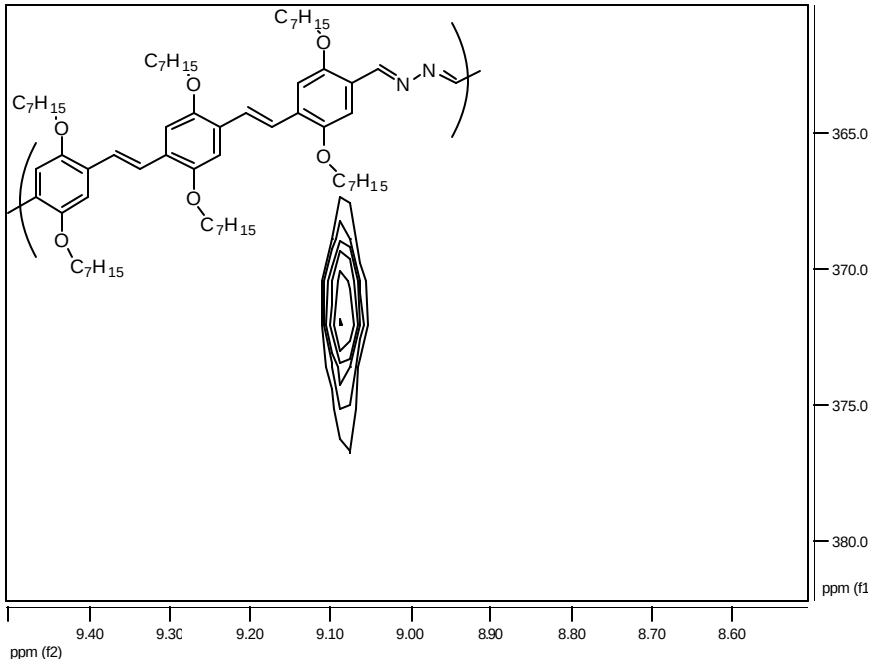

Fig. 5.6 Representative 2D ^{1}H-^{15}N-NMR spectra of **P2**

5.2.2.1.2 FTIR

ATR/FTIR spectra of **1**, **2**, **P1**, and **P2** (fig. 5.7 and 5.8) indicate the strongly reduced C=O stretching band at 1678 cm^{-1} and the appearance of C=N stretching at 1604 cm^{-1} in **P1** and at 1612 cm^{-1} in **P2** (visible as a shoulder on the C=C stretching at 1595 cm^{-1}). Also, in **P1** there is a noticeable change of the aromatic out-of-plane deformation (875 cm^{-1}), relative to 1 (893 cm^{-1}), and of the aromatic C-H deformations at 1194 and 1036/1017 cm^{-1} versus 1214 and 1039/1006 cm^{-1} respectively. These changes are less pronounced in **P2** due to the larger aromatic segment. The strong C=O vibration is always visible in both products, in accordance with the less sensitive NMR spectra.

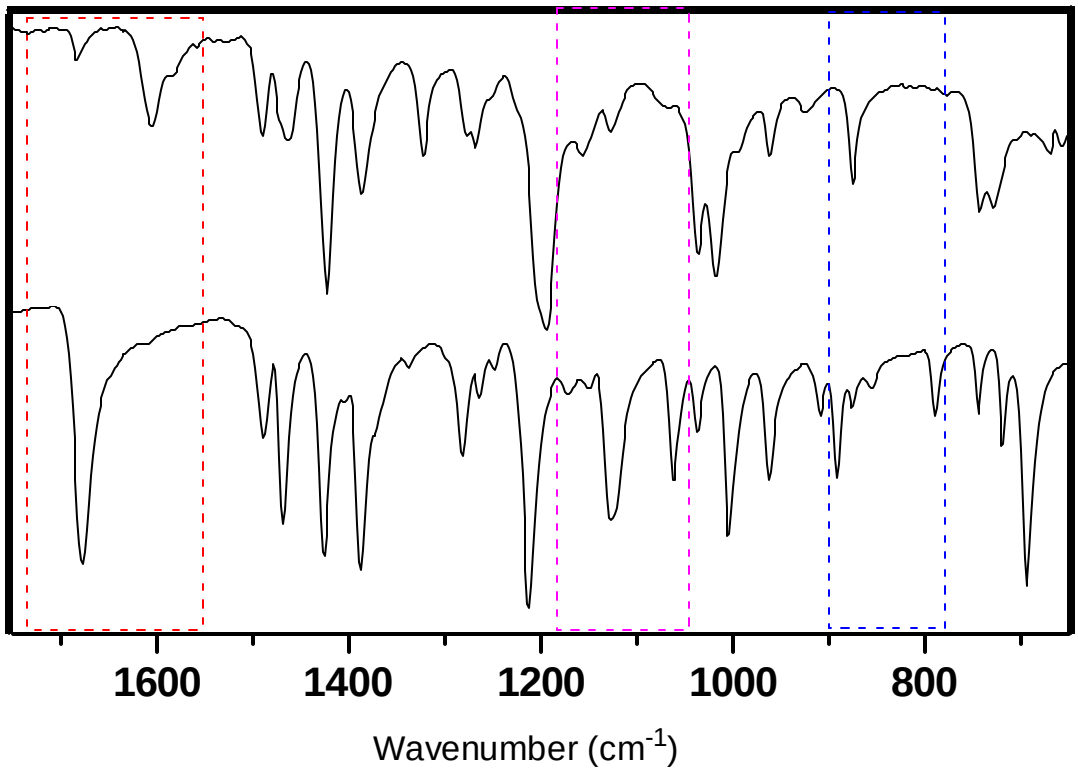

Fig. 5.7 Representative ATR-FTIR (1750-650 cm^{-1}) spectra of **P1** (top) and **1** (bottom).

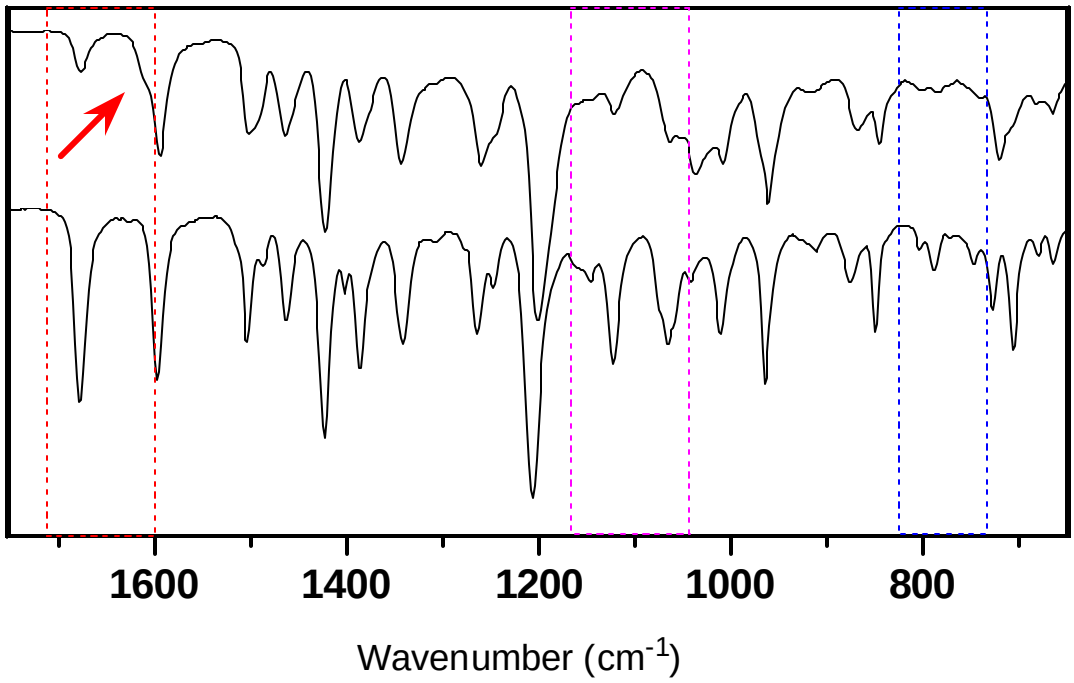

Fig. 5.8 Representative ATR-FTIR (1750-650 cm^{-1}) spectra of **P2** (top) and **2** (bottom).

5.2.2.1.3 Optical properties

The optical properties of **P1** and **P2** were investigated in chloroform (Figure 5.9, 5.10 and 5.11) and THF. Absorptions in $CHCl_3$ show the expected red shifted maxima in **P1** and **P2** (455 and 487 nm respectively) relative to the starting compounds **1** and **2** (404 and 447 nm respectively). This is due to the extended conjugation through *trans*-configured azine double bonds and the aromatic building blocks. The overall shift from **1** to **P1** is larger than the shift from **2** to **P2** (-0.344 versus -0.231 eV, respectively because the chain extension by adding a repeat unit to **1** is a larger change relative to the existing conjugated system. No significant differences between the absorption behaviors of THF soluble and $CHCl_3$ soluble fractions (higher M_n) or between individual product batches were observed. Apparently, the maximum effective conjugation length has been

achieved, [35] yet the products remain soluble and processable. Corresponding solutions of **P1** and **P2** in THF (not shown) exhibit slightly blue-shifted absorption maxima at ~452 and ~482 nm. The observed emission behavior was analogous to the absorption, with maximum emission wavelengths for **1, P1** and **2**, **P2** at ~465, ~515 nm and ~518,~560 nm, respectively (**1**, **2** in Supporting Information). The emission spectrum of **P1** shows shoulders at ~544 and ~646 nm, probably due to aggregation. Similar long wavelength components are observed in the emission spectrum of **P2** (smaller shoulders at ~610 and ~650 nm).

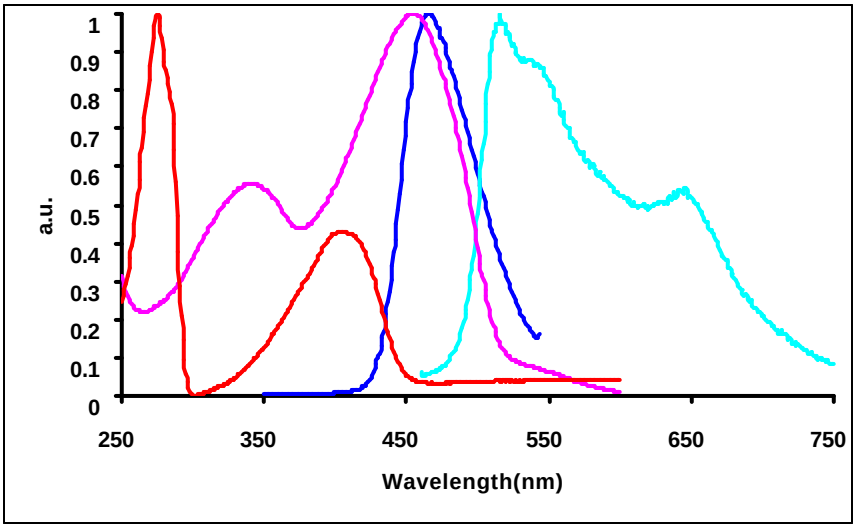

Fig. 5.9 UV and PL data for **1** and **P1** in chloroform.(—) 2,5-diheptyloxy-1,4-diformylbenzene (1)-UV,(—) **P1**-UV,(—) 2,5-diheptyloxy-1,4-diformylbenzene (**1**)-PL, (—)**P1**-PL

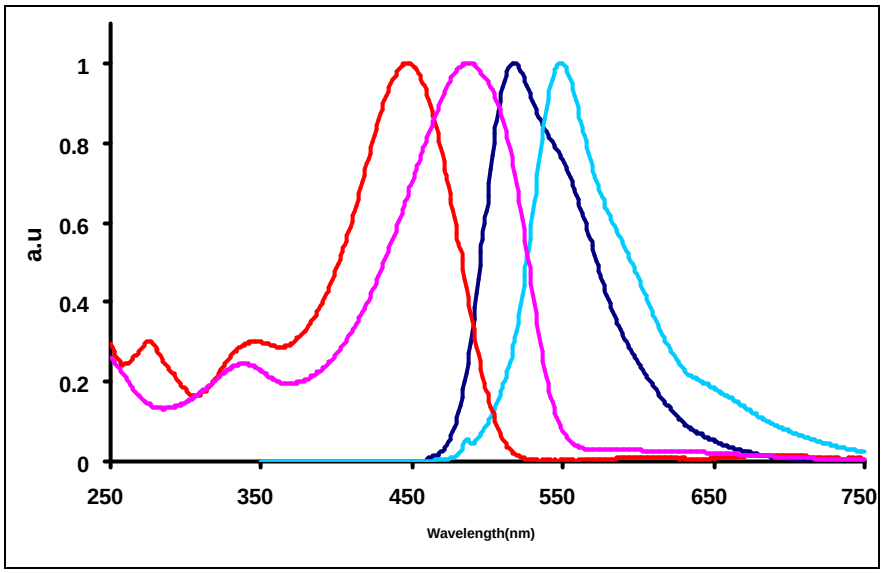

Fig. 5.10 UV and PL data for **2** and **P2** in chloroform.(—) 2,5-Bis(heptyloxy)-1,4-bis[2,5-bis(heptyloxy)-4-formyl-phenylenevinylene]benzene (**2**)-UV, (—) **P2**-UV (—) 2,5-Bis(heptyloxy)-1,4-bis[2,5-bis(heptyloxy)-4-formyl phenylenevinylene] benzene (**2**)-PL, (—) **P2**-PL

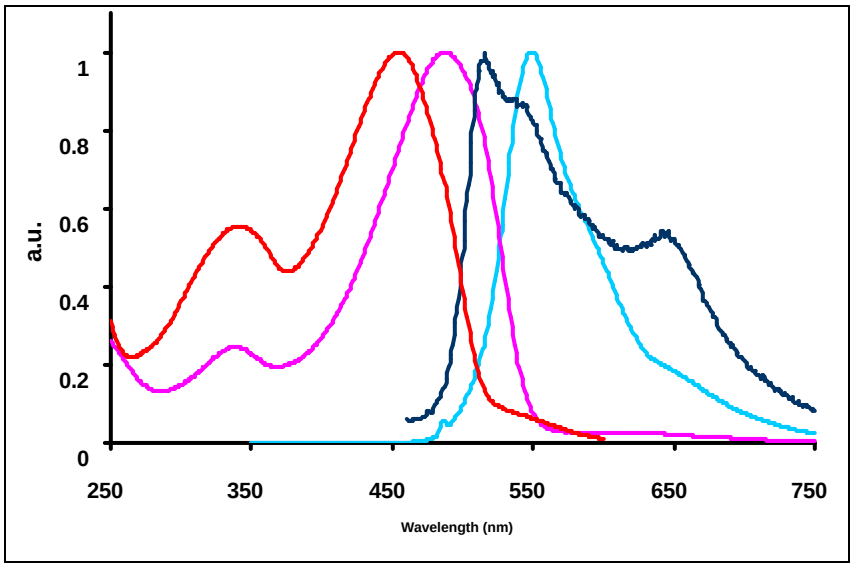

Fig. 5.11 UV and PL data for **P1** and **P2** in chloroform.(—) **P1**-UV, (—) **P2**-UV, (—) **P1**-PL, (—)**P2**-PL

5.2.2.3 Electrochemical

Electrical conductivity measurements indicate that they are insulators, which is supported by the absence of any broad near-IR bands. Differential pulsed voltammetry (DPV) of **P2** film on a Pt electrode was preformed to investigate the electrochemical characteristics. A

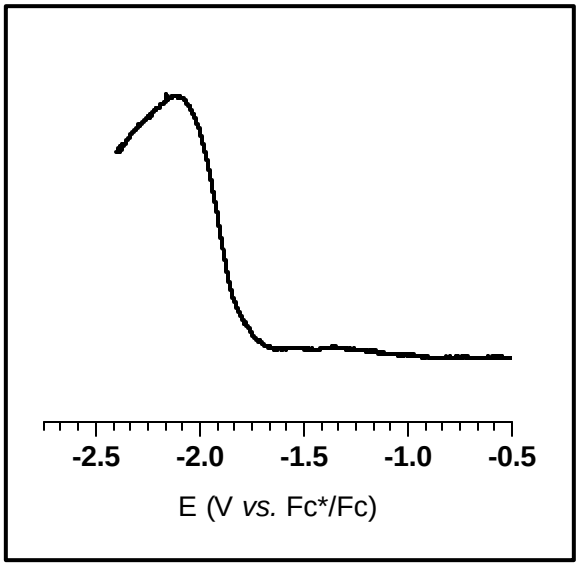

Fig. 5.12 DPV data for **P2** (film).

representative DPV reduction scan is shown as the in fig.5.12. The reduction (*n*-doping) occurred at -2.29V, versus the Fc^{+}/Fc (Fc=ferrocene) couple. Repeating the reduction cycle between 0 and -2.5V leads to gradual degradation of the sample. An oxidation scan (tested from 0 – 2V) results in an irreversible oxidation, indicating that the polymer **P2** has more *n*-type characteristics, whereas conjugated polymers of the PPV type usually display *p*-type behaviors.

5.3 Conclusion and outlook

In summary, we have presented an effective way to synthesize soluble and processable conjugated polymers containing easily customizable aromatic OPV units alternating with azine linkages, thus integrating nitrogen into the conjugated chain. The chains are *trans* configured at the azine bonds, and the azine represents the homologue of a butadienyl bridge in the conjugated chain, leading to a rare example of *n*-type conjugated polymer.

5.4 Experimental

General Information.

All of the experiments using air/moisture sensitive materials were carried out by the use of a dry argon filled dual manifold (inert gas/ vacuum) using standard Schlenk line techniques. All glassware was cleaned and dried for at least 16h in an oven at 120 ^{0}C prior to use.

Chemicals.

2,5-Bis(heptyloxy)terephthaldehyde and 2,5-Bis(heptyloxy)-1,4-bis[2,5-bis(heptyloxy)-4-formyl-phenylenevinylene]benzene were synthesized in analogy to the standard literature [35] using a different side chain substitution and purity was checked by ^{1}H NMR and ^{13}C NMR Solvents e.g. tetrahydrofuran (THF), toluene, hexane, dichloromethane, benzene[anhydrous] and chloroform [anhydrous] were purchased from Fisher scientific. Except acetone, benzene and chloroform all other solvents were dried and degassed by "Pure Solv" solvent purification system (using activated alumina, copper catalyst, molecular sieves column.) by Innovative Technology Inc. before use. Hydrazine [1.0 M solution in THF], acetone [99.9%], and other chemicals were purchased from Sigma-

Aldrich and used as received. Column chromatography was carried out on silica gel 60 (70-230 mesh) form EMD Chemicals Inc.

Instrumentation.

300 MHz or 600 MHz ^{1}H NMR spectra were recorded in $CDCl_3$ on Varian Unity NMR instruments. $CDCl_3$ was used as an internal deuterium lock for ^{1}HNMR spectra. ^{15}N NMR data was calibrated with respect to ^{1}H NMR with the help of the gyromagnetic ratios of ^{1}H and ^{15}N nuclei.

UV-Visible absorption spectra were recorded using a Perkin Elmar Cary Model 650 UV Spectrophotometer with 1-cm path length cells. The samples were prepared with spectroscopic grade chloroform in a sample cell.

Infrared spectra were recorded on Tensor 27 Fourier Transformed Infrared spectrometer from Bruker optics using a Pike ATR accessory and data were processed and analyzed by OPUS software.

Photoluminescence spectra were recorded using Horiba Jobin Yvon Fluoromax-3 spectrofluorometer with 1-cm path length cells. The samples were prepared with spectroscopic grade chloroform in a sample cell.

GPC analysis was carried out on Alliance GPCV 2000 (Waters) GPC instrument equipped with four Waters Styragel HR columns e.g. HR-1, HR-3, HR-4, HR-5E respectively. The instrument was calibrated using polystyrene standards. HPLC grade THF was used as eluent, at a flow rate of 1.0 mL/min at 40 ^{0}C. A third order relative calibration curve was used to measure the molecular weight of unknown samples.

Differential pluse voltametry were recorded on a PARSTAT 2273 potentiostat instrument (Princeton applied research, NJ). The working electrode in all cases consisted of an inlaid

platinum wire (diameter: 0.5mm^2) that was polished with polishing agent (alumina) and sonicated in water and absolute acetone for 2 min (3 times) and then dried before being use. A platinum wire served as a counter electrode, and a silver wire served as a quasi reference electrode. In order to get a thin film coating of polymer, the working electrode was dipped in the polymer solution (1-2 mmolar, in dichloromethane) and the electrode was dried in vacuum for 3h to remove solvent. All measurements were carried out in acetonitrile along with a supporting electrolyte (0.1 M [NBu4$^+$][BF4$^-$], in acetonitrile) to obtain each differential plused voltammogram. All potentials were calibrated by the addition of trace amounts of ferrocene (Fc) as an internal standard taking E (Fc/Fc+) = 0.4 V (with respect to a normal hydrazine electrode) and a scan rate of 20 mV /s was used in all cases. A blank run (with out any sample) was also performed under same condition above to account for possible traces of water.

Typical synthesis of (P1) 0.5 mmol of 2,5-Bis(heptyloxy)terephthaldehyde (1) was dissolved in 5 mL of appropriate dry solvent. 0.5 mmol of Hydrazine [1M solution in THF] was added to it. The reaction was stirred at room temperature until no/ traces amount of aldehyde peak in ^{1}H NMR was observed to ensure the completion of reaction. The reaction mixture was treated with little amount of acetone and the volatiles/solvents were evaporated resulting a deep yellow -orange color solid product. Isolated yield 96%.

P1: ^{1}H NMR (δ in ppm): 9.06(s, 2H), 7.72 (s), 4.11 (m), 1.85-1.1(m), 0.89(t).

^{15}N (δ in ppm): 376

Typical synthesis of (P2) 0.5 mmol of 2,5-Bis(heptyloxy)-1,4-bis[2,5-bis(heptyloxy)-4-formyl-phenylenevinylene]benzene (2) was dissolved in 5 mL of appropriate dry solvent.

0.5 mmol of Hydrazine [1M solution in THF] was added to it. The reaction was stirred at slightly elevated temperature (50 ^{0}C) and monitored by ^{1}H NMR. The reaction was continued until no more significant change in imine peak was observed. The reaction mixture was treated with little amount of acetone and the volatiles/solvents were evaporated resulting a deep yellow -orange color solid product. Isolated yield 92%.

P2: ^{1}H NMR (δ in ppm): 10.431 (s), 9.14(br), 7.72(br), 7.54(m), 7.31 (s), 7.16(br), 4.07(m), 1.87-1.1 (m), 0.87(t).

^{15}N (δ in ppm): 372.7

Table 5.2 ATR-FTIR data for **1, 2, P1, P2**

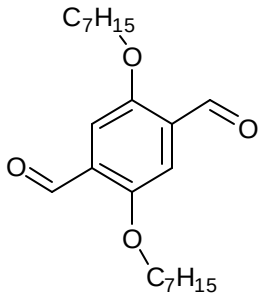

Monomer (1)	**Assignments**
3052	Aromatic C-H stretching
2946	Aromatic. C-H stretching -CH_3 stretching-doublet asymmetrical mode
2918	-CH_2 asymmetrical stretching vibration of H atom
2880	Aliphatic C-H stretching
2870	-CH_3 stretching-doublet symmetrical mode
2854	-CH_2 symmetrical stretching vibration of H atom
1678	Aromatic aldehyde C=O stretching vibration with extended conjugation
1490	Aromatic C=C stretching vibration
1469	Methylene C-H scissoring deformation -CH_3 asymmetrical bending vibration Aromatic C=C stretching vibration with extended conjugation [overlapped]
1428	-CH_3 asymmetrical bending vibration
1389	-CH_3 symmetrical bending vibration Aromatic -C(O)-H in plane bending .
1283	Phenylene. C-H in plane bending
1214	Asymmetric. C-O-C stretching for aromatic ether
1039	Symmetric C-O-C stretching for aromatic ether
857	1,2,4,5 substituted [benzene] Phenylene –CH- out of plane bending deformation
746	Phenylene. C-H out of plane bending
720	Aliphatic C-C vibration Long aliphatic chain -CH_2 rocking deformations
695	-CH_2 rocking

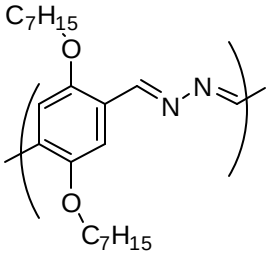

Polymer (P1)	Assignments
3012	Aromatic C-H stretching
2940	Aromatic. C-H stretching -CH_3 stretching-doublet asymmetrical mode
2927	-CH_2 asymmetrical stretching vibration of H atom
2880	Aliphatic C-H stretching
2866	-CH_3 stretching-doublet symmetrical mode
2853	-CH_2 symmetrical stretching vibration of H atom
1682	Unreacted aldehyde/ overtone from aromatic C-H
1604	Aromatic C=N stretching vibration with extended conjugation
1584	Aromatic C=C stretching vibration with extended conjugation
1489	Aromatic C=C stretching vibration with extended conjugation
1463	Methylene C-H scissoring deformation Aromatic C=C stretching vibration vibration with extended conjugation [overlapped]
	-CH_3 asymmetrical bending vibration
1422	-CH_2 symmetrical stretching vibration of H atom
1386	-CH_3 symmetrical bending vibration
1267	Phenylene. C-H in plane bending
	Asymmetric. C-O-C stretching for aromatic ether
1126	Symmetric C-O-C stretching for aromatic ether
875	1,2,4,5 substituted [benzene] Phenylene –CH- out of plane bending deformation
791	Phenylene. C-H out of plane bending
777	Aliphatic C-C vibration Long aliphatic chain -CH_2 rocking deformations
700	-CH_2 rocking

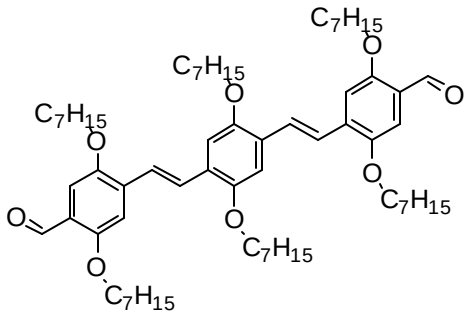

Monomer (2)	**Assignments**
3058	Aromatic C-H stretching
2955	Aromatic. C-H stretching -CH_3 stretching-doublet asymmetrical mode
2919	-CH_2 asymmetrical stretching vibration of H atom
2871	-CH_3 stretching-doublet symmetrical mode
2851	-CH_2 symmetrical stretching vibration of H atom
1677	Aromatic aldehyde C=O stretching vibration with extended conjugation
1597	Conjugated C=C stretching vibration
1503	Aromatic C=C stretching vibration
1463	-CH_2 C-H bending deformation -CH_3 asymmetrical bending vibration Aromatic C=C stretching vibration with extended conjugation [overlapped]
1422	-CH_3 asymmetrical bending vibration
1385	-CH_3 symmetrical bending vibration Aromatic -C(O)-H in plane bending .
1283	Phenylene. C-H in plane bending
1206	Asymmetric. C-O-C stretching for aromatic ether
1146	-CH_3 rocking vibration
1066	Symmetric C-O-C stretching for aromatic ether
964	Inter vinylene C=C out of plane deformation
848	1,2,4,5 substituted [benzene] Phenylene –CH- out of plane bending deformation
746	Phenylene. C-H out of plane bending
726	Aliphatic C-C vibration Long aliphatic chain -CH_2 rocking deformations
705	-CH_2 rocking

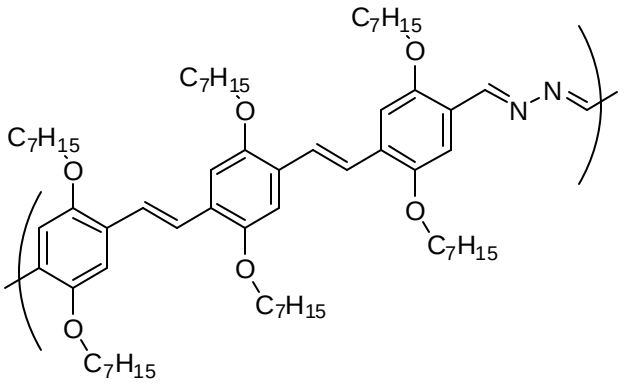

Polymer (P2)	**Assignments**
3058	Aromatic C-H stretching
2952	Aromatic. C-H stretching -CH_3 stretching-doublet asymmetrical mode
2921	-CH_2 asymmetrical stretching vibration of H atom
2871	-CH_3 stretching-doublet symmetrical mode
2852	-CH_2 symmetrical stretching vibration of H atom
1677	Aromatic aldehyde C=O stretching vibration with extended conjugation
1612	C=N stretching vibration with extended conjugation
1596	Conjugated C=C stretching vibration
1502	Aromatic C=C stretching vibration
1465	-CH_2 C-H bending deformation -CH_3 asymmetrical bending vibration Aromatic C=C stretching vibration with extended conjugation [overlapped]
1423	-CH_3 asymmetrical bending vibration
1388	-CH_3 symmetrical bending vibration Aromatic -C(O)-H in plane bending .
1203	Asymmetric. C-O-C stretching for aromatic ether
1146	-CH_3 rocking vibration
1066	Symmetric C-O-C stretching for aromatic ether
964	Inter vinylene C=C out of plane deformation
848	1,2,4,5 substituted [benzene] Phenylene –CH- out of plane bending deformation
726	Aliphatic C-C vibration Long aliphatic chain -CH_2 rocking deformations
705	-CH_2 rocking

6. References and Notes

1. Shirakawa, H.; Louis, E. J.; MacDiarmid, A. G.; Chiang, C. K.; Heeger, A. J. *J. Chem. Soc., Chem. Commun.* **1977**, 578.

2. (a) Skothein, T. A. Ed., *Handbook of Conducting Polymers*, Marcel & Dekker: New York; **1986**; Vol. 1 & 2 (b) Friend, R. H.; Gymer, R. W.; Holmes, A. B.; Burroughes, J. H.; Marks, R. N.; Taliani, C.; Bradley, D.D.C.; Dos Santos, D. A.; Bredas, J. L.; Logdlund, M.; Salaneck, W. R. *Nature* **1999**, *397*, 121 and references therein.

3. Tang, C. W.; Van Slyke, S. A. *Appl. Phys. Lett.* **1987**, *51*, 913.

4. (a) Burroughes, J. H.; Bradley, D. D. C.; Brown, A. R.; Marks, R. N.; Mackay, K.; Friend, R. H.; Burns, P. L.; Holmes, A. B. *Nature (London)* **1990**, *347*, 539 and references therein. (b) Ohmori, Y.; Uchida, M.; Muro, K.; Yoshino, K. *Jpn. J. Appl. Phys.* **1991**, *30*, L1941. (c) Gustafasson, G.; Cao, Y.; Treacy, G. M.; Klavetter, F.; Colaneri, N.; Heeger, A. J. *Nature (London)* **1992**, *357*, 477. (d) Grem, G.; Leditzky, G.; Ullrich, B.; Leising, G. *Adv. Mater.* **1992**, *4*, 36. (e) Akcelrud, L. *Prog. Polym. Sci.* **2003**, *28*, 875 and references therein.

5. Kraft, A.; Grimsdale, A. C.; Holmes, A. B. *Angew. Chem. Int. Ed.* **1998**, *37*, 402 and references therein.

6. (a) Baigent, D. R.; Greenham, N. C.; Gruener, J.; Marks, R. N.; Friend, R. H.; Moratti, S. C.; Holmes, A. B *Synth. Met.* **1994**, *67(1-3)*, 3 and references therein. (b) Dai, L.; Berthold, W.; Dong, L.; Tong, L.; Mau, A. W. H. *Adv. Mater.* **2001**, *13*, 915 and references therein.

7. (a) Skothein, T. A. Ed., *Handbook of Conducting Polymers*, Marcel & Dekker: New York; **1986**; Vol. 1 & 2 (b) Zhang, C.; Seggern, H. von; Parbaz, K.; Kraabel, B.; Schmidt, H. W.; Heeger, A. J. *Synth. Met.* **1994**, *62*, 35. (c) Berggrenm, M.; Inganas, O.; Gustafsson, G.; Rasmusson, J.; Andersson, M. R.; Hjertberg, T.; Wennerstrom, O. *Nature (London)* **1994**, *372*, 444. (d) Fisher, T. A.; Lidzey, D. G.; Pate, M. A.; Weaver, M. S.; Whittaker, D. M.; Skolnick, M. S.; Bradley, D. D. C. *Appl. Phys. Lett.* **1995**, *67*, 1355. (e) Chang, S. C.; Bharathan, J.; Yang, Y.; Helgeson, R.; Wudl, F.; Ramey, M. B.; Reynolds, J. R. *Appl. Phys. Lett.* **1998**, *73*, 2561. (f) Skotheim, T.A.; Elsenbaumer, R.L.; Reynolds, J.R. *Handbook of Conducting Polymers*, 2nd Ed.; Marcel Dekker: New York, **1998**. (g) Dai, L.; Mau, A. W. H. *J. Phys. Chem. B* **2000**, *104*,1891. (h) Zhang, X; Jenekhe, S. A. *Macromolecules* **2000**, *33*, 2069. (i) Kim, D. Y.; Cho, H. N.; Kim, C. Y. *Prog. Polym. Sci.* **2000**, *25*, 1089.

8. Kraft, A., Grimsdale, A.C.; Holmes, A.B. *Angew. Chem* **1998**, *110*, 416.

9. Petty, M. C.; Bryce, M. R.; Bloor, D. Ed., *Introduction to Molecular Electronics*, Edward Arnold: London **1995** and references therein.

10. Meier, H. *Angew. Chem.* **1992**, *104*, 1425.

11. Zerbi, G. Ed., *Organic Materials for Photonics: Science and Technology*, Elsevier: Amsterdam **1993** and references therein.

12. Lupton, J. M.; Samuel, I. D. W.; Beavington, R.; Burn, P. L.; Bassler, H. *Adv. Mater.* **2001**, *13*, 258.

13. (a) Bernius, M. T.; Inbasekaran, M.; O'Brien, J.; Wu, W. *Adv. Mater.* **2000**, *12*, 1737 and references therein. (b) Fumitomo, H.; Maria, A. D-G.; Schwartz, B. J.; Hegger, A. J. *Acc. Chem. Res.* **1997**, *30*, 430 and references therein.

14. Martin, R. E.; Diederich, F. *Angew. Chem* **1999**, *111*, 1444.

15. Meier, H.; Stalmach, U.; Kolshorn, H. *Acta Polymer*. **1997,** *48*, 379 and references therein.

16. Aviram, A.; Ratner, M. *Molecular Electronics: Science and Technology*, The New York Academy of Sciences: New York **1998**; Vol. 852

17. (a) McDonald, R. N.; Campbell, T. W. *J. Am. Chem. Soc.* **1960**, *82*, 4669.(b) Manecke, G.; Zerpner, D. *Makromol. Chem.* **1969**, *129*, 183. (c) Kossmehl, V. G.; Härtel, M.; Manecke, G. *Makromol. Chem.* **1970**, *131*. (d) Hörhold, H. H.; Raabe, D. *Acta Polym*. **1979**, *30*, 86.

18. Müllen, K., Wegner, G. Ed., *Electronic Materials: The Oligomer Approach*, Wiley-VCH: Weinheim **1997** and references therein.

19. Hörhold H. -H. *Z. Chem.* **1972**, *12*, 41.

20. (a) Kanbe, M.; Okawara, M. *J. Polym. Sci. Part A* **1968**, *6*, 1058. (b) Wessling, R. A.; Zimmerman, R. G. *US 3706677*, 1972. (c) Gagnon, D. R.; Capistran, J. D.; Karasz, F. E.; Lenz, R. W. *Polym. Bull.* **1984**, *12*, 293. (d) Wessling, R. A. *J. Polym. Sc. Polym. Symp*. **1985**, *72*, 55. (e) Murase, I.; Ohnishi, T.; Noguchi, T.; Hiroka, M.; Murakami, S. *Mol. Cryst. Liq. Cryst.* **1985**, *118*, 333. (f) Karasz, F. E.; Capistran, D.; Gagnon, D. R.; Lenz, R. W. *Mol. Cryst. Liq. Cryst.* **1985**, *118*, 327. (g) Lenz, R. W.; Han, C. C.; Stenger-Smith, J.; Karasz, F. E. *J. Polym. Sci. Part A* **1988**, *26*, 3241. (h) Lahti, P. M.; Sarker, A.; Garay, R. O.; Lenz, R. W.; Karasz, F. E. *Polymer* **1994**, *35*, 1312.

21. (a) (b)Gustafasson, G.; Cao, Y.; Treacy, G. M.; Klauetter, F.; Colaneri, N.; Heeger, A. J. *Nature* **1992**, *357*, 477.

22. (a) Louwet, F.; Vanderzande, D.; Gelan, J.; Mullens, J. *Macromolecules* **1995**, *28*, 1330. (b) Louwet, F.; Vanderzande, D.; Gelan, J. *Synth. Met*. **1995**, *52*, 125. (c) Louwet, F.; Vanderzande, D.; Gelan, J. *Synth. Met*. **1995**, *69*, 509. (d) Vanderzande, D. J.; Issaris, A. C.; Van Der Borght, M. J.; Van Breemen, A. J.; de Kok, M. M.; Gelan,J. M. *Polym. Prepr.* **1997**, *38* (1), 321.

23. Jin, S. -H. ; Koo, D-S.; Seo, H. -U.; Kim, Y-I.; Gal, Y. -S.; Park, D. -K. *J. Polym. Sci. Part A* **2004**, 42, 2347.

24. Thakur, M. *Macromolecules* **1988**, *21*, 661.

25. Thakur, M.; Elman, B. S. *J. Chem. Phys.* **1989**, *90(3)*, 2042.

26. (a) Cholli, A. L.; Thakur, M. *J. Chem. Phys.* **1989**, *91(12)*, 7912. (b) Cholli, A. L.; Thakur, M. *Polym. Mater. Sci. Eng.* **1991**, *64*, 180. (c) Yu, G.-Q.; Thakur, M. *J. Polymer Science, Part B: Polymer Physics* **1994**, *32(12)*, 2099. (d) Thakur, M. *J. Macromolec. Science, Pure and Applied Chemistry* **2001**, *A38(12)*, 1337. (e) Thakur, M.; Khatavkar, S.; Parish, E. J. *J. Macromolec. Sci., Part A—Pure and Applied Chem.* **2003**, *40(12)*, 1397. (f) Thakur, M.; Swamy, R.; Titus, J. *Macromolecules* **2004**, *37*, 2677. (g) Xu, L.; Li, X.; Gao, Y. *Faming Zhuanli Shenqing Gongkai Shuomingshu* **2005**, *CN 1587346.*

27. (a) Takeda, K. *Polym. Prep.* **1990**, *31(2)*, 236. (b) Abkowitz, M. A.; Stolka, M. *Polym. Prepr.* **1990**, *31(2)*, 254. (c) Mercuri, F.; Re, N.; Sgamellotti, A. *THEOCHEM* **1999**, *489(1)*, 35.

28. (a) Luneva, L. K.; Sladkov, A. M.; Korshak, V. V. Vysokomolekulyarnye Soedineniya **1965**, *7(3)*, 427. (b) Dong, J. *Gaofenzi Tongbao* **1999**, 4, 71 and references therein. (c) Fang, M.-C.; Watanabe, A.; Matsuda, M. *Polymer* **1996**, 37*(1)*, 163. (d) Ohshita, J.; Kunai, A. *Acta Polym.* **1998**, 49*(8)*, 379. (e) Hoshino, S.; Suzuki, H.; Fujiki, M.; Morita, M.; Matsumoto, N. *Mol. Cryst. Liq. Cryst.* **1998**, *315*, 507. (f) Kakimoto, M.; Takiguchi, T.; Kunai, K.; Oshita, J. *Jpn. Kokai Tokkyo Koho* **2000**, *JP 2000143812*. (g) Kakimoto, M.; Takiguchi, T.; Kunai, K.; Ohshita, J. *Jpn. Kokai Tokkyo Koho* **2000**, *JP 2000351836*. (h) Kwak, G.; Masuda, T. *Macromol. Rapid Commun.* **2002**, *23(1)*, 68. (i) Morisaki, Y.; Fujimura, F.; Chujo, Y. *Organometallics* **2003**, 22(17), 3553. (j) Kwak, G.; Fujiki, M.; Masuda, T. *Macromolecules* **2004**, *37(7)*, 2422. (k) Yamaguchi, S.; Xu, C. *Yuki Gosei Kagaku Kyokaishi* **2005**, *63(11)*, 1115. (l) Kunai, A. *Organometallic News* **2007**, *(3)*, 82. (m) Song, S. *U.S. Pat. Appl. Publ.* **2007**, *US 2007249800.*

29. **(**a) Kolesnikov, G. S.; Davydova, S. L.; Klimentova, N. V. *Mezhdunarod. Simpozium po Makromol. Khim., Doklady, Moscow* **1960**, *Sektsiya 1*, 156. (b) Glockling, G.; Hooton, K. A. *J. Chem. Soc.* **1963**, 1849. (c) Mironov, V. F.; Dzhurinskaya, N. G Izvestiya Akademii Nauk SSSR, Seriya Khimicheskaya **1963**, 75. (d) Bedford, J. A.; Bolton, J. R.; Carrington, A.; Prince, R. H. *Trans.*

Faraday Soc. **1963**, 59, 53. (e) Luneva, L. K. *Uspekhi Khimii* **1967,** *36(7),* 1140. (f) Egorochkin, A. N.; Vyazankin, N. S.; Khorshev, S. Ya. *Izvestiya Akademii Nauk SSSR, Seriya Khimicheskaya* **1971**, *9*, 2074. (g) Egorochkin, A. N.; Khorshev, S. Ya.; Ostasheva, N. S.; Sevastyanova, E. I.; Satge, J.; Riviere, P.; Barrau, J. *J. Organomet. Chem.* **1976**, 105(3), 311. (h) Soderquist, J. A.; Hassner, A. *J. Am. Chem. Soc.* **1980**, *102(5)*, 1577. (i) Brefort, J. L.; Corriu, R. J. P.; Gerbier, P.; Guerin, C.; Henner, B. J. L.; Jean, A.; Kuhlmann, T.; Garnier, F.; Yassar, A. *Organometallics* **1992**, *11(7)*, 2500.

30. (a) Tahara, T; Seto, K; Takahashi, S. *Polymer Journal* **1987**, 19*(3),* 301. (b) Seto, K; Takahashi, S; Tawara, T. *Jpn. Kokai Tokkyo Koho* **1987**, *JP 62283129.* (c) Okano, M.; Watanabe, K. *Electrochem. Commun.* **2000,** *2(7),* 471. (d) Baek, N. S.; Kim, H. K.; Chae, E. H.; Kim, B. H.; Lee, J. –H. *Macromolecules* **2002**, *35*, 9282.

31. (a) Dragutan, V.; Balaban, A. T.; Dimonie, M. *Olefin Metathesis and Ring-Opening Polymerization of Cycloolefins*, Wiley, J. & Sons Ltd.: Chichester/Editura Academiei, Bukarest, **1985.** (b) Ivin, K. J.; Mol, J. C. *Olefin Metathesis and Metathesis Polymerization*, Academic Press: London, **1997.** (c) Fürstner, A. *Alkene Metathesis in Organic Synthesis*; Springer: Berlin, **1998**. (d) Grubbs, R. H.; Chang, S. *Tetrahedron* **1998**, *54*, 4413. (f) Ivin, K. J. *J. Mol. Catal. A* **1998**, *133*, 1. (e) Fu¨rstner, A. *Angew. Chem.* **2000**, *112*, 3140; *Angew.Chem., Int. Ed. Engl.* **2000**, *39*, 3013. (f) Trnka, T. M.; Grubbs, R. H. *Acc. Chem. Res.* **2001**, *34*, 18. (g) Grubbs, R.H. *Handbook of Metathesis*, Wiley-VCH: Germany, **2003**. (h) Grubbs, R.H. *Tetrahedron* **2004,** *60*, 7117.

32. Eleuterio, H.S. *U.S.Pat. 3074918*, filed **20th June 1957**.

33. Peters, E.F.; Evering, B.L. *U.S.Pat. 2963447* **1960**.

34. W.L. Truett, D.R. Johnson, I.M. Robinson, B.A. Montague, *J. Am. Chem. Soc.* **1960**, *82,* 2337.

35. Dall'Asta, G.; Mazzanti, G.; Natta, G.; Porri, L. *Makromol. Chem.* **1962**, *56,* 224.

36. (a) Natta, G.; Dall´Asta, G.; Mazzanti, G. *Makromol Chem*. **1963**, *69,* 163. (b) Natta, G.; Dall´Asta, G.; Mazzanti, G. *Angew. Chem*. **1964**, *76*, 765. (c) Natta, G.; Dall´Asta, G.; Bassi, I. W.; Carella, G. *Makromol. Chem.* **1966**, *91*, 87.

37. (a) Calderon, N.; Chen, H. Y.; Scott, K. W. *Tetrahedron Lett.* **1967**, *34,* 3327. (b) Calderon, N.; Ofstead, E. A.; Judy, W. A. *J. Polymer Sci* A-1 **1967**, *5,* 2209. (c) Calderon, N. *Chem. Eng. News* **1967**, *12*, 98.

38. Calderon, N.; Ofstead, E. A.; Ward, J. P.; Judy, W. A.; Scott, K. W. *J. Am. Chem. Soc.* **1968**, *90*, 4133.

39. (a) Mango, F.O.; Schachtschneider, J. H. *J. Am. Chem. Soc.* **1967**, *89*, 2484. (b) Hérisson, J.-L.; Chauvin, Y. *Makromol. Chem.* **1971**, *141*, 161.

40. Grubbs, R. H.; Brunck, T. K. *J. Am. Chem. Soc.* **1972**, *94*, 2538.

41. Levisalles, J.; Rudler, H.; Villemin, D. *J. Organometal. Chem.* **1975**, *87* C7

42. G.S. Lewandos, R. Pettit, *Tetrahedron Lett*. **1971**, *28*, 789.

43. Hérisson, J. L., Chauvin, Y. *Makromol. Chem.* **1971**, *141*, 161.

44. (a) Katz, T. H, McGinnis, J. *J. Am. Chem. Soc.* **1977**, *99* 1903. (b) Grassmann, P. C.; Johnson, T. H. *J. Am. Chem. Soc.* **1976**, *98*, 6055.

45. Calderon, N. *Adv. Chem. Ser*. **1969**, *91*, 399.

46. Natta, G., Dall'Asta, G., Mazzanti, G., *Angew. Chem. Int. Ed.* **1964**, *3*, 723.

47. Pampus, G.; Witte, J.; Hoffmann, M. *Rev. Gen. Caout. Plast.* **1970**, *47*, 1343.

48. Bailey, G. C. *Catalysis Rev.* **1969**, *3*, 37.

49. Warwel, S.; Jägers, H. -G.; Thomas, S. *Fat Sci.Technol* **1992**, *94*, 323.

50. (a) Schrock, R. R. *J. Organomet. Chem*. **1986**, *300*, 249. (b) Schrock, R. R.; Murdzek, J. S.; Bazan, G. C.; Robbins, J.; DiMare, M.; O'Regan, M. *J. Am. Chem. Soc.* **1990**, *112*, 3875. (c) Schrock, R. R. *Acc. Chem. Res.* **1990**, *23*, 158. (c) Schrock, R. R. *Tetrahedron* **1999**, *55*, 8141.

51. Schrock, R. R.; Williams, D. S. *Organometallics* **1994**, *13*, 635 and references therein.

52. (a) Basset, J. L.; Couturier, J. L.; Paillet, C.; Lenconte, M.; Weiss, K. *Angew. Chem.* **1992**, *104*, 622. b) Grubbs, R. H.; Fu, G. C. *J. Am. Chem. Soc.* **1992**, *114*, 5426. (c) Schrock, R. R.; Oskam, J. H.; Fox, H. H.; Yap, K. B.; McConville, D. H.; O'Dell, R.; Lichtenstein, B. J. *J. Organomet. Chem.* **1993**, *459*, 185.

53. Zilles, J. U. *Dissertation*, University of Hamburg: Shaker Verlag GmbH: Germany **1995.**

54. (a) Schwab, P.; France, M. B.; Ziller, J. W.; Grubbs, R. H. *Angew. Chem. Int. Ed. Engl.* **1995**, *34*, 2039; Angew. *Chem.* **1995**, *107*,2179 and references therein. (d) Schwab, P.; Grubbs, R. H.; Ziller, J. W. *J. Am. Chem. Soc*. **1996**, *118*, 110. (d) Dias, E. L.; Nguyen, S. T.; Grubbs, R. H. *J. Am. Chem. Soc.* **1997**, *119*, 3887.

55. (a) Scholl, M.; Ding, S.; Lee, C. W.; Grubbs, R. H. *Org. Lett*. **1999**, *1*, 953. (b) Chatterjee, A. K., Grubbs, R. H. *Org. Lett.* **1999**, *1*, 1751. (c) Romero, P. E.; Piers, W. E.; McDonald, R. *Angew. Chem. Int. Ed. Engl.* **2004**, *41*, 6161 and reference therein.

56. (a) Harrity, J. P. A.; La, D. S.; Cefalo, D. R.; Visser, M. S.; Hoveyda, A. H. *J. Am. Chem. Soc.* **1998,** *120*, 2343. (b) Kingsbury, J. S.; Harrity, J. P. A.; Bonitatebus, Jr., P. J.; Hoveyda, A. H. *J. Am. Chem. Soc.* **1999,** *121*, 791.

57. Garber, S. B.; Kingsbury, J. S.; Gray, B. L.; Hoveyda, A. H. *J. Am. Chem. Soc.* **2000,** *122*, 8168 and references therein.

58. Hong, S. H.; Grubbs, R. H. *J. Am. Chem. Soc.* **2006,** *128*, 3508.

59. Recent developement in metathesis catalyst: (a) Zhu, S.; Cefalo, D. R.; La, D. S.; Jamieson, J. Y.; Davis, W. M.; Hoveyda, A. H.; Schrock, R. R. *J. Am. Chem. Soc.* **1999**, *121*, 8251. (b) Jafarpour, L.; Stevens, E. D.; Nolan, S. P. *J. Organomet. Chem.* **2000**, *606*, 49. (c) Ackermann, L.; El Tom, D.; Furstner, A. *Tetrahedron***2000**, *56*, 2195. (d) Aeilts, S. L.; Cefalo, D. R.; Bonitatebus, P. J.; Houser, J. H.; Hoveyda, A. H.; Schrock, R. R. *Angew. Chem. Int. Ed. Engl.* **2001**, *40*, 1452. (e) Van Veldhuizen, J. J.; Garber, S. B.; Kingsbury, J. S. Hoveyda, A. H. *J. Am. Chem. Soc.* **2002**, *124*, 4954.

60. (a) Schneider, M. F.; Blechert, S. *Angew. Chem. Int. Ed. Engl.* **1996**, *35*, 410. (b) Tallarico, J. A.; Bonitatebus, Jr. P. J.; Snapper, M. L. *J. Am. Chem. Soc.* **1997**, *119*, 7157. (c) Schneider, M. F.; Lucas, N.; Velder, J.; Blechert, S.; *Angew. Chem. Int. Ed. Engl.* **1997**, *36*, 257. (d) Seiders, T. J.; Ward, D. W.; Grubbs, R. H. *Org. Lett.* **2001**, *3*, 3225.

61. (a) Armstrong, S. K.; *J. Chem. Soc., Perkin Trans.* **1998**, *1*, 371. (b) Maier, M. E. *Angew. Chem. Int. Ed. Engl.* **2000**, *39*, 2073.

62. (a) Brumer, O. ; Ruckert, A. ; Blechert, S. *Chem. Eur. J.* **1997**, *3*, 441. (b) Diver, S. T.; Schreiber, S. L. *J. Am. Chem. Soc.* **1997**, *119*, 5106. (c) Schuster, M.; Lucas, N.; Blechert, S. *Chem. Commun.* **1997**, 823.

63. (a) Lindmark-Hamberg, M.; Wagener, K. B. *Macromolecules* **1987**, *20*, 2951. (b) Wagener, K. B., Boncella, J. M., Nel, J. G., Duttweiler, R. P., Hillmyer, M. A. *Makromol. Chem.* **1990**, *191*, 365. (c) Wagener, K. B.; Boncella, J. M.; Nel, J. G. *Macromolecules* **1991**, *24*, 2649 and references therin. (d) Patton, J. T.; Boncella, J. M.; Wagener, K. B. *Macromolecules* **1992**, *25*, 3862. (e) Schuster, M.; Blechert, S. *Angew. Chem. Int. Ed.* **1997**, 36, 2036. (f) Tindall, D.; Pawlow, J. H.; Wagener, K. B. *Adv. Top. Organomet. Chem.* **1998**, *1*, 183. (g) Furstner, A. *Angew. Chem. Int. Ed.* **2000**, *39*, 3012. (h) Schwendenman, J. E.; Church, A. C.; Wagener, K. B. *Adv. Synth. Catal.* **2002**, *344*, 597 and references therein. (i) Courchay, F. C.; Sworen, J. C.; Wagener, K. B. *Macromolecules* **2003,** *36*,

8231. (j) Baughman, T. W.; Wagener, K. B. *Adv. Polym. Sci.* **2005**, *176*, 1 and references therein. (k) Gorodetskaya, I. A.; Choi, T. -L.; Grubbs, R. H. *J. Am. Chem. Soc.* **2007**, *129*, 12672.

64. Dall'Asta, G.; Stigliani, G.; Greco, A.; Motta, L. *Chim. Ind. (Milan)* **1973**, *55*, 142.

65. Korshak, Y. V.; Tlenkopatchev, M. A.; Dolgoplosk, B. A.; Avdeikina, E. G.; Kutepov, D. F. *J. Mol. Catal.* **1982**, *15*, 207.

66. (a) Ivin, K. J.; Saegusa, T. *Ring-Opening Polymerization*; Elsevier: London, **1984**. (b) Buchmeiser, M. R. *Chem. Rev.* **2000**, *100*, 1565 and references therein. (c) Ivin, K. J. *NATO Science Series, II: Mathematics, Physics and Chemistry* **2002**, *56*, 1.

67. (a) Kumar, A.; Eichinger, B.E. *Makromol. Chem., Rapid Commun.* **1992,** *13* , 311. (b) Thorn-Csányi, E.; Pflug, K.P. *Makromol. Chem., Rapid Commun.* **1993**, *14*, 619. (c) Thorn-Csányi E.; Pflug, K. P. *J. Mol. Catal.* **1994**, *90*, 69. (d) Tao, D.; Wagener, K. B. *Polym. Prepr. (Polym. Chem.)* **1994**, *35(2)*, 522. (d) Thorn-Csányi, E.; Kraxner, P. *Macromol. Rapid Commun.* **1995**, *16*, 147. (e) Thorn-Csányi, E.; Kraxner, P. *Macromol. Chem. Phys.* **1997,** *198*, 3827. (f) Thorn-Csányi, E.; Kraxner, P. *J. Mol. Catal. A: Chemical* **1997**, *115(1)*, 21. (g) Thorn-Csányi, E.; Kraxner, P.; Strachota, A. *Macromol. Rapid Commun.* **1998,** *19*, 223. (h) Kraxner, P.; Thorn-Csanyi, E. *NATO ASI, Ser. C*, **1998**, *506*, 297.

68. (a) Herzog, O.; Narwark, O.; Thorn-Csanyi, E. *Synth. Met.* **2001**, *119(1-3)*, 141. (b) Peetz, R.; Narwark, O.; Herzog, O.; Brocke, S.; Thorn-Csanyi, E. *Synth. Met.* **2001**, *119(1-3)*, 539. (c) Peetz, R.; Strachota, A.; Thorn-Csanyi, E. *Macromol. Chem. Phys.* **2003**, *204(11)*, 1439 and references therein. (d) Peetz, R.; Thorn-Csanyi, E. *Polym. Prepr. (Polym. Chem.)* **2003**, *44(2)*, 653.

69. (a)Peetz, R. *Doctoral Thesis* **2000**, University of Hamburg. (b) Strachota, A. *Doctoral Thesis* **2000**, University of Hamburg.

70. (a) Schlick, H.; Stelzer, F.; Tasch, S.; Leising, G. *J. Mol. Catal. A: Chemical* **2000**, *160(1)*, 71. (b) Miller, C. G.; Harper, A. W. *Polym. Prepr. (Polym. Chem.)* **2003**, *44(1)*, 816.

71. Thorn-Csanyi, E; Herzog, O. *J. Mol. Catal. A: Chemical* **2004**, *213(1)*, 123.

72. Nomura, K.; Miyamoto, Y.; Morimoto, H.; Geerts, Y. *J. Polym. Sci., Part A: Polym. Chem.* **2005**, *43(23)*, 6166.

73. (a) Wagener, K. B.; Smith, D. W. *Macromolecules* **1991**, *24*, 6073. (b) Smith, D. W., Wagener, K. B. *Macromolecules* **1993**, *26*, 1633. (c) Smith, D. W.; K. B. Wagener, *Macromolecules* **1993**, *26*, 3533. (d) Cummings, S.; Smith, D.;

Wagener, K.; Miller, R.; Ginsburg, E. *Polym. Prepr. (Polym. Chem.)* **1995**, *36(1),* 697. (e) Cummings, S.; Ginsburg, E.; Miller, R.; Portmess, J.; Smith, Dennis W., Jr.; Wagener, K. ACS Symposium Series **1996**, *624*, 113. (f) Wolfe, P. S.; Gomez, F. J.; Wagener, K. B. *Macromolecules* **1997**, 30*(4)*, 714. (g) Gomez, F. J.; Wagener, K. B. *J. Organomet. Chem.* **1999**, *592*, 271. (h) Brzezinska, K. R.; Wagener, K. B.; Burns, G. T. *J. Polym. Sci., Part A: Polym. Chem.* **1999**, *37(6),* 849. (i) Brzezinska, K. R.; Schitter, R.; Wagener, K. B. *J. Polym. Sci., Part A: Polym. Chem.* **2000**, *38*, 1544. (j) Church, A. Cameron; Pawlow, James H.; Wagener, K. B. *Macromolecules* **2002**, *35*, 5746. (k) Gomez, F. J.; Wagener, K. B. *NATO Science Series, II: Mathematics, Physics and Chemistry* **2002**, *56*, 285. (l) Matloka, P. P.; Wagener, K. B. *J. Mol. Catal. A: Chemical* **2006**, *257(1-2),* 89.

74. (a) Solmaz, K.; Cemil, A.; Buelent, D.; Imamoglu, Y. *J. Mol. Catal. A: Chemical* **2006**, 254*(1-2),* 186. (b) Karabulut, S.; Aydogdu, C.; Duez, B.; Imamoglu, Y. *J. Inorg. Organomet. Polym.* **2006**, *16(2),* 115.

75. (a) Wu, Z.; Papandrea, J. P.; Apple, T.; Interrante, L. V. *Macromolecules* **2004,** *37*, 5257 and references therein. (b) Hyun, J. Y.; Oh, K.; Ryu, C. Y.; Interrante, L. V. *Polym. Prepr. (Polym. Chem.)* **2005**, *46(2),* 1053.

76. Schrock, R. R.; De Pue, R. T.; Feldman, J.; Schverin, C. J.; Dewan, S. C.; Liu, A. H. *J. Am. Chem. Soc.* **1988**, *110*, 1423.

77. (a) Marciniec, B; Lewandowski, M. *J. Inorg. Organomet. Polym.* **1995**, *5(2),* 115. (b) Marciniec, B. *NATO Science Series, II: Mathematics, Physics and Chemistry* **2002**, *56*, 331. (c) Malecka, E.; Marciniec, B.; Pietraszuk, C.; Church, A.C.; Wagener. K.B. *J. Mol. Catal. A-Chem.* **2002**, *190***,** 27. (d) Marciniec, B.; Majchrzak. M. *J. Organomet. Chem.* **2003**, *686*, 228. (e) Marciniec, B.; Pietraszuk, C. *Curr. Org. Chem*. **2003**, *7*, 691. (f) Pietraszuk, C.; Marciniec, B.; Rogalski, S.; Fischer, H. *J. Mol. Catal. A-Chem*. **2005**, *240*, 67. (g) Pawluc, P.; Marciniec,B. ; Kownacki, I.; Maciejewski, H. *Appl. Organomet. Chem.* **2005**, *19*, 49. (h) Majchrzak. M.; Marciniec,B. ; Itami. Y. *Adv. Synth. Catal.*, **2005**, *347,*1285. (i) Pietraszuk, C.; Rogalski, S.; Majchrzak. M.; Marciniec,B. *J. Organomet. Chem.* **2006**, *69,1* 5476. (j) Marciniec,B. *Coord. Chem. Rev*. **2005,** *249*, 2374 and references therein.

78. Miao, Y.-J.; Bazan, G. C. *Macromolecules* **1997**; *30(24);* 7414.

79. Kawai, T.; Shiga, K.; Iyoda, T. *J. Mol. Catal. A-Chem*. **2000**, *160*, 173.

80. (a) Kim, H. K.; Ryu, M.-K.; Lee, S.-M. *Macromolecules* **1997**, *30*, 1236. (b) Kim, H. K.; Ryu, M. K.; Kim, K. D.; Lee, J. H. *Synth. Met*. **1997**, *91*, 297. (c) Kim, H. K.; Ryu, M. K.; Kim, K. D.; Lee, S. M.; Cho, S. W.; Park, J. W.; *Macromolecules* **1998**, *31*, 1114. (d) Kim, K. D; Park, J.S.; Kim, H. K.; Lee, T.B.; No, K. T. *Macromolecules* **1998**, *31*, 7267. (e) Park, J. S.; Kim, K. D.; Jung, S. H.; Kim, H.

K.; Jeoung, S.C.; Kim, Y. H.; Kim, D. *Synth. Met*. **1999**, *102*, 1063. (f) Kim, H. K.; Kim, K. D.; Park, D. S.; Song, H. H. *Nonlinear Opt.* **1999**, *20*, 297. (g) Kim, H. K.; Park, J. –S.; Kim, K.-D.; Jung, S.-H.; Jeoung, S. C.; Kim, Y. H.; Kim, D. *Mol. Cryst. Liq. Cryst. Sci. Technol., Sect. A* **1999**, *327, 175*. (h). Jung, S. H.; Kim, H. K.; Kim, S. H.; Jeoung, S. C.; Kim, Y. H.; Kim, D.; *Macromolecules* **2000**, *33*, 9277. (i) Baek, N. S.; Jung, S. H.; Oh, D. J.; Kim, H. K.; Hwang, G. T.; Kim, B. H. *Synth. Met.* **2001**, *121*, 1743. (j) Yoshida, Y.; Nichihara, Y.; Ootake, R.; Fujii, A.; Ozaki, M.; Yoshuno, K.; Kim, H. K.; Baek, N. S.; Choi, S. K. *J. Appl. Phys.* **2001**, *90*, 6061. (k) Paik, K. Lim; B., Nam S.; Kim, H. K.; Lee, Y.; Lee, K. J. *Thin Solid Films* **2002**, *417*, 132. (l) Baek, N. S.; Kim, H. K.; Chae, E.H.; Byeang Hyean Kim, B.H.; Lee,J.-H. *Macromolecules* **2002,** *35*, 9282. (m) Paik, K. L.; Baek, N. S.; Kim, H. K.; Lee, J. H.; Lee, Y. *Opt. Mater.* **2003**, *21(1-3)*, 135.

81. (a) Abkowitz, M. A.; Stolka, M. *Synth. Met.* **1996**, *78*, 333. (b) Suzuki, H.; Hoshino, S.; Yuan, C. -H.; Fujiki, M.; Toyoda, S.; Matsumoto, N. *IEEE J. Sel. Top. Quantum Electron.* **1998**, *4*, 129. (c) Chen, Z-K.; Lai, Y.-H.; Chan, H. S-O; Ng, S.-C.; Huang, W. *Chem. Lett.* **1999**, 6, 477. (d) Hoshino, S.; Yuan, C. H.; Furukawa, K.; Suzuki, H. *Oyo Butsuri* **1999**, *68(2)*, 166. (e) Lucht, B. L.; Buretea, M. A.; Tilley, T. D. *Organometallics* **2000**, 19, 3469. (f) Law, C. C. W.; Chen, J.; Lam, J. W. Y.; Peng, H.; Tang, B. Z. *J. Inorg. Organomet. Polym.* **2004**, 14, 39. (g) Sumiya, Ken-Ichi; Kwak, Giseop; Sanda, Fumio; Masuda, Toshio. *J. Polym. Sci., Part A: Polym. Chem.* **2004**, *42*, 2774. (h) Takagi, K.; Kunii, S.; Yuki, Y. *J. Polym. Sci., Part A: Polym. Chem.* **2005**, *43*, 2119.

82. (a) Brouwer, H. J.; Krasnikov, V.; Hil- berer, A.; Hadziioannou,G. *Adv. Mater.* **1996**, *8, 935*. (b) Mercuri, F.; Re, N.; Sgamellotti, A. *J. Mol. Struct.* (Theochem) **1999**, *489*, 35. (c) Ohshita, J.; Sugimoto, K.; Kunai, A.; Harima, Y.; Yamashita, K. *J. Organomet. Chem.* **1999**, *580*, 77. (d) Yamashita, H.; de Leon, M. S.; Channasanon, S.; Suzuki,Y.; Uchimaru, Y.; Takeuchi, K. *Polymer* **2003**, *44*, 7089.

83. Tidwell, T. T. *Angew. Chem. Int. Ed*. **2007**, *46*, 2 and references therein.

84. (a) Marvel, C. S.; Bonsignore, P. V. *J. Am. Chem. Soc.* **1959**, *81(11)*, 2668. (b) Weng, J.; Sun, W.; Jiang, L.; Shen, Z. *Macromol. Rapid Commun.* **2000,** *21*, 1099. (c) Annaraj, J.; Srinivasan, S.; Ponvel, K. M.; Athappan, P. R. *J. Inorg. Biochem*. **2005**, *99*, 669. (d) Chen, Q.; Huang, J.; *Appl. Organometal. Chem.* **2006**, *20*, 758. (e) Guo, L.; Wu, S.; Zeng, F.; Zhao, J. Eur. Polym J. **2006**, *42*, 1670.

85. (a) Guerriero, P.; Tamburini, S.; Vigato, P.A. *Coord. Chem. Rev*. **1995,** *139*, 17 and reference therein. (b) Vigato, P.A.; Tamburini, S. *Coord. Chem. Rev*. **2004**, *248*, 1717 and reference therein. (c) Drozdzak, R.; Allaert, B.; Ledoux, N.; Dragutan, I.; Dragutan, V.; Verpoort , F. *Coord. Chem. Rev*. **2005**, *249*, 3055 and reference therein.

86. Adams, R.; Bullock, R.E.; Wilson, W.C. *J. Am. Chem. Soc.* **1923,** *45*, 521.

87. (a) D'Alelio, G. F.; Crivello, J. V.; Schoenig, R. K.; Huemmer, T. F. *J. Macromol. Sci. Chem.* **1967**, *A1*, 1161. (b) D'Alelio, G. F.; Crivello, J. V.; Schoenig, R. K.; Huemmer, T. F. *J. Macromol. Sci. Chem. A* ***1*967**, *1*, 1321. (c) D'Alelio, G. F.; Crivello, J. V.; Dehner, T. R.; Schoenig, R. K. *J. Macromol. Sci. Chem*. **1967**, *A1 (7)*, 1331. (d) D'Alelio, G. F.; Kurosaki, T.; Ostdick, T. *J. Macromol. Sci. Chem. A*, **1968**, *2*, 285. (e) D'Alelio, G. F.; Strazik, W. F.; Feigl, D. M.; Schoenig, R. K. *J. Macromol. Sci. Chem. A* **1968**, *2*, 1457.

88. (a) Patel, M. S.; Patel, S. R. *J. Polym. Sci. Part A: Polym. Chem*. **1982**, *20*, 1985. (b) Lee, K. S.; Won, J.C.; Jung, J. C. *Makromol. Chem*. **1989**, *190*, 1547. (c) Saegusa, Y.; Sekiba, K.; Nakamura, S. *J. Polym. Sci Part A: Polym. Chem.* **1990**, *28*, 3647. (d) Al-Jumah, K. B.; Wagener, K. B.; Hogen-Esch, T. E.; Musfeldt, J. L.; Tanner, D.B. *Polym. Prepr. (Polym. Chem.)* **1990**, 31, 173. (e) Kim, H.; Park, S.B.; Jung, J.C.; Zin, W.C. *Polymer* **1996**, *37*, 2845. (f) Thomas, O.; Inganas, O.; Andersson, M. R. *Macromolecules* **1998,** *31*, 2676 and reference therein. (g) Krebs, F. C.; Jorgensen, M. *Synth. Met*. **2004**, *142*, 181. (h) Liu, C.L.; Chen, W. C. *Macromol.Chem.Phys*. **2005,** *206*, 2212. (i) Liu, C.L.; Tsai, F. C.; Chang, C. C.; Hsieh, K.H.; Lin, J.L.; Chen, W. C. *Polymer* **2005**, *46*, 4950.

89. Davydov, B. É.; Drabkin, I. A.; Korshak, Y. V.; Rozenshtein, L. D. *Russ. Chem. Bull.* **1963**, *12(9)*, 1521 and reference therein.

90. Salamone, J. C. Ed., *Polymeric Materials Encyclopedia*, CRC Press, Inc. **1996**, Vol. 9.

91. (a) Millaud, B.; Thierry, A.; Skoulios, A. *Mol. Cryst. Liq. Cryst.* **1978**, *41 (10)*, 263. (b) Millaud, B.; Strazielle, C. *Polymer* **1979,** *20 (5)*, 563. (c) Millaud, B.; Thierry, A.; Strazielle, C.; Skoulios, A. *Mol. Cryst. Liq. Cryst*. **1979**, *49 (10)*, 299. (d) Barbera, J.; Oriol, L.; Serrano, J.L. *Liq. Cryst.* **1992**, *12 (1)*, 37.

92. (a) D'Alelio, G.F.; Schoenig, R.K. *J. Macromol. Sci. Rev. Macromol. Sci.* **1969**, *3 (1)*, 105. (b) D'Alelio, G.F. *Encyc. Polym. Sci. Technol*. **1969**, *10*, 659. (a) Pron, A. *Prog. Polym. Sci.* **2001**, *27 (1)*, 135.

93. Grigoras, M.; Catanescu, C.O.; *J. Macromol. Sci. Part C – Polym. Rev.* **2004**, *C44*, *2*, 131 and references therein.

94. Yang, H.H. *Aromatic High-Strength Fibers*; Wiley-Interscience: New York, **1989**; p 641.

95. (a) Yang; C. J.; Jenekhe, S.A *Chem. Mater*.**1994**, *6*,196-203. (b) Wang, C.; Shieh, S.; LeGoff, E.; Kanatzidis, M.G. *Macromolecules* **1996**, *29***,** 3147. (c) Euler, W.V. *Conducting polymers: Transport, Photophysics and Applications;* Nalwa, H.S.,

Ed.; John Wiley & Sons: New York, **1997**; Vol. 2, p 719 (d) McElvain, J.; Tatsuura, S.; Wudl, F.; Heeger, A. J. *Synth. Met*. **1998**, *95*, 101.

96. Park, S.B.; Kim, H.; Zin, W.C.; Jung. J.C. *Macromolecules* **1993**, *26*, 1627.

97. (a) Destri, S.; Porzio, W.; Dubitsky, Y. *Synth. Met*. **1995**, *75*, 25. (b)Destri, S.; Pasini, M.; Pelizzi, C.; Porzio, W.; Perdieri, G.; Vignali, C. *Macromolecules* **1999**, *32*, 353 – 360 and refrecens therein.

98. (a) Conwell, E.M.; Stolka, M.; Miller, M.R. *Electroluminescent materials, devices and large-screen displays*. International Society for Optical Engineering (SPIE) Proceedings **1993**, San Jose, CA. (b) Miyata, S.; Nalwa, H. S. *Organic electroluminescent materials and devices*, Gordon & Breach: Amsterdam, **1997**. (c) Hsieh, B.R.; Wei, Y. Semiconducting polymers: properties and synthesis. ACS Symp Series 735, American Chemical Society; **1999**. (d) Kippelen, B.; Bradley, D. *Polymer photonic devices. IV*. International Society for Optical Engineering (SPIE) Proceedings **1998**, vol. 3281, San Jose CA. (e) Akcelrud, L. *Prog. Polym. Sci.* **2003,** *28*, 875 and references therein.

99. Kasim, R. K.; Cheng, Y.; Pomerantz, M.; Elsenbaumer, R. L. *Synthetic Metals* **1997**, *85*, 1213.

100. (a) Brown, A. R.; Greenham, N. C.; Burroughes, J. H.; Bradley, D. D. C.; Friend, R. H.; Burn, P. L.; Kraft, A.; Holmes, A. B. *Chem. Phys. Lett*. **1992**, *200*, 46. (b) Misra, A.; Kumar, P.; Kamalasanan, M. N.; Chandra, S. *Semicond. Sci. Technol*. **2006** , *21*, 35 and references therein. (c) Bernardo, G.; Charas, A.; Alcacer, L.; Morgado, J. Appl. Phys. Lett. **2007**, 91*(6)*, 063509-1.

101. Kumagai, T; Itsuno, S. *Tetrahedron: Asymmetry* **2001**, *12(18)*, 2509.

102. Marsmann, H. *29Si-NMR spectroscopic results. In: NMR. Basic Principles and Progress.* Diehl, P.; Fluck, E.; Kosfeld, R. Ed.; Springer-Verlag: Berlin **1981**, Vol. 17, 65-235.

103. Kvaran1, A´.; Konra´ðsson, A´. E.; Evans, C.; Geirsson, J.K.F. *J. Mol. Struct.* **2000**, *553*,79.